ESTRATÉGIAS PARA OBTENÇÃO DE COMPÓSITOS FERTILIZANTES VIA SOLUBILIZAÇÃO BIOLÓGICA DE MINERAIS

UNIVERSIDADE FEDERAL DE SÃO CARLOS

CENTRO DE CIÊNCIAS EXATAS E TECNOLOGIA

PROGRAMA DE PÓS-GRADUAÇÃO EM ENGENHARIA QUÍMICA

ESTRATÉGIAS PARA OBTENÇÃO DE COMPÓSITOS FERTILIZANTES VIA SOLUBILIZAÇÃO BIOLÓGICA DE MINERAIS

Rodrigo Klaic

São Carlos, SP, Brasil.

2018

UNIVERSIDADE FEDERAL DE SÃO CARLOS

CENTRO DE CIÊNCIAS EXATAS E TECNOLOGIA

PROGRAMA DE PÓS-GRADUAÇÃO EM ENGENHARIA QUÍMICA

Rodrigo Klaic

ESTRATÉGIAS PARA OBTENÇÃO DE COMPÓSITOS FERTILIZANTES VIA SOLUBILIZAÇÃO BIOLÓGICA DE MINERAIS

Tese de doutorado apresentada ao Programa de Pós-Graduação em Engenharia Química da Universidade Federal de São Carlos como parte dos requisitos necessários para a obtenção do título de Doutor em Engenharia Química, área de concentração em Pesquisa e Desenvolvimento de Processos Químicos.

Orientadora: Dra. Cristiane Sanchez Farinas

Coorientadora: Prof. Dra. Teresa Cristina Zangirolami

São Carlos, SP, Brasil.

2018

MEMBROS DA BANCA EXAMINADORA DA DEFESA DE TESE DE RODRIGO KLAIC APRESENTADA AO PROGRAMA DE PÓS-GRADUAÇÃO EM ENGENHARIA QUÍMICA DA UNIVERSIDADE FEDERAL DE SÃO CARLOS, EM 27 DE MARÇO DE 2018.

BANCA EXAMINADORA:

Cristiane Sanchez Farinas
Orientadora, EMBRAPA/UFSCar

Teresa Cristina Zangirolami
UFSCar

Cauê Ribeiro de Oliveira
EMBRAPA

Alberto Carlos de Campos Bernardi
EMBRAPA

Alberto Colli Badino Junior
UFSCar

Agradecimentos

Agradeço a meus pais, Henrique Klaic e Lídia Alicia Karlec Klaic, e a meu irmão Tiago Klaic, pelo apoio incondicional e pela compreensão.

Agradeço em especial aos meus orientadores Dra. Cristiane Sanchez Farinas e Prof. Dra. Teresa Cristina Zangirolami, e também ao Dr. Cauê Ribeiro de Oliveira pela orientação, ensinamentos, amizade, conselhos e apoio no desenvolvimento deste trabalho.

Agradeço à UFSCar (Universidade Federal de São Carlos), PPGEQ (Programa de Pós-Graduação em Engenharia de Química) e à Embrapa Instrumentação pela estrutura física disponibilizada.

Agradeço aos funcionários da UFSCar e Embrapa Instrumentação pela amizade e apoio.

Agradeço ao CNPq (Conselho Nacional de Desenvolvimento Cientifico e Tecnológico) pela bolsa de incentivo à pesquisa disponibilizada.

Agradeço a todos os colegas e amigos pelo apoio e incentivo ao longo desses quatro anos de Doutorado e a todos aqueles que por um lapso não mencionei, mas que colaboraram para esta pesquisa.

"A ciência ensina ao homem o amor e o respeito pela verdade, a ideia do dever e a necessidade do trabalho, não como um castigo, mas como mais elevado meio de empregar sua atividade"

(Marcelin Berthelot)

Resumo

Fertilizantes fosfatados são amplamente utilizados para melhorar a produtividade agrícola. Entretanto, o processo de produção destes fertilizantes envolve altos custos e pode causar danos ambientais. A aplicação de microrganismos capazes de solubilizar fosfatos (MSP) tem sido considerada uma potencial estratégia para obter biofertilizantes via solubilização biológica da rocha fosfática (RF), porém, a eficiência desse processo ainda é baixa. Dessa forma, o objetivo desse trabalho foi desenvolver estratégias para aumentar a solubilização da RF pela ação de MSP usando processos de cultivo microbiano por rota submersa (CSm) e estado sólido (CES), além de propor novos produtos empregando o uso de MSP como agente promotor de solubilização. Inicialmente foi realizada a seleção de um potencial MSP, na qual o fungo *Aspergillus niger* se destacou. Em seguida, foi avaliada uma nova estratégia mecânico-biológica para aumentar a solubilização da RF. Nessa estratégia, a RF Bayóvar (origem sedimentar) foi ativada mecanicamente para diminuir o tamanho de partícula, assim a solubilidade pode ser aumentada em decorrência da maior área superficial juntamente com a alteração local do pH. Os resultados mostraram um aumento de solubilidade de 60% quando utilizado o CSm e 115% em CES. A estratégia da ativação mecânica também foi estudada com a RF Itafós (origem ígnea), a qual mostrou um comportamento diferente da RF Bayóvar, com ganhos de solubilidade de 57% por CSm e 45% por CES. Ainda para a RF Itafós, foi investigada uma estratégia utilizando fornecimento de sólidos por batelada alimentada integrada à ativação mecânica, que levou a aumento de 78% na solubilização desta rocha. A fim de elucidar o mecanismo de ação no processo de biosolubilização, realizou-se um estudo sobre o efeito dos ácidos orgânicos sob diferentes fontes de RFs. Os resultados mostraram que o ácido cítrico e oxálico são os ácidos orgânicos com maior potencial para solubilizar RF. Foi constatada sinergia entre os ácidos cítrico/oxálico e oxálico/gluconico quando presentes na razão 1:1 e 2:1, respectivamente, que potencializou a solubilização. A partir dos conhecimentos obtidos, desenvolveu-se um compósito-fertilizante baseado na gelatinização de amido com simultânea dispersão de partículas de RF mecanicamente ativadas e esporos de *A. niger*. As caracterizações dos compósitos mostraram um elevado grau de dispersão das partículas de RF na matriz de amido, além de um considerável teor de P_2O_5 entre 10-22%. A solubilidade do fósforo contido no compósito foi superior a 70% em somente 96 h. Além disso, os esporos mantiveram-se viáveis após o processamento e estocagem, garantindo um tempo de prateleira de no mínimo dois meses ao produto. Devido ao potencial dessa tecnologia, foram também desenvolvidos compósitos-fertilizantes a partir de óxidos de minérios e de enxofre elementar, os quais são importantes para a nutrição de plantas. Os resultados mostraram que a matriz foi capaz de comportar uma alta carga de óxidos (ZnO, MnO e CuO) e enxofre elementar, assim como observado quando utilizado a RF. Os experimentos de bio-ativação mostraram uma elevada solubilização dos óxidos quando utilizado enxofre na matriz de amido. O produto final obtido foi um grânulo multi-nutriente, fonte de Zn, Mn, Cu e S para as plantas. O compósito multi-nutriente também foi avaliado no sistema solo-planta e os resultados mostram que foi tão eficiente quanto as fontes comerciais utilizadas. Conclui-se que os nanocompósitos-fertilizantes obtidos neste trabalho constituem um inovador conceito de "biorreator em grânulo" como muitas possibilidades de aplicação na nutrição de plantas.

Palavras Chaves: Biofertilizantes, rocha fosfática, solubilização biológica, *Aspergillus niger*, nanocompósito.

Abstract

Phosphate fertilizers are widely used to improve agricultural productivity. However, the process of producing these fertilizers involves high costs and can cause environmental damage. The application of phosphate solubilising microorganisms (PSM) has been considered a potential strategy to obtain biofertilizers by biological phosphate rock (PR) solubilization, but the efficiency of this process is still low. Thus, the objective of this work was to develop strategies to increase the solubilization of RF by the action of PSM using microbial culture processes by submerged route (SmC) and solid state (SSC), besides proposing new products employing the use of PSM as agent promoter. Initially the selection of a potential PSM was performed, in which the fungus *Aspergillus niger* was highlighted. Then, a new mechanical-biological strategy was evaluated to increase the solubilization of the PR. In this strategy, PR Bayóvar (sedimentary origin) was mechanically activated to decrease particle size, so the solubility can be increased as a result of the larger surface area together with the local pH change. The results showed an increase of solubility of 60% when using SmC and 115% in SEC. The mechanical activation strategy was also studied with the Itafós PR (igneous origin), which showed a different behavior of Bayóvar PR, with solubility gains of 57% by SmC and 45% by ESC. Also for the PR Itafós, a strategy was proposed using a system of solids supply by fed-batch integrated to the mechanical activation step increased the solubilization of this rock in 78%. In order to elucidate the mechanism of action in the biosolubilization process, a study was carried out to evaluated the effect of organic acids under different RF sources. The results showed that citric acid and oxalic acid are the organic acids with the greatest potential to solubilize PR. A synergistic relationship was found between citric/oxalic acids as well as oxalic/gluconic acids when presented in molar ratio of 1:1 and 2:1, respectively, that potentiates the solubilization. Using the knowledge obtained, a composite-fertilizer based on starch gelatinization was developed with simultaneous dispersion of PR particles mechanically activated and encapsulation of *A. niger* spores. The characterization of the composites showed a high degree of dispersion of the PR particles in the starch matrix, besides a considerable content of P_2O_5 between 10-22%. The solubility of the phosphorus contained in the composite was greater than 70% in only 96 h. In addition, the spores remained viable after processing and storage, ensuring a minimum shelf-time of two months. Due to the potential of this technology, composites-fertilizers were also developed from mineral oxides and elemental sulfur. The results showed that the matrix was capable of carrying a high load of oxides (ZnO, MnO and CuO) and elemental sulfur, as observed when using PR. The bio-activation experiments showed a high solubilization of the oxides when sulfur was used in the starch matrix. The final product obtained was a multi-nutrient granule source of Zn, Mn, Cu and S for the plants. The multi-nutrient composite was also evaluated in the soil-plant system and the results show that they were as efficient as the commercial sources used. Concludes, that the nanocomposite-fertilizers proposed in this work constituting an innovative concept of "bioreactor in granule" with many possibilities of application in the nutrition of plants.

Keywords: Biofertilzers, phosphate rock, biological solubilization, *Aspergillus niger*, nanocomposite.

Lista de Figuras

Capítulo 3

Capítulo 4

Lista de Tabelas

Capítulo 6

Sumário

Introdução

O fósforo (P) é um dos principais nutrientes limitantes para o crescimento das plantas, sendo necessário para desempenhar as diversas funções vitais no desenvolvimento das plantas. Alguns fatores de crescimento associado ao fósforo são a melhoria na qualidade da plantação, maior resistência a doenças e suporte ao desenvolvimento da planta por todo ciclo de vida (Maravolta, 1980; Novais, 1991). Portanto, realizar uma fertilização/suplementação fosfatada adequada é essencial para aumentar o rendimento e produtividade na agricultura. A suplementação de P é realizada principalmente na forma de fertilizantes fosfatados solúveis, como o superfosfato simples (SSP) e superfosfato triplo (TSP). O consumo mundial de P para agricultura entre no biênio 2016/2017 foi em torno de 46,9 Mt P_2O_5 e há previsão de aumento de 2% ao ano até 2020 (Heffer, 2017). Os fertilizantes fosfatados são produzidos pelo processamento químico da rocha fosfática (RF), sendo que esse processo envolve alto consumo de energia, uso de ácidos inorgânicos fortes como o ácido sulfúrico e fosfórico, liberação de contaminantes gasosos, além da geração de subprodutos indesejáveis como o fosfogesso (Canovas et al., 2018; CONAMA, 2011). Estudos tem mostrado que para cada tonelada de P_2O_5 são produzidas 5 toneladas de fosfogesso ($CaSO_4.H_2O$), o acumulo de subproduto pode gerar problemas como eutrofização de lagos e rios (Canovas et al., 2018; Tayibi et al., 2009). De acordo com os resultados de estudos divulgados pela Organização Mundial da Saúde, os poluentes gasosos gerados pela indústria de fertilizantes levaram a um aumento da mortalidade e da morbidade na população local onde estas indústrias estão instaladas (CONAMA, 2011).

Uma alternativa quem vem sendo estudada para minimizar estes problemas, além de diminuir os custos de processo, é a solubilização da RF por rota biotecnológica (Mendes et al., 2015; Avdalovic et al., 2015; Vassilev et al., 2017). A solubilização da RF por rota biotecnológica consiste em aplicar um microrganismo para promover a solubilização da RF, sendo que o produto resultante desse processo de solubilização vem sendo denominado de biofertilizante fosfatado (Vassilev et al., 2006; Vassilev and Vassileva, 2003; Vassilev et al., 2015; Vassileva et al., 2010). Nesse processo, o microrganismo atua como agente solubilizador, transformando o fósforo insolúvel presente na RF em formas solúveis principalmente pela acidificação resultante da produção de ácidos orgânicos (Illmer and Schinner, 1995; Kpomblekoua and Tabatabai, 1994; Mendes et al., 2014a; Nahas, 1996). Os grupos hidroxila e carboxila dos ácidos orgânicos podem sequestrar os cátions (principalmente o cálcio) ligados ao fosfato e, posteriormente, converter o fosfato insolúvel

em formas solúveis (Kpomblekoua and Tabatabai, 1994). Por estas razões é de grande interesse estudar e desenvolver processos e novas tecnologias aplicando microrganismos solubilizadores de fósforo (MSP) para produção de biofertilizantes fosfatados, visto que a solubilização da RF por rota biotecnológica tem menor impacto ao meio ambiente comparado aos métodos clássico de produção de fertilizantes fosfatados.

Cultivos de MSP por suspensão aerada (cultivo submerso, CSm) e em meio sólido (cultivo em estado sólido, CES) são os principais processos utilizados para realizar a solubilização da RF pela rota biotecnológica. No CES, o substrato sólido umedecido é suplementado com nutrientes e empregado para sustentar o crescimento e o metabolismo do microrganismo (Stanton, 2002). Já no CSm, as células microbianas se desenvolvem em um meio líquido gaseificado, com adição de nutrientes para promover o crescimento do microrganismo (Fazenda et al., 2008). Estudos realizados têm demonstrado o potencial de utilizar MSP para solubilizar RF por ambas técnicas de cultivo, utilizando diferentes tipos de RF, diferentes MSP e condições de processo (Mendes et al. 2015; de Oliveira et al., 2015; Ogbo et al., 2010). Embora muitos fungos e bactérias tem sido reportado como bons MSP, fungos filametosos são reconhecidos pela alta taxa de produção de ácidos orgânicos e podem ser mais eficientes para promover a solubilização da RF (Mendes et al. 2015; de Oliveira et al. 2015). Os produtos obtidos a partir desses processos de solubilização têm demonstrado bons resultados como fonte de P para as plantas quando avaliados no sistema solo-planta (Mendes et al., 2017; Vassilev et al., 2017). Entretanto, a eficiência de solubilização da RF por ambas rotas biotecnologias ainda é baixa, o que leva à necessidade de desenvolver bioprocessos mais eficientes, para aumentar a competitividade dos biofertilzantes frente aos produtos já disponíveis no mercado.

Uma classe de novos produtos para a agricultura baseada no desenvolvimento de compósitos-fertilizantes para promover a liberação controlada de nutrientes vem se destacando recentemente (Giroto et al., 2014; Giroto et al., 2017). Entretanto, compósitos com a função de promover o aumento de solubilidade de fontes de nutrientes de baixa reatividade (como as RFs) ainda são pouco explorados. Existem trabalhos que promovem o encapsulamento de MSP em materiais como alginato de cálcio para posterior adição destes materiais ao solo ou mesmo a biorreatores, para a solubilização de RP por cultivo submerso (Jain et al., 2010; Schoebitz et al., 2013; Vassilev et al., 2017; Vassilev et al., 2015). Entretanto, na maioria das matrizes utilizadas para o encapsulamento de microrganismos não se obtém uma boa dispersão de material particulado, ou quase nenhum material pode ser

dispersado conjuntamente com o encapsulamento devido a limitações dos tradicionais métodos de processamento. Portanto, desenvolver um compósito a partir de um material compatível para promover boa dispersão de minerais de baixa solubilidade e simultaneamente encapsular microrganismos para promover a solubilização dessas fontes de nutrientes seria um conceito inovador de uma nova classe de fertilizantes.

Dessa forma, este estudo propõe novas estratégias para melhorar a eficiência de solubilização da RF por ambas as rotas biotecnológicas para tonar estes processos viáveis economicamente e ambientalmente corretos, além de contribuir para o desenvolvimento de tecnologia para a produção de biofertilizantes em larga escala. Também faz parte deste trabalho, propor diferentes alternativas para produzir novos produtos fertilizantes baseados na ação biológica do microrganismo para promover a solubilização da RF e outras fontes de nutrientes para as plantas.

Estrutura do trabalho

A apresentação dos estudos desenvolvidos ao longo do doutorado está estruturada no formato de Capítulos. Inicialmente, no Capítulo 1 é apresentada uma revisão da literatura, na qual se encontram informações relevantes para o entendimento do trabalho desenvolvido, juntamente com os objetivos propostos.

No Capítulo 2 são apresentados os resultados obtidos durante o desenvolvimento da primeira etapa do trabalho e refere-se ao estudo de seleção do microrganismo com maior potencial para solubilizar fosfato e de uma estratégia para aumentar a solubilidade da rocha fosfática Bayóvar. A estratégia proposta neste estudo combina a ativação mecânica da rocha fosfática associada à biosolubilização por cultivo submerso e no estado sólido. Além disso, também é apresentada a caracterização química e física desta rocha. Esses resultados estão apresentados na forma de artigo, publicado na revista *International Journal of Mineral Processing*, intitulado "A novel combined mechanical-biological approach to improve rock phosphate solubilization".

No Capítulo 3 são apresentados os resultados obtidos no estudo do efeito do tamanho de partícula na solubilização da rocha fosfática Itafós por cultivo submerso e em estado sólido. A caracterização detalhada desta rocha fosfática assim como a análise do efeito do teor de sólidos (concentração de rocha fosfática) no processo de solubilização são apresentados. A estratégia de processo proposta para contornar os problemas oriundos da alta carga de sólidos

e aumentar a eficiência de solubilização também é discutida. Os resultados estão apresentados na forma de artigo submetido à revista *Sustainable Chemistry & Engineering*. O artigo é intitulado "A fed-batch strategy integrated with mechanical activation improves the biological solubilization of phosphate rock".

A fim de melhor entender os mecanismos envolvidos na biosolubilização do fosfato, foi realizado um estudo de solubilização de rochas fosfáticas de diferentes origens em ácidos orgânicos de baixa massa molecular, cujos resultados são apresentados no capítulo 4. As solubilizações das diferentes fontes de fosfatos minerais também foram realizadas em ácidos inorgânicos e água, para comparação dos resultados. Um estudo avaliando o sinergismo dos ácidos orgânicos também foi realizado, além de um estudo cinético de solubilização. Os resultados desta etapa do trabalho estão apresentados na forma de artigo em elaboração. O artigo é intitulado "Solubilization of mineral phosphate by organic acids".

No capítulo 5 são apresentados os resultados relativos ao estudo do desenvolvimento de um novo produto, um compósito-fertilizante. Assim, é proposto um conceito inovador de um "biorreator em grânulo", no qual os microrganismos se desenvolvem na estrutura do grânulo consumindo a matriz como fonte de carbono e produzindo ácidos orgânicos. Consequentemente, a acidez local aumenta promovendo a solubilização das partículas de rocha fosfática dispersas na matriz. Esses resultados estão apresentados na forma de artigo submetido à revista *Minerals Engineering*. O artigo é intitulado "Nanocomposite of starch-phosphate rock bio-activated for environmentally-friendly fertilization".

No capítulo 6 são apresentados os resultados da etapa de aplicação da estratégia proposta de "biorreator em grânulo" para a obtenção de compósitos-fertilizantes com outras fontes de nutrientes de baixa solubilidade, como os óxidos metálicos e enxofre elementar. Nesta etapa, também foram realizados ensaios em casa de vegetação para avaliar o efeito dos compósitos-fertilizantes no sistema solo-planta. Os resultados estão apresentados na forma de artigo em elaboração intitulado "Nanocomposites fertilizers biologically activated for an efficient supply of sulfur and micronutrients to plants".

Por fim, no Capítulo 7 são apresentadas as conclusões e perspectivas do presente trabalho.

Capítulo 1

1. Revisão Bibliográfica

1.1. O fósforo e sua importância para as plantas

O fósforo (P) é um elemento químico de número atômico 15 (15 prótons e 15 elétrons), massa atômica igual a 31. Existe naturalmente na natureza e pode ser encontrado em todo globo terrestre, sendo vital para existência da vida no planeta. Nas plantas, o P é um dos principais nutrientes limitantes para o crescimento e corresponde a aproximadamente 0,2% da massa seca e, apesar da pequena quantidade, é indispensável para melhorar a produção agrícola de diversas culturas (Mullins, 2009).

O P (como fosfato, PO_4^{3-}) é um componente de compostos importantes das células vegetais, incluindo fosfocarboidratos e fosfolipídios que compõem as membranas vegetais de todas as plantas (Goldstein et al., 1993). Este elemento é essencial na transferência de energia, respiração e fotossíntese (Krishnaraj and Dahale, 2014). A energia absorvida pela clorofila durante a fotossíntese é convertida em adenosina trifosfatada (ATP) e atua como primeira fonte de energia requerida nos processos biológicos (Krishnaraj and Dahale, 2014). Dessa forma, o P torna-se essencial para desempenhar as diversas funções vitais nas plantas. A ausência de P pode afetar a floração, a formação e maturação de frutos, o crescimento das raízes e a multiplicação das células, sendo que o fósforo deve estar presente em uma forma inorgânica simples para que possa ser assimilado (Krishnaraj and Dahale, 2014). O desenvolvimento de manchas arroxeadas nas folhas mais velhas, além do atraso no florescimento, flolhas quebradiças e pequeno número de frutos e de sementes são indícios de falta de fósforo (Krishnaraj and Dahale, 2014). Assim, para obter bons rendimentos no cultivo de qualquer cultura, o fósforo é necessário e indispensável.

O P é geralmente encontrado nos solos na forma de compostos de baixa solubilidade. Em solos ácidos, o fosfato reage com ferro (Fe) e alumínio (Al) formando fosfatos de Fe e Al. Já em solos alcalinos, reage com cálcio (Ca) para formar fosfatos de Ca (Fontes and Weed, 1996). Entretanto, as plantas podem absorver apenas o P que está dissolvido na água presente no solo (fosfato solúvel), que se encontra principalmente na forma de ânions $H_2PO_4^-$ e HPO_4^{2-} (Fontes and Weed, 1996; Krishnaraj and Dahale, 2014; Mullins, 2009). Nesse contexto, estudos tem demonstrado que a concentração de P solúvel na maioria dos solos é baixa,

devido a reações de complexação que ocorrem com elementos como Fe, Al e Ca, como já citado, limitando assim o desenvolvimento das plantas. Estima-se que para obter bons rendimentos para culturas como milho e soja, a concentração de P solúvel deve estar entre 200 e 300 mg Kg^{-1} de solo, entretanto essas concentrações podem variar dependendo do solo e das condições iniciais que o solo se encontra (Maravolta, 1980; Novais, 1991). Isto mostra a necessidade e a importância de realizar fertilização fosfatada para suprir as necessidades nutricionais das plantas aumentado a concentração de fósforo disponível no solo para obter bons rendimentos e produtividade agrícola.

1.2. Reservas e tipos de rochas fosfáticas

As rochas fosfáticas (RFs) são a principal fonte de matéria-prima para produção de fertilizantes fosfatados e estão sendo constantemente exploradas para suprir as altas demandas das indústrias de fertilizantes. Estima-se que as reservas mundiais atuais de RF sejam de aproximadamente 16 trilhões de toneladas (Souza and Fonseca, 2010). As reservas estão distribuídas por mais de 37 países, entretanto apenas cinco países (Marrocos, China, Estados Unidos, África do Sul e Jordânia) detêm aproximadamente 85 % da produção mundial (Souza and Fonseca, 2010). O Brasil ocupa a sétima posição entre os países produtores de RF no mundo (UNEP, 2011). As principais reservas brasileiras estão localizadas em Minas Gerais (67 %), Goiás (14 %) e São Paulo (6 %). A principal jazida se encontra em Tapira (MG), seguida das reservas de Patos de Minas (MG), Araxá (MG), Catalão (GO) e Cajati (SP) (Souza and Fonseca, 2010).

As RFs ou fosfatos naturais são minérios que possuem alguma fase cristalina rica em fósforo. A denominação fosfatos naturais abrange uma gama de variações nesses tipos de minérios, quer seja em composição, textura ou origem geológica. Porém todos apresentam uma característica em comum: são constituídos de minerais do grupo das apatitas (Toledo, 2001). Dessa forma, a apatita é um mineral de fósforo que pode ser representada de forma geral como $Ca_{10}(PO_4)_6X_2$, onde X pode sofrer substituição por flúor (F) (fluorapatita) ou cloro (Cl) (clorapatita) ou hidroxila (OH) (hidroxiapatita) (Toledo, 2001). A apatita também pode apresentar substituição do grupo fosfato por um grupo carbonato, formando a carbonato-fluorapatita $(Ca,Na,Mg)_{10}(PO_4,CO_3)_6(F,OH)_2$ ou carbonato-hidroxiapatita $Ca_{10}(PO_4,CO_3)(OH)_2$ (Chien, 1993; Toledo, 2001; Zapata, 2004). Normalmente, nenhuma destas composições simplificadas é observada na apatita natural, devido às inúmeras substituições ocasionadas pela complexa formação desses minerais.

Os minerais apatíticos formaram-se sob diferentes regimes geológicos, além de terem sofrido transformações por intemperismo, lixiviação, reprecipitação e diversas contaminações, o que justifica a diversidade mineralógica deste material (Toledo, 2001). Os depósitos naturais podem ser divididos principalmente em duas categorias: os depósitos sedimentares ou metamórficos e os depósitos ígneos ou magmáticos. Os depósitos sedimentares possuem uma origem complexa e variada, constituem aproximadamente 85 % da oferta mundial e, estão localizados principalmente nos Estados Unidos, sudeste do México, Marrocos, noroeste do Saara e Oriente Médio (Toledo, 2001). Neste tipo de depósito, os minerais predominantes são apatitas com alto grau de substituição isomórfica de fosfato por carbonato e este tipo de mineral é muitas vezes denominado de francolitas ou fosforitas (Chien, 1993; Toledo, 2001). Já os depósitos ígneos, ou magmáticos, estão presentes principalmente na África do Sul, Rússia, Finlândia e Brasil, representando aproximadamente 15 % das reservas mundiais. O principal tipo de apatita associado com este depósito é a fluorapatita com baixa substituição isomórfica (Toledo, 2001). No Brasil aproximadamente 95% das reservas de RFs são de origem ígnea (Loureiro et al., 2008).

As RFs também podem ser classificadas em fosfatos "duros" e "moles". Os fosfatos "duros" são apatitas que não têm ou apresentam baixa substituição isomórfica, geralmente de origem ígnea. Este tipo de fosfato constitui a maioria das reservas de RFs brasileiras (Toledo, 2001). Os fosfatos "moles", geralmente de origem sedimentar, são apatitas de alto grau de substituição isomórfica do fosfato por carbonato, resultando em um cristal imperfeito, poroso, de alta área superficial. Geralmente este tipo de fosfato apresenta uma maior solubilização que os fosfatos "duros" (Chien, 1993).

Sendo assim, a grande diversidade de RFs existente é devido principalmente à sua complexa formação. A caracterização física e química é essencial para descobrir o tipo de apatita e o grau de substituição isomórfica. Geralmente fosfatos de baixa substituição isomórfica (duros) são de difícil solubilização, o que contribui para aumentar os custos de processamento na produção dos fertilizantes fosfatados. Essas caracterizações também são importantes para desenvolver estudos de solubilização via processo biotecnológico.

1.3. Fertilizantes químicos fosfatados e impactos ambientais

A produção tradicional de fertilizantes fosfatados é baseada no processamento químico da rocha fosfática para obter fósforo inorgânico solúvel. Fertilizantes fosfatados também

podem ser definidos como o produto resultante do tratamento químico do concentrado fosfático, que apresenta parte do P_2O_5 solúvel disponível para as plantas e que pode ter ainda outros constituintes nutrientes ou micronutrientes agregados, além de estar com a forma e tamanho adequados para sua utilização na agricultura (CONAMA, 2011). Os principais produtos originados desse processo são fosfato monoamônico (MAP); fosfato diamônico (DAP); superfosfato triplo (TSP) e superfosfato simples (SSP).

O conjunto de operações unitárias no processo de produção de fertilizantes fosfatados envolve um alto consumo de energia, elevado gasto de ácido sulfúrico e ácido fosfórico assim como a liberação de contaminantes no efluente gasoso, dentre os quais destacam-se material particulado, tetrafluoreto de silício (SiF_4), fluoreto de hidrogênio (HF), amônia (NH_3), óxidos de enxofre (SO_x) e óxidos de nitrogênio (NO_x), além da obtenção de subprodutos tóxicos indesejáveis (CONAMA, 2011). De acordo com a Organização Mundial da Saúde, estudos sobre os efeitos destes resíduos gasosos evidenciam o aumento da mortalidade e da morbidade na população exposta aos poluentes gerados pela indústria de fertilizantes (CONAMA, 2011). A geração de subprodutos indesejáveis como o fosfogesso resultante do processo de acidificação também é um problema que gera poluição ambiental devido ao baixo consumo desse material (Canovas et al., 2018; Tayibi et al., 2009).

Além desses problemas, a aplicação massiva de fertilizantes químicos solúveis como o super fosfato simples e triplo para promover o crescimento de diversas culturas, tem resultado na poluição dos solos e corpos hídricos, levando a problemas como eutrofização de corpos d'água próximo a áreas agrícolas (Vassilev et al., 2015). Efeitos indiretos incluem a elevada proliferação de algas e a mortalidade dos peixes devido à redução do nível de oxigênio (Conley et al., 2009; Nemery & Garnier, 2016). Frente a estes problemas, existe uma tendência global em adotar práticas de agricultura sustentável e a utilização de biofertilizantes é uma alternativa que vem sendo proposta em diversas conferências ambientais (Kontic and Kontic, 2012).

1.4. Microrganismos solubilizantes de fosfatos e mecanismos

O solo é um sistema que permite o desenvolvimento de diversos microrganismos (MOs) e muitos deles são capazes de metabolizar e solubilizar formas insolúveis de fosfatos inorgânicos presentes no solo (Krishnaraj and Dahale, 2014). Esta capacidade é conhecida desde o início do século XX, quando pesquisas reportaram a importância dos microrganismos

para o ciclo do P (Goldstein et al., 1993). Desde então, muitos estudos têm sido conduzidos para identificar e isolar microrganismos solubilizantes de fosfatos inorgânicos a partir de amostras de solos utilizando técnicas de screening (Hamdali et al., 2008; Mendes et al., 2014a; Nautiyal, 1999). Embora existam muitos microrganismos solubilizantes de fosfatos, poucos são eficazes, destacando-se os gêneros de bactérias *Bacillus*, *Pseudomonas* e *Agrobacterium* e de fungos *Aspergillus* e *Penicillium* (Krishnaraj and Dahale, 2014). O tipo de fosfato que cada microrganismo consegue solubilizar pode variar bastante entre as diferentes culturas. A grande maioria pode solubilizar fosfato de cálcio ($Ca_3(PO_4)_2$), entretanto poucos MOs conseguem solubilizar fosfato de alumínio ($AlPO_4$) e ferro ($FePO_4$) (Mendes et al., 2014a). A eficiência de solubilização ainda é menor para RFs devido à complexidade e a diversidade da constituição mineralógica (Mendes et al., 2014a).

O principal mecanismo de solubilização de fosfatos inorgânicos ocorre pela habilidade bioquímica que alguns microrganismos têm de produzir metabólicos de baixa massa molecular como ácidos orgânicos (Kpomblekoua and Tabatabai, 1994; Nahas, 1996; Nautiyal, 1999). Nesse contexto, a solubilização e a produção dos ácidos orgânicos ocorre simultaneamente com a redução do pH. Os grupos hidroxila e carboxila dos ácidos orgânicos podem sequestrar os cátions (principalmente o cálcio) ligados ao fosfato e, posteriormente, converter o fosfato insolúvel em formas solúveis (Kpomblekoua and Tabatabai, 1994). Deste modo, alguns ácidos orgânicos como os ácidos glucônico, oxálico e, principalmente, o cítrico tem sido reportados como bons agentes quelantes e, deste modo podem agir solubilizando fontes de fosfato (Illmer and Schinner, 1995; Kpomblekoua and Tabatabai, 1994; Mendes et al., 2014a). Entretanto, como as fontes de fosfatos minerais tem diferentes origens, são muito heterogêneas e apresentam diferentes propriedades físico-químicas, os ácidos orgânicos podem ter ação diferente dependendo do tipo de mineral fosfatado.

A solubilização também pode acontecer por outros mecanismos, porém o efeito desses outros mecanismos tem baixo impacto na solubilização quando comparado à ação dos ácidos orgânicos. Enzimas como fitase e fosfatase podem ser produzidas por microrganismos como *A. niger* e a partir de reações enzimáticas podem catalisar a solubilização de fosfatos inorgânicos (Vassilev et al., 2007). A solubilização também pode acontecer pela acidificação do meio devido ao lançamento de prótons (H^+) pela enzima ATPase durante a respiração celular (Illmer and Schinner, 1995). Alguns microrganismos, como as bactérias do gênero *Thiobacillus,* podem promover a solubilização por métodos indiretos, uma vez que essas bactérias podem oxidar o enxofre elementar a sulfato que gera acidez no meio e promove a

solubilização do fosfato (Avdalovic et al., 2015; Calle-Castaneda et al., 2018). Entretanto, para isso é necessário adicionar enxofre elementar, e o processo de oxidação é lento e muitas vezes não é suficiente para promover uma solubilização significativa da RF. No solo, a solubilização do fosfato também pode ocorrer por ácidos húmicos e fúlvicos, que são produzidos durante a degradação de resíduos vegetais (Krishnaraj and Dahale, 2014). O mecanismo de solubilização é similar ao dos ácidos orgânicos, no qual os grupos hidroxila e carboxila presentes nos ácidos húmicos e fúlvico sequestram cátions ligados ao fosfato e, posteriormente, convertem o fosfato insolúvel para forma solúvel.

Dessa forma, a seleção de um microrganismo eficiente em solubilizar diferentes fontes de fosfatos e a compreensão do mecanismo de solubilização são etapas fundamentais para obtenção de um processo eficiente. Entretanto, fungos filamentosos como o *Aspergillus. niger* são reconhecidos pela alta taxa de produção de ácidos orgânicos (Papagianni, 2007) e podem ser mais eficientes que as bactérias para promover a solubilização da RF (Mendes et al. 2015; de Oliveira et al. 2015). A forma de cultivo também pode interferir na eficiência do processo. Nesse contexto, o cultivo destes microrganismos pode ser conduzido por suspensão aerada (cultivo submerso, CSm) ou meio sólido (cultivo em estado sólido, CES). Na sequência, estão comentados alguns dos principais trabalhos de solubilização de fosfato via processo biotecnológico.

1.5. Estado da Arte: Produção de biofertilizantes fosfatados a partir de microrganismos solubilizadores

1.5.1. Cultivo submerso (CSm)

O CSm é o tipo de cultivo no qual as células de microrganismos são dispersas em um meio líquido gaseificado suplementado com nutrientes para promover o crescimento (Fazenda et al., 2008). Este tipo de cultivo apresenta grande potencial e vem sendo utilizado para solubilizar RF. O CSm apresenta vantagens principalmente na instrumentação e controle do bioprocesso, o que contribui para aumentar a eficiência de solubilização da RF, além de versatilidade na operação utilizando biorreatores (Fazenda et al., 2008). Nesse contexto, alguns trabalhos têm sido desenvolvidos utilizando biorreatores para aumentar a eficiência de solubilização das RFs. Ahuja e Souza (2009) cultivaram *Paecilomyces marquandii* (imobilizado em espuma de poliuretano) usando meio de cultivo Pikovskaya (modificado) para solubilizar RF Hirapur (fluorapatita, 10% P) em biorreator airlift (4 L). Após 48 h de cultivo obtiveram uma concentração no final do processo de 370 mg L^{-1} de P solúvel. O

processo foi repetido por seis bateladas e a eficiência foi mantida. A RF foi adicionada ao meio em uma concentração de 8 g L^{-1} e a fonte de carbono usada foi amido 10 g L^{-1}.

O uso de microrganismos encapsulados também é mencionado como possível estratégia para aumentar a eficiência de solubilização. Jain et al. (2010) estudaram a solubilização da RF (Fluorapatiata, Marrocos, 12,8% P) avaliando o efeito de *Aspergillus awamori* encapsulado e disperso no meio de cultivo. Os resultados mostraram que o cultivo do fungo encapsulado em alginato de cálcio (340 mg L^{-1} de P) e Agar (345 mg L^{-1} de P) proporcionou uma maior solubilização da RF em relação ao cultivo com células dispersas (291 mg L^{-1}). Trabalhos posteriores do mesmo grupo de pesquisa mostraram que os fungos encapsulados conservaram o mesmo rendimento após 5 bateladas (Jain et al., 2011). Este aumento na solubilização também foi observado em outros estudos que utilizaram fungos encapsulados do gênero *Aspergillus* (Vassilev et al., 1997; Vassilev et al., 2001; Vassilev et al., 2015; Vassileva et al., 1998). O aumento na solubilização é proporcionado pela maior produção de ácidos orgânicos nessas condições e, consequentemente, maior solubilização do fosfato (Vassilev and Vassileva, 1992).

A composição do meio de cultivo é outro fator determinante para otimizar qualquer processo fermentativo. Dessa forma, muitos estudos têm avaliado o efeito de diferentes fontes de carbono e nitrogênio sobre o processo de solubilização. Bhattacharya et al. (2015) estudou o efeito de diferentes fontes de carbono e nitrogênio no cultivo de *Aspergillus niger* para solubilizar fosfato de tricálcio. Os resultados mostraram que maltose, seguida de sacarose e glicose, foram as fontes de carbono que proporcionaram maior solubilização. Entre as melhores fontes de nitrogênio se destacam o sulfato de amônio e nitrato de amônio. Srividya e Pooja (2009) observaram a mesma relação de eficiência entre as fontes de carbono. Por outro lado, Saber et al. (2009) reportaram a frutose seguida da glicose e xilose como melhores fontes de carbono. Barosso et al. (2006) verificaram que a solubilização do fosfato de cálcio foi aumentada na presença de fontes de carbono como: manitol, maltose, galactose e glicose. Entretanto, quando o fosfato de cálcio foi substituído por fosfato de ferro, as fontes de carbono que mais favoreceram a solubilização foram galactose, sacarose e maltose. Estas diferenças comportamentais têm sido constantemente relatadas na literatura principalmente em relação à fonte de carbono. De forma geral, monossacarídeos e alguns dissacarídeos (sacarose e maltose) são constantemente reportados como boas fontes de carbono, enquanto fontes de nitrogênio amoniacal proporcionam maior produção de ácidos orgânicos e solubilização de fosfatos.

A suplementação adequada de minerais no meio de cultivo também é muito importante para qualquer processo fermentativo. Geralmente meios de cultivo para solubilização de RF tem baixa concentração de minerais (Nautiyal, 1999; Srividya et al., 2009), principalmente Fe, Al e Mn, que exercem forte inibição na produção de ácidos orgânicos (Papagianni, 2007), principal mecanismo de solubilização das RFs (Fontes and Weed, 1996). Entretanto, recentemente Oliveira et al. (2015) avaliaram a influência da suplementação dos minerais em meio de cultivo definido Czapek's. Os resultados mostraram que a adição dos minerais não é necessária pois como as RFs possuem diversos minerais integrados à sua estrutura, os quais são solubilizados simultaneamente ao longo da solubilização do fósforo, fornecendo as quantidades mínimas necessárias para suprir as funções básicas do fungo.

Também em relação ao meio de cultivo, durante a solubilização do P outros elementos químicos presentes na RF também são solubilizados e passam a acumular no meio e alguns desses elementos podem exercer efeito inibitório na solubilização. Nesse contexto, Mendes et al. (2013) estudaram a solubilização da RF Araxá (Fluorapatita, Brasil, 13% P) por CSm com *Aspergillus niger* utilizando meio sintético NBRIP (Nautiyal, 1999) suplementado com 3 g L^{-1} de RF. Este tipo de RF, por ser uma fluorapatita, possui uma elevada quantidade de fluor (F) presente na composição química e a caracterização físico-química mostrou, além do F, a presença de 52 elementos químicos. A solubilização do P foi monitorada juntamente com os dos outros 53 elementos químicos por 240 h e amostras foram coletadas a cada 12 h. Os resultados mostraram forte inibição por íons F^{-} na solubilização da RF, no crescimento do celular e na produção de ácido cítrico. Esta inibição também foi reportada posteriormente por Silva et al. (2014), sendo que outros íons como Fe, Al, Mn e Cu também provocaram inibição moderada. Entretanto, apenas o Sr proporcionou um efeito positivo na solubilização de RF. Mendes et al. (2014b) estudaram formas de adsorver íons F^{-}, utilizando alumina e biochar e os resultados mostraram que a biochar foi mais eficiente para adsorver F^{-}, aumentando a solubilização da RF.

O extrato líquido obtido da solubilização via cultivo submerso também já foi avaliado no sistema solo-planta usando sistema de fertirrigação (Mendes et al., 2017; Vassilev et al., 2017). Os resultados têm mostrado aumento do crescimento e absorção de fósforo pelas plantas.

1.5.2. Cultivo em estado sólido (CES)

O CES também é muito utilizado para produção de biofertilizantes, sendo que neste tipo de cultivo o substrato sólido umedecido é suplementado com nutrientes, o qual é empregado para sustentar o crescimento e metabolismo do microrganismo (Stanton, 2002). O cultivo em CES simula as condições de crescimento mais favoráveis presentes no habitat natural do microrganismo (Stanton, 2002) e, muitas vezes, proporciona uma maior solubilização da RF (Mendes et al., 2015). Uma importante vantagem da CES é a possibilidade de utilizar resíduos agroindustriais como fonte de carbono e energia para crescimento do microrganismo (Farinas, 2015).

Dentre os estudos de CES para solubilização de fosfato, Vassilev et al. (1995) reportaram o cultivo *Aspergillus niger* para solubilizar RF (fluorapatita, Marrocos, 12,8% P) em três diferentes tipos de substratos. Os resultados mostraram uma eficiência de 69% (292 mg L^{-1} de P solúvel) de solubilização em resíduo de casca beterraba suplementado com meio Czapek após 10 dias de cultivo. Vassielv et al. (1998) utilizaram as mesmas condições de cultivo e RF, porém como substrato foi usado torta de oliva (resíduo da extração do óleo de oliva) e obtiveram uma solubilização com eficiência de 42% (168 mg L^{-1} de P solúvel). Ogbo (2010) também estudou a produção de biofertilizante a partir da solubilização da RF, comparando *Aspergillus niger* e *Aspergillus fumigatus* isolados a partir da casca da mandioca em decomposição. O meio para CES foi composto de 1% de mandioca crua como amido, 3% de excrementos de aves e 96% casca seca de mandioca. O processo fermentativo durou 14 dias e foi conduzido com três tipos de fosfato. Os resultados mostraram que *Aspergillus fumigatus* obteve 41 mg L^{-1}, 10 mg L^{-1} e 4 mg L^{-1} enquanto *Aspergillus niger* 47 mg L^{-1}, 10 mg L^{-1} e 6 mg L^{-1}, respectivamente, de fósforo solúvel a partir de fosfato de tricálcio, fosfato de alumínio e fosfato de ferro. Os resultados de solubilização de ambos os fungos foram similares, entretanto quando comparados com outros estudos da literatura podem ser considerados baixos (Vassilev et al., 1995; 1998), o que pode ser atribuído ao tipo de substrato utilizado.

Mendes et al. (2013) utilizaram um planejamento experimental para avaliar a influência da fonte de carbono (sacarose) e da fonte de nitrogênio (sulfato de amônia) como suplementação para um meio composto por bagaço de cana, além de avaliar a dosagem máxima de RF. O efeito das variáveis foi avaliado frente à solubilização de duas RFs (Catalão, 14,8% P e Araxá 14% P, Brasil) por 4 diferentes fungos. Entre os fungos analisados, o *Aspergillus niger* conseguiu solubilizar mais fosfato para as duas RFs. Os resultados do

planejamento experimental demonstraram que o aumento na quantidade de sulfato de amônio diminuía a solubilização para o fungo *A. niger*, porém para os outros fungos a solubilização aumentava. Tanto o aumento na quantidade de sacarose como de RF suplementada favoreceu a solubilização para todos os fungos estudados.

Mendes et al. (2015) estudaram a solubilização de RF Araxá por CES a partir do cultivo de *Aspergillus niger*. Após otimização, obtiveram uma formulação com 856 mg de biochar (proporciona principalmente a adsorção de F^-), 250 mg de RF e 270 mg de sacarose e 6,2 ml de água por grama de bagaço de cana, e nessas condições conseguiram 8,6 mg de P solúvel. Após o processo de solubilização, foi realizada a secagem do biofertilizante a 70 °C, 350 °C e 500 °C. A secagem do material proporcionou uma redução de massa de 64% e concentrou o P_{Total} para 4,4% a 350 °C, enquanto uma redução de massa de 77% e P_{Total} de 7,4% a 500 °C foram observados. O pH mudou para 3,5 (70 °C), 7,6 (350 °C) e 9,5 (500 °C). Posteriormente foram realizados bioensaios em casa de vegetação e os resultados foram comparados aos do fertilizante comercial superfosfato triplo (TSP). Todas as formulações de biofertilizantes propostas proporcionaram maior crescimento e maior absorção de P pelas plantas quando comparadas com o controle (sem fertilização) e com o ensaio no qual foi apenas adicionado a RF. Entre as formulações de biofertilizante, o melhor rendimento foi obtido quando seco a 500 °C, sendo que este rendimento foi equivale a 60 % do TSP.

1.5.3. Novas alternativas de produtos

A grande maioria dos trabalhos de solubilização de RFs concentram-se nas rotas clássicas de cultivo microbiano onde a solubilização acontece em um sistema fechado e depois o material é aplicado ao campo (Mendes et al., 2017; Vassilev et al., 2017). Existem trabalhos que promovem o desenvolvimento de formulações por CSm e CES e posteriormente estas formulações com alta concentração de microrganismos é lançado ao solo juntamente com a RF. Entretanto, a eficiência desse processo é baixa devido à alta mortalidade dos microrganismos no solo e baixo contato entre microrganismo e RF. Uma alternativa é realizar o encapsulamento do microrganismo em matrizes como alginato e quitosa, para aumentar a resitencia do microrganismo a oscilações climáticas e choques mecânicos para posterior adição ao solo. Porém, o contato entre microrganismo e RF ainda é baixo resultando na baixa solubilização do P (Jain et al., 2010; Schoebitz et al., 2013; Vassilev et al., 2017; Vassilev et al., 2015). Apenas recentemente Mattiello et al. (2017) desenvolveram uma pastilha à base de

enxofre elementar, oxido de zinco e Na-bentonita inoculada com células da bactéria *Acidithiobacillus thiooxidans*, e mostraram que as bactérias inoculadas promoveram aumento da oxidação do enxofre e a acidez gerada promoveu a solubilização do óxido de zinco quando acicionado ao solo. Portanto, esse estudo mostra que é possível desenvolver materiais fertilizantes bioativados por microrganismos, o que inaugura uma nova rota de desenvolvimento de fertilizantes granular com aplicação de microrganismo solubilizadores para aumentar a solubilidade de fontes de nutrientes de baixa solubilidade, que é uma interessante estratégia ainda pouco explorada.

1.6. Objetivos

1.6.1. Objetivo geral

O objetivo deste trabalho foi desenvolver estratégias de processo para aumentar a solubilização de rochas fosfáticas e minérios de baixa solubilidade pela ação de microrganismos via cultivo microbiano e propor novas alternativas de produtos fertilizantes baseados na ação biológica.

1.6.2. Objetivos específicos

Para atender o objetivo geral, fez-se necessário o cumprimento das seguintes etapas:

1. Selecionar os microrganismos mais eficientes na solubilização de rocha fosfática;

2. Avaliar da influência do tamanho de partícula no processo de solubilização com diferentes tipos de rochas fosfáticas;

3. Avaliar a influência do teor de sólidos no processo de solubilização e desenvolvimento de estratégias para aumentar a solubilidade da rocha fosfática usando uma alta concentração de sólidos;

4. Avaliar a influência de diferentes ácidos orgânicos na solubilização de diferentes rochas fosfáticas;

5. Desenvolver de novas alternativas de produtos para aumentar a solubilidade de rochas fosfática e de outras fontes de nutrientes de baixa solubilidade a partir a ação de microrganismos solubilizadores;

6. Avaliar a eficácia dos biofertilizantes propostos no sistema solo-planta em casa de vegetação.

Capítulo 2

"A novel combined mechanical-biological approach to improve rock phosphate solubilization"

Artigo publicado na revista International Journal of Mineral Processing, volume 161, páginas 50-58, ano 2017.

O artigo apresentado propõe uma nova estratégia combinando os processos mecânico e biológico para aumentar a solubilidade da rocha fosfática. A alternativa para acelerar o processo de solubilização foi promover a ativação mecânica da rocha fosfática para reduzir o tamanho de partícula. Dessa forma, a solubilidade pode ser aumentada como consequência da maior área superficial juntamente com a alteração local do pH, causada pela liberação de ácidos orgânicos produzidos durante o cultivo. Uma etapa inicial foi realizada para seleção do microrganismo com maior potencial para solubilizar fosfatos minerais. Caracterizações detalhadas desta rocha foram realizadas mostrando que se trata de uma rocha fosfática de origem sedimentar com um teor de P_2O_5 em torno de 30%. Este artigo se refere aos objetivos específicos 1 e 2: (1) Selecionar microrganismos mais eficientes para solubilizar fosfato de rocha; (2) Avaliar a influência do tamanho de partícula da rocha fosfática no processo de solubilização. Os resultados mostraram que a estratégia proposta aumentou em 60% a solubilidade da rocha quando utilizado o cultivo submerso e 115% quando utilizado o cultivo em estado sólido do fungo filamentoso *A. niger*. Esta estratégia pode contribuir para avaços no desenvolvimento de fertilizantes via solubilização biológica buscando uma agricultura sustentável.

Abstract

Phosphate chemical fertilizers are extensively used to improve agricultural productivity. However, the production of these fertilizers is expensive and can cause environmental damage. Alternatively, microbial solubilization of rock phosphate (RP) is a potential strategy for obtaining biofertilizers. This paper proposes the use of a novel combined mechanical-biological approach to produce soluble phosphate by cultivation of a selected strain of *Aspergillus niger* using RP with particle sizes in the nanometric range. The effect of Bayóvar RP particle size on phosphate solubilization was analyzed for cultivations under submerged (SmF) and solid-state fermentation (SSF). The RP particle size played a key role in phosphate solubilization, with gains of up to 60% for SmF and 115% for SSF. The mechanical treatment of RP, combined with the biological cultivation process, resulted in an optimized solubilization of P, and it was shown that even short periods of milling could be highly effective. This proposed strategy could contribute to advances in the current bio-based economy and assist future developments in large-scale industrial production of biofertilizers.

1. Introduction

The manufacture of phosphate fertilizers constitutes one of the largest markets for fertilizers in the agribusiness field, as phosphorus (P) is one of the main limiting nutrients for plant growth. Global consumption of processed phosphate fertilizers in 2013/2014 was 40.3 Mt P_2O_5, and an annual increase of 1.5-2% is expected during the next five years (Heffer, 2015). Although phosphorus is abundant in many soil types, most of the P is not usually readily available to plants, due to leaching and/or immobilization. The reason of decrease in P availability is the formation of less soluble Fe, Al or Ca phosphates due to contact with phosphate anions in soil (Fontes & Weed, 1996; Mendes et al., 2014). As a result, frequent applications of soluble inorganic forms of P are required to ensure satisfactory plant growth. Such applications of P to the soil are usually made in the form of chemical fertilizers. However, traditional P fertilizer production is based on chemical processing of insoluble high-grade mineral phosphate ore, which includes an energy-intensive treatment with sulfuric acid at high temperature, in a process that is expensive and can potentially lead to environmental damage (Vassilev et al., 2006; Vassilev & Vassileva, 2003).

The direct application of rock phosphate (RP) to the soil could be one way to minimize pollution and reduce the costs of chemical treatment. However, it is widely accepted that direct application of RP is not feasible, mainly due to limitations in terms of soil characteristics and the long period of time required for the P to become available (Vassilev & Vassileva, 2003). A potential strategy to accelerate this process is to reduce the RP particle size to the nanometric range, where the solubility increases as a consequence of the greater surface area (Enustun & Turkevich, 1960). Although this strategy has been shown to be effective for some phosphate ores (Lim et al., 2003; Tonsuaadu et al., 2011), the associated energy demand can be high, making the process not economically viable. Therefore, there is a need for the development of novel strategies associated with particle size reduction that could improve the solubilization of RP, such as local pH changes caused by organic acids released during microbial growth.

There has been renewed interest in manipulating RP by means of biotechnological processes, with emphasis on the use of P-solubilizing microorganisms (PSMs) (Vassilev et al., 2015). The P-solubilizing activity of PSMs is determined by their ability to produce and release metabolites such as organic acids that, through their hydroxyl and carboxyl groups, chelate the cations (mainly calcium) bound to phosphate, with the latter being converted into soluble forms (Kpomblekoua & Tabatabai, 1994). Although both bacterial and fungal PSMs

have been reported (Chang & Yang, 2009), the aerobic fungi are especially recognized for their high rates of organic acid production (Mendes et al., 2014).

Besides finding a suitable PSM, it is necessary to identify the most appropriate cultivation method for accessing all of the phosphate present in RP. PSM cultures can be performed as aerated suspensions (submerged fermentation - SmF), or using solid media (solid-state fermentation - SSF). Although SmF has well-known industrial-scale advantages related to bioreactor instrumentation and process control, SSF can be particularly advantageous for the cultivation of filamentous fungi, because it simulates the natural habitat of these microorganisms (Farinas, 2015). From the environmental perspective, an important advantage of SSF is the ability to use agro-industrial wastes as low-cost sources of carbon and energy for microorganism growth and product formation. Recent studies have described the potential of using microbial cultivations to improve phosphate solubilization under both SmF (de Oliveira et al., 2015) and SSF (Mendes et al., 2015; Mendes et al., 2013b; Ogbo, 2010), employing different rock phosphate sources, fungal strains, and process conditions. A recent comprehensive review has gathered a large amount of information on strategies to obtain biofertilizers by microbial cultivation (Vassilev et al., 2015). However, to the best of our knowledge, there have been no previous studies exploiting the potential of a reduced particle size to improve the solubilization of RP during microbial cultivation for biofertilizer production.

The present work proposes a novel combined mechanical-biological strategy for the production of soluble phosphate. The alternative approach employed to accelerate the P solubilization process involved reducing the RP particle size to the nanometric range, so that phosphate solubility was increased because of the greater surface area and the local change of pH caused by the release of organic acids during fungal growth. A preliminary screening of fungal strains was carried out in order to select the PSM with greatest potential. The effect of particle size on P solubilization by a selected strain of *A. niger* cultivated under SSF and SmF processes was then evaluated using Bayóvar rock phosphate (BRP) as a model material, since this rock contains a significant amount of phosphatic phase (around 33% of P_2O_5). A detailed physical-chemical characterization of the Bayóvar rock was performed (using X-ray diffraction, X-ray fluorescence, field emission scanning electron microscopy, and total surface area measurements), and the kinetics of P solubilization were assessed for each cultivation method.

2. Materials and Methods

2.1. Bayóvar rock phosphate (BRP)

2.1.1. Milling

The BRP powders were prepared by milling a commercial sample of BRP (from Sechura, Peru) for periods of 2.5, 5, 10, 20, 40, 80, and 160 min, using an orbital mill (Servitech CT 241, 0.5 HP) consisting of a porcelain jar (1000 mL) and alumina balls.

2.1.2. Physical-chemical characterization

X-ray diffraction (XRD) analyses were performed using a LabX XRD-6000 diffractrometer (Shimadzu, Japan) operated with Cu-Kα radiation ($\lambda = 1.54056$ Å), voltage of 30 kV, and current of 30 mA. The XRD patterns were recorded for 2θ from 5° to 55°, using a continuous scanning speed of 2° min^{-1}.

X-ray fluorescence (XRF) employing the lithium tetraborate fusion technique was used to analyze the ten most common oxides found in the ores. In addition, fluorine was determined by potentiometric method using a selective ion electrode (ISE). The carbon was determined using an inductive combustion furnace in an oxygen atmosphere with infrared spectroscopy determination.

The morphology of the BRP samples was observed by field emission gun scanning electron microscopy (FEG-SEM), using a JSM-6701F FEG microscope (JEOL, Japan). Images were acquired using an accelerating voltage of 2 kV and secondary electron detection.

Total surface area measurements of the BRP samples were made by isothermal nitrogen adsorption, using a Micrometritics ASAP 2020 instrument and the 5-point B.E.T. (Brunauer–Emmett–Teller) method.

The solubilities of the BRP materials were evaluated in 2% (w/w) citric acid solution. The solubilization experiments were carried out for 30 days in Falcon tubes. During the first 10 days of the experiment, daily samples were collected for determination of the degree of phosphate solubilization. For the following 10 days, samples were collected every two days, and for the last 10 days of the experiment, samples were taken every 5 days, giving 17 aliquots in total. The analysis of soluble phosphorus employed the colorimetric method described in Section 2.5.

2.2. Microorganisms

A preliminary screening of eight fungal strains was carried out to determine their capacity for phosphate solubilization. Isolates of *Aspergillus niger* C (BRMCTAA 82), *Aspergillus niger* 11T53A14 (BRMCTAA 20), and *Aspergillus niger* 3T5B8 were from the Embrapa Food Technology collection (Rio de Janeiro, Brazil). Isolates of *Penicillium pinophilum* F14 (BRMCMPC 483), *Talaromyces rotundus* F102 (BRMCMPC 485), *Talaromyces rotundus* F105 (BRMCMPC 486), *Penicillium pimiteouiense* F40 (BRMCMPC 941), and *Acremonium strictum* F87 (BRMCMPC 484) were from the Embrapa Maize and Sorghum collection (Sete Lagoas, MG, Brazil). Spore suspensions of the strains were kept at -18 °C and were activated by incubation on Petri dishes containing potato dextrose agar for 96 h at 30 °C. The spore concentrations were determined using a Neubauer chamber.

2.3. Submerged fermentation (SmF)

The nutrient medium used in the pre-culture and during P solubilization was adapted from the medium described by Pikovskaya (1948) and contained (w/v): glucose, 1%; $(NH_4)_2SO_4$, 0.5%; NaCl, 0.2%; $MgSO_4.7H_2O$, 0.1%; KCl, 0.2%; $MnSO_4.H_2O$, 0.002%; $FeSO_4.7H_2O$, 0.002%; yeast extract, 0.5%. Bayóvar RP was added at 0.5% as the source of insoluble phosphate. In the submerged fermentation process, the pre-culture was initiated in 500 mL Erlenmeyer flasks by adding a volume of spore suspension calculated to give a concentration of 1.2×10^7 spores per mL of the nutrient medium. A 100 mL volume of the nutrient medium was used in each experiment. The incubation was carried out for 48 h in an orbital shaker incubator, at 30 °C and 220 rpm. Solubilization of P was initiated by transferring a volume of pre-culture suspension corresponding to 10% (v/v) to the culture medium with the same composition, with agitation for 96 h in an orbital shaker incubator at 30 °C and 220 rpm. After this period, the resulting material was vacuum filtered using Whatman No. 1 filter paper and then centrifuged for 20 min at 12000 rpm and 20 °C. The clear supernatant was analyzed using the colorimetric method described in Section 2.5. The initial screening step carried out with the eight fungal strains described in Section 2.2 was performed using the same SmF procedure outlined above, except that the insoluble phosphate source was changed to tricalcium phosphate $(Ca_3(PO_4)_2)$. All experiments were carried out in triplicate, and the data were calculated as means ± standard deviations.

2.4. Solid-state fermentation (SSF)

Sugarcane bagasse (SB) ground to a particle size of 2 mm was used as a substrate for SSF. The experiments were carried out in 250 mL Erlenmeyer flasks, with 5 g of SB in each experiment and addition of BRP to a concentration of 5.0 g L^{-1}. After sterilization at 120 °C for 20 min, the medium containing SB and BRP was inoculated with $1.2x10^7$ spores per g of substrate. The initial moisture content of the treated SB was adjusted to 80% using the nutrient solution (Pikovskaya medium), and the fermentation was performed at 30 °C for 96 h. Analyses of the solid-state fermentation products were performed after homogenization of 5 g of sample in 50 mL of distilled water (shaking the suspension at 200 rpm for 60 min). The resulting material was vacuum-filtered using Whatman No. 1 filter paper and then centrifuged for 20 min at 12000 rpm and 20 °C. Soluble P in the clear supernatant was determined by the colorimetric method described in Section 2.5. All experiments were carried out in triplicate, and the data were calculated as means ± standard deviations.

2.5. Analytical method for determination of soluble P

The soluble P content was determined using a colorimetric method adapted from Murphy and Riley (1986). Briefly, a 5 mL aliquot of the clear supernatant sample was reacted with 2 mL of ascorbic acid solution (0.4 mol L^{-1}), 0.2 mL of citric acid (0.03 mol L^{-1}), and 2 mL of a reagent consisting of 25 mL of a sulfuric acid solution (4.7 mol L^{-1}), 5.5 mL of ammonium molybdate solution (0.08 mol L^{-1}), and 0.6 mL of antimony and potassium tartrate solution (0.05 mol L^{-1}). This mixture was reacted at 50 °C for 15 min, forming a phosphoantimonylmolybdenum blue complex. The concentration of the complex was determined by UV-Vis spectrometry at a wavelength of 880 nm.

3. Results and Discussion

3.1. Fungal strain screening

Figure 1 shows the final pH values (pH_{final}) of the media after SmF cultivations of the eight prospective fungal strains, together with the corresponding soluble phosphorus concentrations when tricalcium phosphate ($Ca_3(PO_4)_2$) was used as the source of insoluble phosphate. This compound was used in the fungal screening step because it is a source of

readily solubilized phosphate and is commonly used in growth media for the screening of PSMs (Nautiyal, 1999).

It was observed that the increase in the available phosphate concentration was accompanied by a decrease in the pH of the medium, compared to the non-inoculated medium used as a control. Hence, there was a significant negative correlation between the amount of soluble phosphorus and the pH_{final} of the cultivation media (r = -0.83). Gomes et al. (2014) studied the solubilization of rock phosphate using soil microorganisms isolated from the maize rhizosphere and obtained a similar negative correlation between pH_{final} and phosphate solubilization (r = -0.89 for Itafós rock phosphate and r = -0.82 for Araxá rock phosphate). Similar increases in the available phosphate concentration with decrease in the pH of the medium were reported by Nahas et al. (1996) and Mendes et al. (2014).
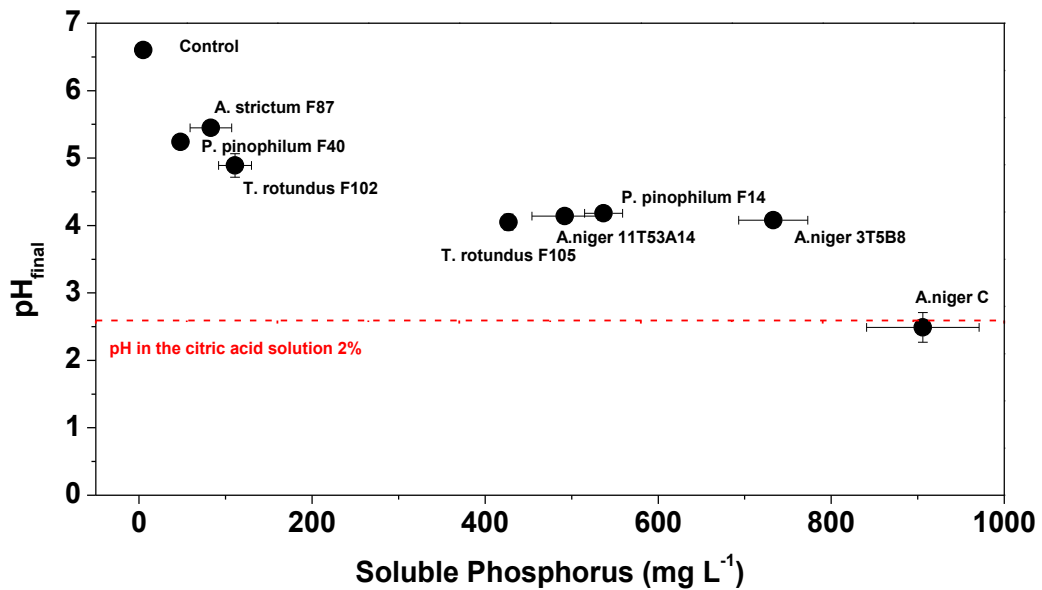
Figure 1. Final medium pH versus phosphate concentration solubilized by different microorganisms cultivated under submerged fermentation using Pikovskaya medium, 96 h, 30 °C, 220 rpm, $pH_{initial}$ 7, and 5 g L^{-1} of $Ca_3(PO_4)_2$. The dotted line in red represents the pH of a reference 2% citric acid solution.

The beneficial effect of a more acidic solution on the solubilization of minerals phosphates is the result of release of low molecular weight organic acids by the microorganisms (Nahas, 1996). These organic acids exhibit chelation and complexing

properties and can form soluble complexes with polyvalent cations from contact with rock or minerals, thus releasing phosphate to medium (Kpomblekoua & Tabatabai, 1994; Nahas, 1996; Salih et al., 1989). It is important to note that the type of organic acid affects the degree of phosphorus solubilization, and that solubilization can also occur due to the release of protons resulting from respiration or the assimilation of NH_4^+ present in the nutrient medium (Illmer & Schinner, 1995).

Among the eight strains of filamentous fungi evaluated here, the *Aspergillus niger* fungi showed the greatest potential for phosphate solubilization (Figure 1), with the highest rate of solubilization achieved using *A. niger* C. This strain produced an acidic environment that was comparable to that of a 2% (w/w) citric acid solution, which is the standard condition used in tests of phosphate solubilization or releasing from rock phosphate and chemical fertilizers (MAPA, 2013). The potential of strains of the filamentous fungus *A. niger* to solubilize phosphate has been reported previously. Mendes et al. (2014) evaluated 57 strains of *Penicillium* and *Aspergillus* isolated from soil samples and showed that P solubilization varied from 6 to 100%, with the *A. niger* strains presenting the highest levels of solubilization. Nevertheless, it is important to consider the potential of the other fungal species that presented lower acidification profiles, because these fungi could exhibit symbiotic effects or lead to the production of biostimulant substances when applied directly to the soil (Vassilev et al., 2015).

Based on the results of fungal screening using the solubilization of tricalcium phosphate in a liquid medium, the three most effective fungal strains (*A. niger* C, *A. niger* 3T5B8, and *A. niger* 11T53A14) were selected for further evaluation. Their potential to solubilize phosphorus during submerged (SmF) and solid-state fermentation (SSF) cultivation processes was studied using a Bayóvar rock phosphate (employed here as a model RP material).

3.2. Bayóvar rock phosphate (BRP) characterization

Detailed characterizations of the original and milled samples of BRP were carried out in order to understand the physical and chemical nature of the source of phosphate used in the fermentation processes. The crystalline phases of the BRP were assessed using X-ray diffractometry (Figure S1, Supplementary Material). The main crystalline phases observed were quartz (SiO_2, PDF2 diffractogram file #01-089-8935) and a phosphate phase corresponding to a type of apatite, fluorapatite ($Ca_{10}(PO_4)_6.F_2$, PDF2 diffractogram file #01-087-2462). In previous studies (Chien, 1993; Lim et al., 2003; McArthur, 1985; Zapata,

2004), using rock phosphates from the Sechura region of Peru, it was shown that the main mineralogical phase in this rock is a carbonate-fluorapatite composite, francolite ($Ca_{10}[(PO_4)_{6-x}(CO_3)_x]F_2$), which characteristically shows the substitution in crystal structure of some of the phosphate groups in the molecule by carbonate groups.

Table 1 displays the chemical analysis results for 10 oxides determined by X-ray fluorescence, fluorine determined by specific ion analysis, and carbon measured by infrared spectroscopy. These results confirmed the identification of the quartz phase observed using XRD, as well as the presence of a phosphate-rich phase. A simple mineralogical analysis showed that this phosphate phase represented about 75% (by mass) of the rock.

Table 1: Chemical analysis of the Bayóvar rock phosphate.

Oxide	% mass
SiO_2	4.42
Al_2O_3	0.96
Fe_2O_3	0.87
CaO	46.6
MgO	0.53
TiO_2	0.07
P_2O_5	30.73
Na_2O	1.98
K_2O	0.30
MnO	0.01
Loss on ignition	10.57
Total	97.04
F(*)	2.236
C(**)	2.23

(*) – Fluorine determined by specific ion analysis.
(**) – Carbon determined by infrared spectroscopy.

Physical characterization of the BRP samples obtained using the different milling times was performed by SEM. The micrographs showed that a longer milling time resulted in a smaller rock phosphate particle size (Figure 2), and that for a short milling time (such as 2.5

min), there was only deagglomeration of the particles. An effect on particle size only occurred after 5 min of grinding, when the first submicron particles were evident. These observations were supported by the surface area results (Figure 2), which showed that while the specific surface area of the sample milled for 2.5 min was approximately the same as that of the original sample, the values increased by more than 50% for the samples milled for 80 and 160 min. Previous studies of grinding mills (Lim et al., 2003; Tonsuaadu et al., 2011) have shown that each specific assembled system (mill and grinding medium) has an optimal time for obtaining the smallest particle size and consequently the greatest relative surface area. After this time, particle deformation can cause agglomeration, resulting in a constant or decreased total surface area available for adsorption.

The energy consumption for BRP grinding was calculated for all time according to the Bond Law (Table S1, Supplementary Material) (Sadrai et al., 2006; Thomas & Filippov, 1999). The results showed a high reduction in particle size in the first 10 min of grinding which was confirmed by increasing surface area. The energy consumption in 10 min of grinding (0.0549 HP) is about 1/3 smaller than energy consumed in 160 min (0.1489 HP), moreover, the particle size obtained at 10 min of grinding was as efficient as 160 min when evaluated the effect of BRP particle size on solubilization (Section 3.4). This shows that the grinding can be stopped in 10 min, avoiding energy expenditure. In the next step, evaluation was made of the effect of particle size on the BRP solubilization process in the presence of *A. niger* cultivated under SmF and SSF.
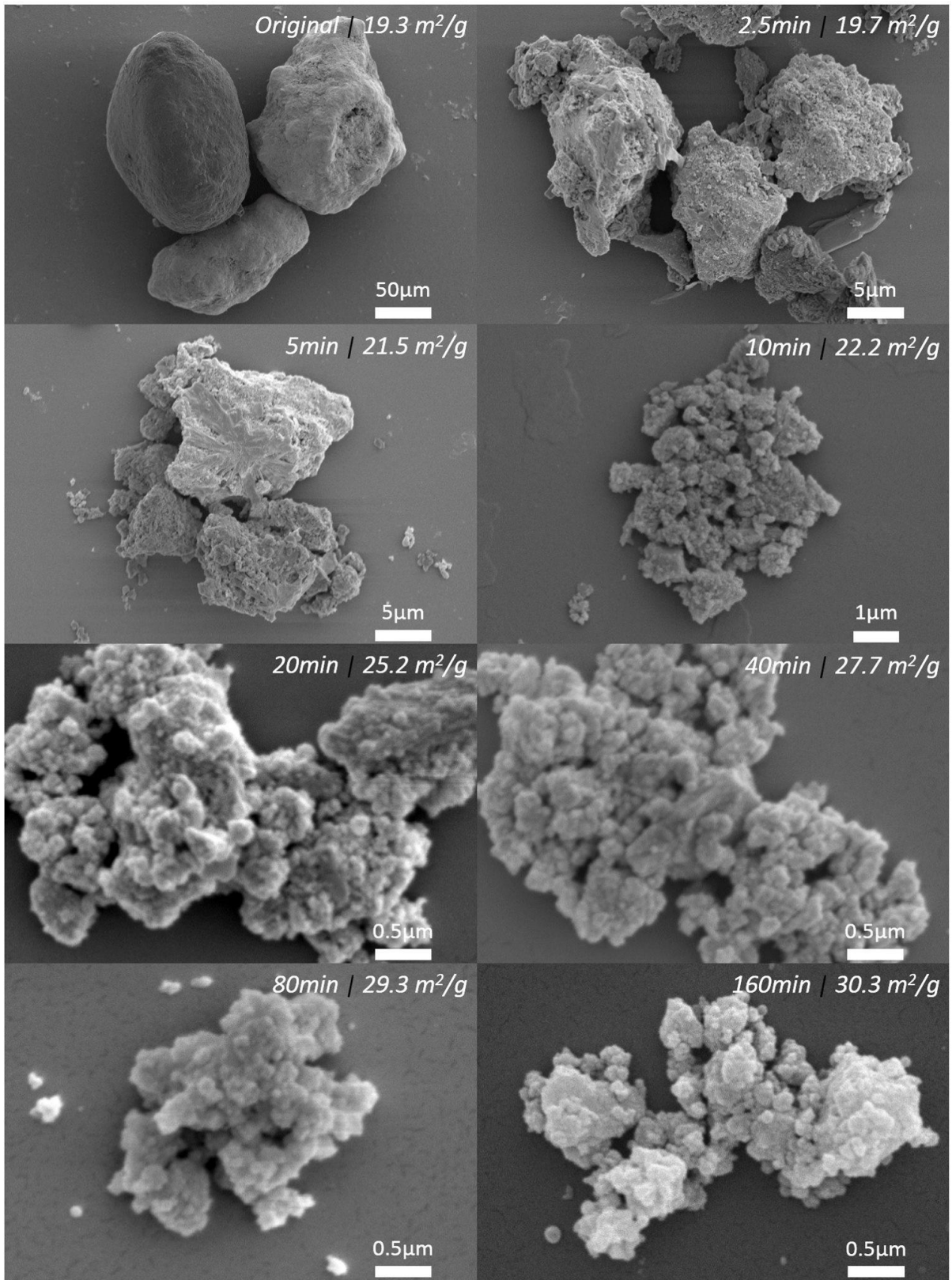
Figure 2. FEG-SEM micrographs and specific surface area of Bayóvar rock phosphate subjected to different milling times.

3.3. Bayóvar rock phosphate solubilization under SmF and SSF

Figure 3 shows the concentrations of solubilized phosphorus obtained using the three selected strains of *A. niger* cultivated under submerged fermentation (Figure 3a) and solid-state fermentation (Figure 3b), with the original Bayóvar RP (without milling, surface area of 19.3 m^2 g^{-1}) as the insoluble phosphate source. The solubilization patterns were the same as those obtained for the solubilization of $Ca_3(PO_4)_2$ using these three strains (Figure 1), indicating that the Bayóvar RP was suitable for use as a model of mineral phosphates.
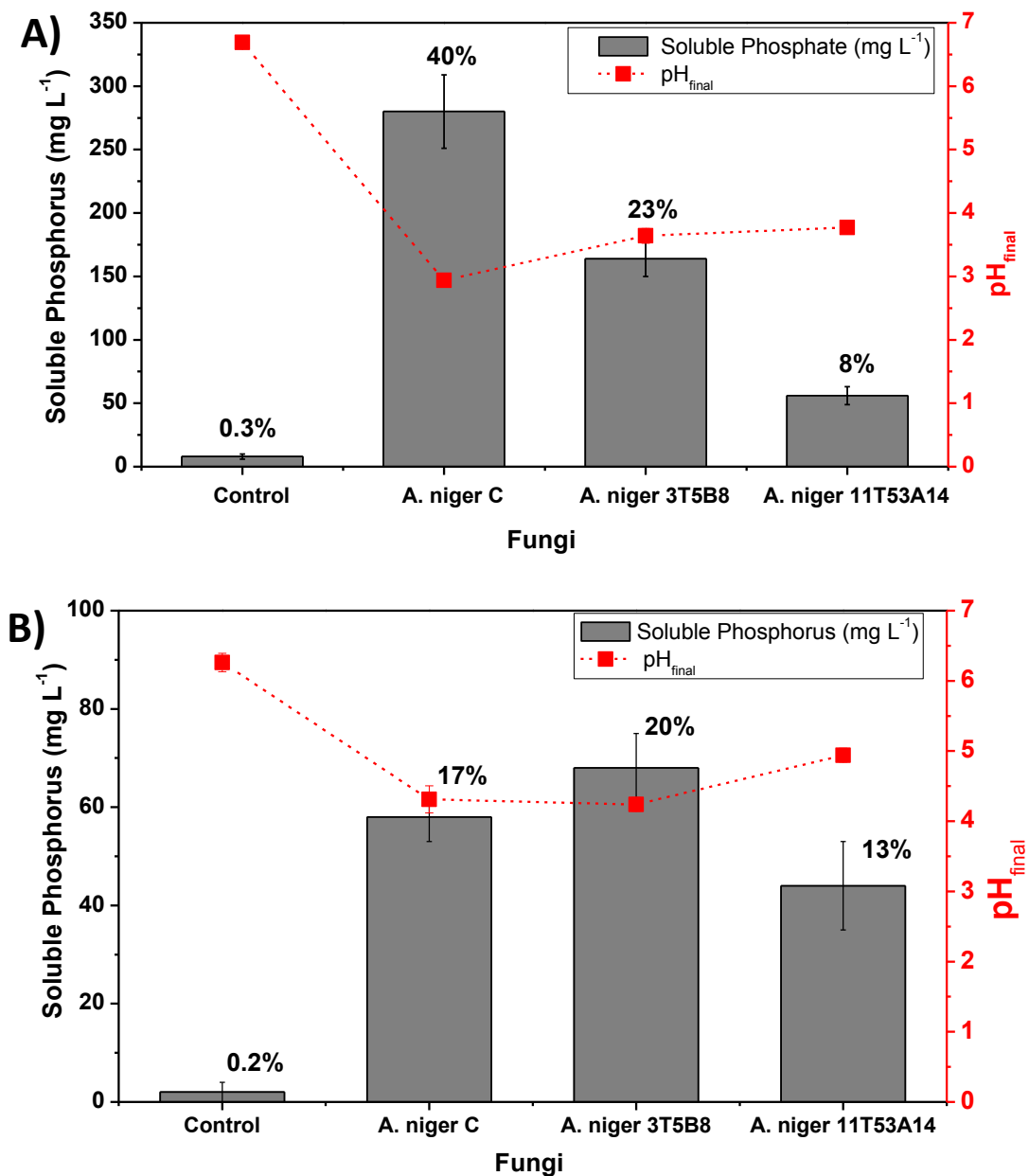
Figure 3. Phosphorus solubilization and pH$_{final}$ for three different strains of *Aspergillus niger*. **a)** Submerged fermentation using Pikovskaya medium, 96 h, 30 °C, 220 rpm, pH$_{initial}$ 7, and 5

g L^{-1} Bayóvar RP. **b)** Solid-state fermentation using sugarcane bagasse, 96 h, 30 °C, moisture 80%, pH$_{initial}$ 7, and 5 g L^{-1} Bayóvar RP.

For cultivations under SmF, the maximum solubilized phosphate concentration was 280 mg L^{-1} (corresponding to 40% solubilization), achieved using the *A. niger* C strain (Figure 3a), which also exhibited the lowest final pH. For SSF cultivations, the maximum solubilized phosphate concentration was 67 mg L^{-1} (20% solubilization), using the *A. niger* 3T5B8 strain (Figure 3b). However, for SSF the *A. niger* C strain also presented a very satisfactory solubilization of 58 mg L^{-1} (17% solubilization) (Figure 3b). Application of Tukey's test (95% confidence level) showed that there was no significant difference between the phosphate solubilization results achieved using these two *Aspergillus* strains under SSF. In both cases, the final culture pH remained above pH 4. However, there were significant differences between the P solubilizations obtained in the SmF and SSF cultivations. These differences were expected, because SmF provided greater contact between the particles and the acidic medium, compared to SSF. Consequently, there were greater differences among the strains in the case of SmF.

The results demonstrated the versatility of these microorganisms in solubilizing an insoluble source of phosphate under different cultivation systems. However, as expected, phosphate solubilization using the Bayóvar RP (Figure 3) was lower than using tricalcium phosphate (Figure 1). This was because the solubilization capacity of microorganisms varies according to the type of phosphate present. Tricalcium phosphate is a pure source of phosphate that is readily solubilized at pH around 4 (Bengtsson et al., 2007; Mendes et al., 2014), while Bayóvar RP is a highly insoluble phosphate source that has a more complex structure (fluorapatite, as found in the characterization assays) containing many chemical elements including Mn, Zn, Fe, and Al (Table 1). Thus RFs needs more strong conditions than tricalcium phosphate for solubilization, for example, a higher concentration of organic acid and lower pH (Mendes et al., 2014). In this way, organic acids production during the solubilization process as mentioned above is the main mechanism for RFs solubilization, because they promote the reduction of pH and can complex cations (metals) present in the RF that are released to the medium together with the phosphorus solubilization (Bengtsson et al., 2007). Fluoride present in fluorapatite rocks can also be released (Bengtsson et al., 2007) and it has a negative effect on biomass production and organic acid production, this causes a strong reduction on RP solubilization (Mendes et al., 2013a).

Based on these findings, the *A. niger* C strain was selected for further evaluation of the effect of the Bayóver RP particle size on phosphorus solubilization under SmF and SSF, since this fungal strain presented the greatest potential for phosphorus solubilization among the microorganisms tested.

3.4. Effect of rock phosphate particle size during SmF and SSF

The effect of the Bayóvar RP particle size on phosphorus solubilization was evaluated using the selected *A. niger* C strain cultivated under both SmF and SSF with BRP that had been milled for different times (Figure 4). It was observed that reduction of the RP particle size to the nanometric range could potentially increase the solubility of the phosphate due to the greater surface area.
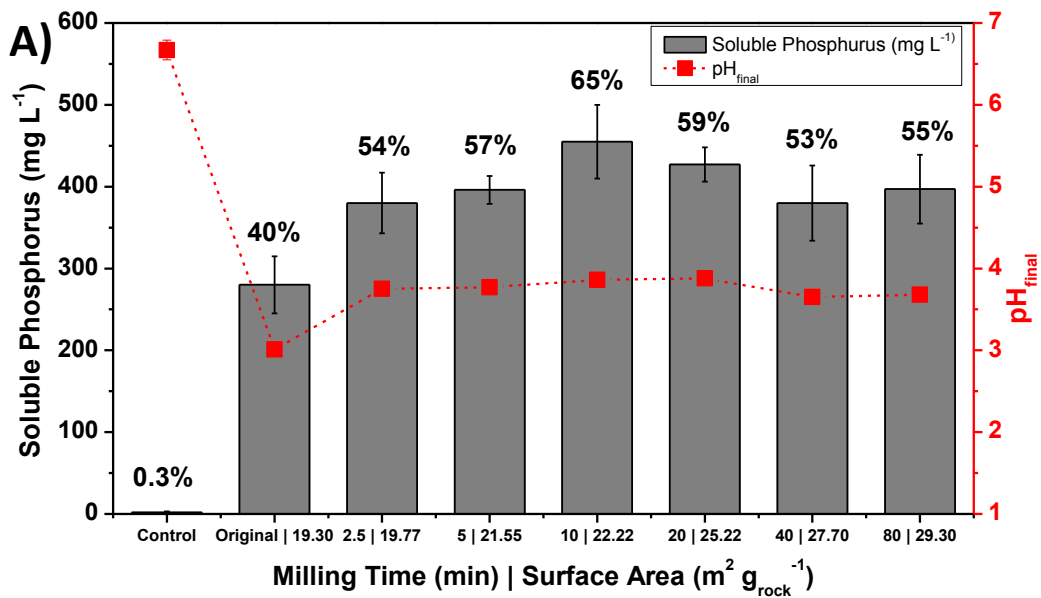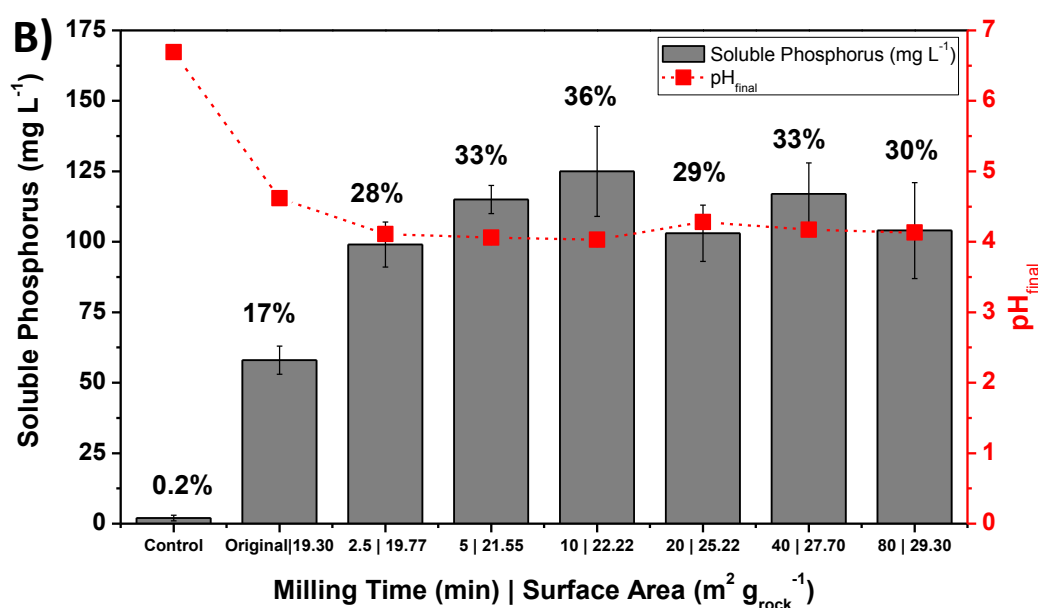
Figure 4. Phosphorus solubilization and pH_{final} using different particle sizes for *A. niger* C cultivation. **a)** Submerged fermentation using Pikovskaya medium, 96 h, 30 °C, 220 rpm, $pH_{initial}$ 7, and 5 g L^{-1} Bayóvar RP. **b)** Solid-state fermentation using sugarcane bagasse, 96 h, 30 °C, moisture 80%, $pH_{initial}$ 7, and 5 g L^{-1} Bayóvar RP.

Milling of the rock phosphate for 10 min increased the surface area (SA) from 19.30 to 22.22 m^2 g^{-1}, which under SmF resulted in a solubility increase of 60%, compared to the solubility achieved with the original rock particles. Soluble phosphorus values up to 450 mg L^{-1} (65% solubilization) were achieved using SmF and the RP particles obtained from the size reduction process (Figure 4a).

These results are very promising, compared to values reported previously. Vassileva et al. (1998) studied the solubilization of Moroccan RP (a sedimentary rock with solubility similar to that of Bayóvar) and obtained a soluble phosphorus concentration of 200 mg L^{-1} (52% solubilization) using *A. niger* cultivated under SmF. In other work, Vassilev et al. (2001) obtained 226 mg L^{-1} (55%) solubilization of Moroccan RP using *A. niger* under SmF. In both studies, the initial rock concentration was 3 g L^{-1} (with a particle size smaller than 1mm) and the solubilization efficiency was up to 55%. Here, use of an initial rock concentration of 5 g L^{-1} (with a particle size around 1μm) resulted in solubilization efficiency of up to 65%, showing that reduction of particle size was highly effective for improving the efficiency of solubilization of BRP during SmF cultivations.

When *A. niger* C was cultivated under SSF, a maximum phosphorus concentration of 125 mg L^{-1} (36% solubilization) was achieved using reduced size particles with SA of 22.22 m^2 g^{-1} (Figure 4b). This represented an increase in phosphorus solubility of around 115%, compared to the solubilization achieved using the original particle size.

The results therefore indicated that the manipulation of RP particle size could significantly improve phosphorus solubilization under both SmF and SSF. To the best of our knowledge, this is the first work in which RP particle size in the nanometric range has been considered as an important variable affecting the solubilization efficiency. An important finding was that for both SmF and SSF fermentation processes, the increase of surface area favored phosphorus solubilization up to a certain point, after which further increases were no longer effective (or even reduced the solubilization). A possible explanation for this was the agglomeration of particles of reduced sizes. In the case of SmF, the presence of agglomerates in the liquid medium could act to decrease diffusion of the organic acids (the main solubilization agents) produced during fermentation, hence decreasing the solubilization of phosphate. Similarly, in SSF the presence of agglomerates could lead to slower diffusion of organic acids into the interior of the rock particles on the substrate surface.

Since the increase in surface area only promoted solubility up to a certain point, there was also an optimal point for the reduction in particle size. This optimum point can be seen in Figure 4, where the highest solubility for both fermentation processes was obtained at a surface area of 22.22 m^2 g^{-1} (10 min of milling), corresponding to the smallest particle size that could be used without the negative interference of agglomeration. Further reduction in particle size resulted in reduced final phosphate solubility. The existence of this phenomenon, which was observed for the first time in this work, indicates that pretreatment of the RP prior to the solubilization process (obtaining an optimal particle size) may be an important factor to consider for increased efficiency of RP solubilization in fermentation processes.

After determining the best particle size for use in the SmF and SSF cultivation systems, the next step was to consider the kinetics of solubilization, which is a key process parameter in the continuous acidification during fungal cultivation. A study of the solubilization kinetics was carried out using BRP at the selected particle size, with determination of the temporal profiles of phosphorus solubilization under SmF and SSF.

3.5. Kinetics of rock phosphate solubilization

Figure 5 shows the solubilization temporal profiles for the SmF and SSF fermentation processes using the BRP particle size corresponding to 22.22 m^2 g_{rock}^{-1}.
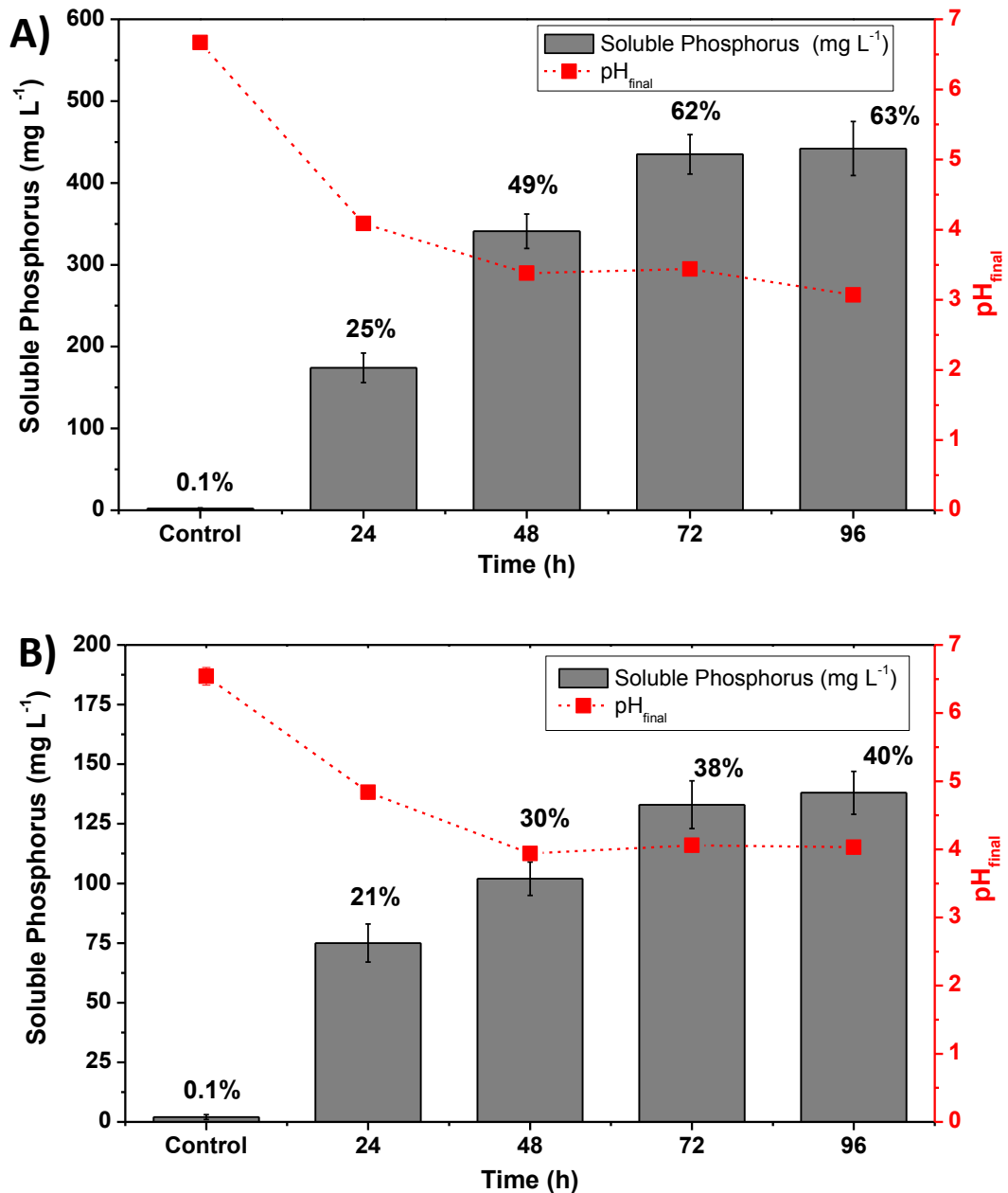
Figure 5. Phosphorus solubilization time profile and pH_{final} for *A. niger* C. **a)** Submerged fermentation using Pikovskaya medium, 96 h, 30 °C, 220 rpm, $pH_{initial}$ 7, and 5 g L^{-1} Bayovar RP (22.22 m^2 g_{rock}^{-1}). **b)** Solid-state fermentation using sugarcane bagasse, 96 h, 30 °C, moisture 80%, $pH_{initial}$ 7, and 5 g L^{-1} Bayovar RP (22.22 m^2 g_{rock}^{-1}).

In both processes, maximum solubilization was achieved within 96 h, with values of 442 mg L^{-1} (63% solubilization) for SmF (Figure 5a) and 138 mg L^{-1} (40% solubilization) for SSF (Figure 5b). However, within 72 h of cultivation, soluble phosphorus concentrations of 435 mg L^{-1} (62% solubilization) for SmF and 133 mg L^{-1} (38% solubilization) for SSF were already achieved. The differences between the values obtained after 72 and 96 h were not significant (Tukey's test, 95% confidence level). The phosphate solubilization period obtained here for SSF (72 h) was shorter than the cultivation periods reported in the literature, which range between 7 and 14 days (Mendes et al., 2015; Ogbo, 2010). This is possibly due to the simultaneous effect between the reduction of the particle size of the phosphate rock and the potential of *A. niger* C strain to solubilize inorganic phosphates.

In order to interpret the kinetics of the rock phosphate solubilization, a reference test was performed using a 2 wt.% citric acid medium (assumed representative of the type of acid produced by the strains) at initial pH 2.5. This reference procedure, widely used for the evaluation of phosphate solubility, was adapted from previous studies (Lim et al., 2003; Tonsuaadu et al., 2011; Zapata, 2004). Figure 6 shows the temporal profiles for solubilization of four BRP particle sizes in the citric acid solution.
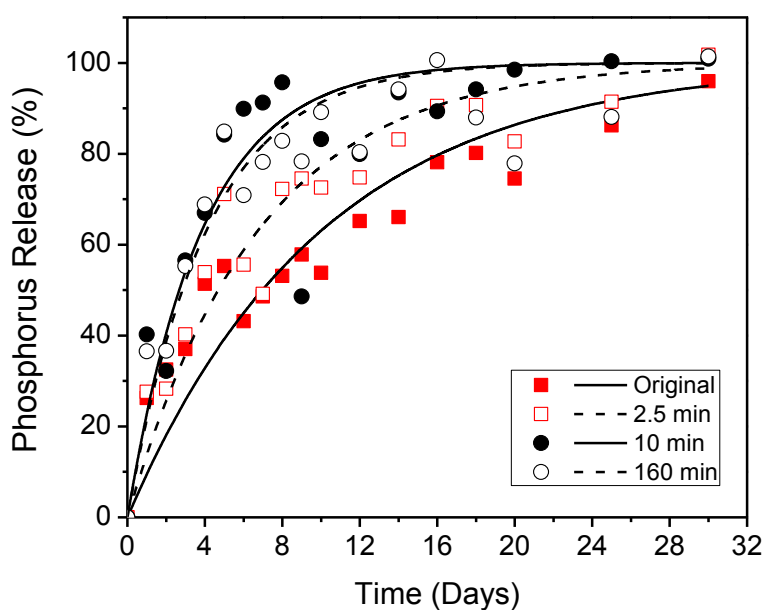
Figure 6. Kinetics of solubilization of Bayóvar RP in 2% (w/w) citric acid solution used as a reference condition for phosphate solubilization.

Almost total phosphate solubilization was found in all cases, confirming that the medium was sufficiently acidic to drive the process. However, differences were observed in the kinetic profiles, with the original material requiring 30 days to be almost completely solubilized, while the material milled for 10 min reached maximum solubilization in 8-10 days. The material milled for 160 min presented almost the same solubilization kinetics, which reinforced the existence of an optimum milling time (under the conditions used).

The results suggested that the maximum phosphate solubilization observed for the *A. niger* C strain was related to the balance of organic acids produced in the medium. It is notable that the maximum solubilization found for the SmF process after 4 days (64%) was approximately the same as the value observed after 4 days in the reference experiment with citric acid. This finding further highlights the potential of the proposed mechanical-biological approach for the solubilization of rock phosphate.

4. Conclusions

The results showed that the manipulation of rock phosphate particle size significantly enhanced phosphorus solubilization under both SmF and SSF, with gains of up to 115%. Phosphate solubilization was favored up to a certain point as the particle size decreased, after which further increase of surface area was no longer effective, highlighting the importance of this variable in bioprocess development to produce biofertilizers. In overall, our findings demonstrated that the mechanical treatment combined with biological cultivation is a potential strategy for phosphorus solubilization, and even short periods of milling can be highly effective in improving the solubilization of RP. To the best of our knowledge, this is the first work in which rock phosphate particle size in the nanometric range has been considered as an important variable affecting the solubilization efficiency during microbial cultivation. This proposed strategy could contribute to advances in the current bio-based economy and assist future developments in large-scale industrial production of biofertilizers.

References

Bengtsson, A., Lindegren, M., Sjoberg, S., Persson, P. 2007. Dissolution, adsorption and phase transformation in the fluorapatite-goethite system. *Applied Geochemistry*, **22**(9), 2016-2028.

Chang, C.H., Yang, S.S. 2009. Thermo-tolerant phosphate-solubilizing microbes for multi-functional biofertilizer preparation. *Bioresource Technology*, **100**(4), 1648-1658.

Chien, S.H. 1993. Solubility assessment for ferlilizer containing phosphate rock. *Fertilizer Research*, **35**(1-2), 93-99.

de Oliveira, S.C., Mendes, G.D., da Silva, U.C., da Silva, I.R., Ribeiro, J.I., Costa, M.D. 2015. Decreased mineral availability enhances rock phosphate solubilization efficiency in Aspergillus niger. *Annals of Microbiology*, **65**(2), 745-751.

Enustun, B.V., Turkevich, J. 1960. Solubility of fine particles of strontium sulfate. *Journal of the American Chemical Society*, **82**(17), 4502-4509.

Farinas, C.S. 2015. Developments in solid-state fermentation for the production of biomass-degrading enzymes for the bioenergy sector. *Renewable & Sustainable Energy Reviews*, **52**, 179-188.

Fontes, M.P.F., Weed, S.B. 1996. Phosphate adsorption by clays from Brazilian Oxisols, relationships with specific surface area and mineralogy. *Geoderma*, **72**(1-2), 37-51.

Gomes, E.A. 2014. Rock phosphate solubilizing microorganisms isolated from maize rhizosphere soil. 1 ed, (Ed.) U.C. Silva, Vol. 13, pp. 69-81.

Heffer, P. 2015. Fertilizer Outlook 2015-2019. in: *83rd IFA Annual Conference*, (Ed.) M. Prud'homme. Istanbul (Turquey).

Illmer, P., Schinner, F. 1995. Solubilization of inorganic calcium phosphates—Solubilization mechanisms. *Soil Biology and Biochemistry*, **27**(3), 257-263.

Kpomblekoua, K., Tabatabai, M.A. 1994. Effect of organic-acids on release of phosphorus from phosphate rocks. *Soil Science*, **158**(6), 442-453.

Lim, H.H., Gilkes, R.J., McCormick, P.G. 2003. Beneficiation of rock phosphate fertilisers by mechano-milling. *Nutrient Cycling in Agroecosystems*, **67**(2), 177-186.

MAPA. 2013. Manual de métodos analíticos oficiais para fertilizantes e corretivos, (Ed.) M.d.A.P.e. Abastecimento. Brazil.

McArthur, J.M. 1985. Francolite geochemistry - compositional controls during formation, diagenesis, metamorphism and weathering. *Geochimica Et Cosmochimica Acta*, **49**(1), 23-35.

Mendes, G.D., da Silva, N., Anastacio, T.C., Vassilev, N.B., Ribeiro, J.I., da Silva, I.R., Costa, M.D. 2015. Optimization of Aspergillus niger rock phosphate solubilization in solid-state fermentation and use of the resulting product as a P fertilizer. *Microbial Biotechnology*, **8**(6), 930-939.

Mendes, G.D., de Freitas, A.L.M., Pereira, O.L., da Silva, I.R., Vassilev, N.B., Costa, M.D. 2014. Mechanisms of phosphate solubilization by fungal isolates when exposed to different P sources. *Annals of Microbiology*, **64**(1), 239-249.

Mendes, G.d.O., Bojkov Vassilev, N., Araujo Bonduki, V.H., da Silva, I.R., Ribeiro, J.I., Jr., Costa, M.D. 2013a. Inhibition of Aspergillus niger Phosphate Solubilization by Fluoride Released from Rock Phosphate. *Applied and Environmental Microbiology*, **79**(16), 4906-4913.

Mendes, G.O., Dias, C.S., Silva, I.R., Ribeiro, J.I., Pereira, O.L., Costa, M.D. 2013b. Fungal rock phosphate solubilization using sugarcane bagasse. *World Journal of Microbiology & Biotechnology*, **29**(1), 43-50.

Murphy, J., Riley, J.P. 1986. Citation-classic - a modified single solution method for the determination of phosphate in natural-waters. *Current Contents/Agriculture Biology & Environmental Sciences*(12), 16-16.

Nahas, E. 1996. Factors determining rock phosphate solubilization by microorganisms isolated from soil. *World Journal of Microbiology & Biotechnology*, **12**(6), 567-572.

Nautiyal, C.S. 1999. An efficient microbiological growth medium for screening phosphate solubilizing microorganisms. *Fems Microbiology Letters*, **170**(1), 265-270.

Ogbo, F.C. 2010. Conversion of cassava wastes for biofertilizer production using phosphate solubilizing fungi. *Bioresource Technology*, **101**(11), 4120-4124.

Pikvoskaya. 1948. Mobilization of phosporus in soil connection with the vital activity of some microbial species, Vol. 17. Microbiology, pp. 362-370.

Sadrai, S., Meech, J.A., Ghomshei, M., Sassani, F., Tromans, D. 2006. Influence of impact velocity on fragmentation and the energy efficiency of comminution. *International Journal of Impact Engineering*, **33**(1-12), 723-734.

Salih, H.M., Yahya, A.I., Abdulrahem, A.M., Munam, B.H. 1989. Availability of phosphorus in a calcareous soil treated with rock phosphate or superphosphate as affected by phosphate-dissolving fungi. *Plant and Soil*, **120**(2), 181-185.

Thomas, A., Filippov, L.O. 1999. Fractures, fractals and breakage energy of mineral particles. *International Journal of Mineral Processing*, **57**(4), 285-301.

Tonsuaadu, K., Kaljuvee, T., Petkova, V., Traksmaa, R., Bender, V., Kirsimaee, K. 2011. Impact of mechanical activation on physical and chemical properties of phosphorite concentrates. *International Journal of Mineral Processing*, **100**(3-4), 104-109.

Vassilev, N., Medina, A., Azcon, R., Vassileva, M. 2006. Microbial solubilization of rock phosphate on media containing agro-industrial wastes and effect of the resulting products on plant growth and P uptake. *Plant and Soil*, **287**(1-2), 77-84.

Vassilev, N., Vassileva, M. 2003. Biotechnological solubilization of rock phosphate on media containing agro-industrial wastes. *Applied Microbiology and Biotechnology*, **61**(5-6), 435-440.

Vassilev, N., Vassileva, M., Fenice, M., Federici, F. 2001. Immobilized cell technology applied in solubilization of insoluble inorganic (rock) phosphates and P plant acquisition. *Bioresource Technology*, **79**(3), 263-271.

Vassilev, N., Vassileva, M., Lopez, A., Martos, V., Reyes, A., Maksimovic, I, Eichler-Lobermann, B., Malusa, E. 2015. Unexploited potential of some biotechnological techniques for biofertilizer production and formulation. *Applied Microbiology and Biotechnology*, **99**(12), 4983-4996.

Vassileva, M., Azcon, R., Barea, J.M., Vassilev, N. 1998. Application of an encapsulated filamentous fungus in solubilization of inorganic phosphate. *Journal of Biotechnology*, **63**(1), 67-72.

Zapata, F. 2004. Use of phosphate rocks for sustainable agriculture. *FAO Fertilizer and Plant Nutrition Bulletin*, 1-148.

Supplementary Material

Section I

Determination of the milling energy

The energy consumption for BRP milling was calculated for each time according to the Bond Law (Sadrai et al., 2006; Thomas & Filippov, 1999). This methodology has as main characteristic to use the index friction of the mill that depends on the nature of the solid.

-W = k C W$_i$ [(1 / X$_1^{1/2}$) + (1 / X$_2^{1/2}$)] → Bond model.

W → Energy consumption (HP).

  X$_1$ → Particle size initial (cm).

  X$_2$ → Particle size final (cm).

  W$_i$ → Friction index (kWh ton^{-1}) (13.23).

  C → Capacity of the mill (ton h^{-1}) (0.0003).

  k → Constant of Bond (0.134).

Table S1: Energy consumption for BRP milling for each time

Time Milling (min)	Superficial Area (m^2 g^{-1})	Average Diameter (µm)	Energy (HP)
Original	19.3	138.00 ± 23	0.0000
2.5	19.7	8.00 ± 4	0.0122
5	21.5	7.00 ± 3.00	0.0142
10	22.2	0.70 ± 0.30	0.0549
20	25.2	0.20 ± 0.60	0.1143
40	27.7	0.16 ± 0.04	0.1284
80	29.3	0.15 ± 0.05	0.1327
160	30.3	0.12 ± 0.03	0.1489

Supplementary Material

Section II

Figures

Fig. S1. XRD pattern of original (not milled) Bayóvar phosphate rock.
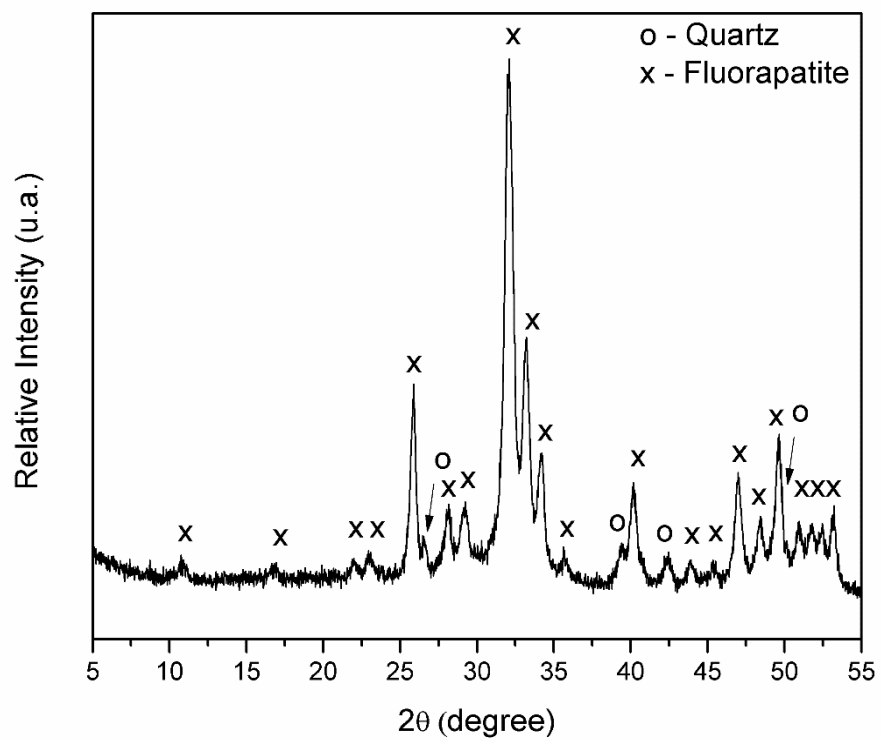
Fig. S1.

Capítulo 3

"A fed-batch strategy integrated with mechanical activation improves the biological solubilization of phosphate rock"

Artigo submetido na revista *Sustainable Chemistry & Engineering*

Nesse estudo foi avaliado o efeito do tamanho de partícula e teor de sólidos da rocha fosfática Itafós na solubilização do fósforo durante cultivo submerso e em estado sólido do fungo filamentoso *Aspergillus niger*. A rocha fosfática Itafós utilizada neste estudo apresenta características diferentes da rocha fosfática Bayóvar estudada no Capítulo 2 e, entender comportamento de diferentes tipos de minerais fosfatados no processo de biosolubilização é necessário para desenvolver bioprocessos eficientes. Caracterizações detalhadas desta rocha foram realizadas e mostraram que se trata de uma rocha fosfática de origem ígnea com um teor de P_2O_5 em torno de 20%. Os resultados mostraram que associar a redução do tamanho de partícula ao processo de biosolubilização da rocha fosfática foi determinante para aumentar a eficiência de solubilização via cultivo microbiano. O aumento na solubilização da rocha fosfática Itafós foi de 57% usando cultivo submerso e de 45% usando cultivo em estado sólido, para uma ativação mecânica de apenas 10 min. Entretanto, ao aumentar o teor de sólidos no meio (concentração da rocha fosfática) foi observado um efeito de inibição no crescimento microbiano e na acidez produzida, consequentemente, a eficiência de solubilização reduziu para altas concentrações de rocha fosfática. Nesse sentido, foram propostas estratégias de processo para minimizar os efeitos de inibição e aumentar a eficiência de solubilização. Utilizando uma estratégia de batelada alimentada de sólidos foi possível reduzir os efeitos de inibição e aumentar a eficiência de solubilização. O processo integrado usando uma ativação mecânica junto ao sistema de batelada alimentada de sólidos proporcionou um aumento de 78% na solubilização da rocha fosfática Itafós, quando comparado ao processo convencional. Este artigo se refere ao objetivo específico 2 e 3: (2) Avaliação da influência do tamanho de partícula da rocha fosfática e, (3) Avaliação do efeito do teor de sólidos no processo de solubilização.

Abstract

Solubilization of phosphate rock (PR) by microorganisms is an environmentally sustainable alternative to chemical processing for production of phosphate fertilizers. However, the biosolubilization efficiency has been limited by the PR solids content of cultivation systems, and is still low for practical applications. Here, we propose a fed-batch strategy coupled with mechanical activation to improve the biological solubilization of PR. An initial systematic study of the effect of the particle size of Itafós phosphate rock (IPR), a low reactivity phosphate mineral (P_2O_5, 20%), on the microbial solubilization of P revealed that the particle size played a key role in IPR solubilization. Increases of available phosphate of up to 57% under submerged cultivation and 45% for solid-state culture were observed for rocks that been milled for only 10 min. A fed-batch procedure was proposed in order to increase the solids content while maintaining the P solubilization efficiency, resulting in a remarkable increase of 78% in P solubilization, compared to the conventional process. This proposed strategy could potentially contribute to the future development of biotechnological processes for the large-scale industrial production of phosphate fertilizers that are environmentally sustainable.

Keywords: Phosphate rock, Particle size, Biological solubilization, *Aspergillus niger*, Organic acids, Fed-batch.

1. Introduction

Phosphorus (P) is a key nutrient for plants that is usually supplied in the form of soluble fertilizers produced by expensive chemical treatments of phosphate rock (PR), leading to several environmental concerns [1, 2]. Novel technologies have been developed to processing of PR [3] as well as new fertilizers products for a sustainable agriculture [4, 5]. An innovative and attractive alternative for obtaining soluble P fertilizer is the use of P-solubilizing microorganisms (PSMs) to solubilize PR in biotechnological processes [1, 2, 6, 7]. The P-solubilizing activity of PSMs is determined mainly by their ability to produce and release metabolites such as organic acids that chelate cations (principally calcium) bound to phosphate [8-10]. Aerobic fungi are especially noted for their high rates of growth and organic acid production [11], and *Aspergillus niger* has been widely recognized as a potential PSM [8, 12, 13].

Recent studies concerning biotechnological routes for PR solubilization have discussed the selection of PSMs using different screening methods [14-16], as well as process conditions (including C and N sources, initial pH, inoculum size, and duration of cultivation) [17-20] and quantification of the organic acids produced in the microbial cultivation [8, 13, 21]. In previous work by our group, we found that the PR particle size influenced phosphate solubilization, with gains of over 60% for solid-state culture and 115% for submerged culture [12]. However, this effect can vary depending on the type of rock (sedimentary or igneous).

To the best of our knowledge, biosolubilization processes are still strongly limited by the PR solids content in the cultivation system. There is a negative correlation between the amount of P solubilized and the P yield with increasing PR doses [22, 23]. Therefore, the challenge in achieving an economically and industrially feasible process is to develop a strategy to solubilize all the available phosphate in PR at high solids contents. This strategy could contribute to the development of a commercial bioproduct in the form of a liquid biofertilizer with high P concentration, which could be used for direct application in agriculture. The effectiveness of liquid biofertilizers has been demonstrated previously in the fertirrigation of *Trifolium repens* plants, which resulted in a significant improvement in plant growth and increased P uptake [24]. However, novel bioprocess engineering strategies focusing on ways to make this process industrially competitive remain to be further investigated.

Therefore, here we propose a fed-batch strategy coupled to mechanical activation to simultaneously increase the biological solubilization of PR and the effective solids content.

Itafós phosphate rock (IPR), an igneous rock, was selected as a model of a very low solubility phosphate source typically rejected for industrial fertilizer production, despite its high phosphate content (P_2O_5, 20%), due to its difficult chemical processing and high associated costs. The findings indicated that biosolubilization using fed-batch addition of solids, with optimization of PR size and bioprocess conditions (microorganism, pH, and biomass), was more efficient than using sequential or conventional solubilization modes. These results could contribute to the development of a feasible industrial bioprocess for PR treatment and environmentally sustainable fertilizer production.

2. Materials and methods

2.1. Itafós phosphate rock

The Itafós phosphate rock (IPR) was kindly donated by ITAFÓS in Arraias (Tocantins State, Brazil). The IPR was dried at 110 ºC for 48 h in order to reduce the humidity content and was then ground for periods of 2.5, 5, 10, 20, 40, and 80 min in an orbital mill (Model CT-251, Servitec) consisting of a porcelain jar and alumina balls [12, 25]. After treatment, the materials were stored in dry boxes at room temperature for further characterization (Section 2.2) and for use in the solubilization experiments (Sections 2.4 and 2.5).

2.2. Physical-chemical characterizations

X-ray diffraction (XRD) analyses of the IPR samples were performed using a LabX XRD-6000 diffractometer (Shimadzu, Japan) operated with Cu-Kα radiation ($\lambda = 1.54056$ Å), voltage of 30 kV, and current of 30 mA. The diffractograms were recorded for 2θ from 5° to 55°, using a continuous scanning speed of 2° min^{-1}. X-ray fluorescence (XRF) employing the lithium tetraborate fusion technique was used to analyze the ten commonest oxides found in the ores. In addition, fluorine and carbon were determined using specific ion analysis and infrared spectroscopy, respectively. The morphology of the IPR samples was observed by field emission gun scanning electron microscopy (FEG-SEM), using a JSM-6701F FEG microscope (JEOL, Japan). Images were acquired using an acceleration voltage of 2 kV and secondary electron detection. Total surface area measurements of the IPR samples were made by isothermal nitrogen adsorption, using a Micromeritics ASAP 2020 instrument and the 5-point B.E.T. (Brunauer–Emmett–Teller) method.

2.3. Microorganism

The filamentous fungus *Aspergillus niger* C (BRMCTAA 82) was obtained from the Embrapa Food Technology collection (Rio de Janeiro, RJ, Brazil). This fungus was selected from among eight filamentous fungi as the best for rock phosphate solubilization [12]. Spore suspensions of the fungal strain were kept at -18 °C in a solution of water with glycerol (10 wt.%) and NaCl (0.9 wt.%). Spores were germinated at 30 °C in Petri dishes containing potato dextrose agar. After 96 h, a suspension of grown spores was harvested by adding distilled water. The spore concentration was determined using a Neubauer chamber.

2.4. Submerged culture (SmC)

In the microbial cultivations under submerged culture, the pre-culture was initiated in 500 mL Erlenmeyer flasks by adding a volume of spore suspension calculated to give a concentration of 1.2×10^7 spores per mL of the nutrient medium. The nutrient medium was adapted from the medium described by Pikvoskaya [26] and contained (w/v): glucose, 1%; $(NH_4)_2SO_4$, 0.5%; NaCl, 0.2%; $MgSO_4.7H_2O$, 0.1%; KCl, 0.2%; $MnSO_4.H_2O$, 0.002%; $FeSO_4.7H_2O$, 0.002%; yeast extract, 0.5%. A 100 mL volume of the nutrient medium was used in each experiment. The incubation for the pre-culture step was carried out for 48 h in an orbital shaker incubator, at 30 °C and 220 rpm. Solubilization of P was initiated by transferring a volume of pre-culture suspension corresponding to 10% (v/v) to 100 mL of culture medium with the same composition, with agitation for 96 h in an orbital shaker incubator at 30 °C and 220 rpm. In this cultivation step, IPR was added at 5 g L^{-1} as the source of insoluble phosphate. After this period, the resulting suspension was vacuum-filtered using Whatman No. 1 filter paper, followed by centrifugation for 20 min at 12000 rpm and 20 °C. The clear supernatant was analyzed using the colorimetric method described in Section 2.8 and the pH, titratable acidity, and microbial biomass were measured as described in Section 2.11. All experiments were carried out in triplicate and the data were calculated as means ± standard deviations.

2.5. Solid-state culture (SSC)

Sugarcane bagasse (SB) ground to a particle size of 2 mm was used as the solid substrate for SSC. The experiments were carried out in 250 mL Erlenmeyer flasks, with 5 g of

SB in each experiment. After sterilization at 120 °C for 20 min, the medium containing SB and IPR was inoculated with 1.2×10^7 spores per g of substrate. The initial moisture content of the treated SB was adjusted to 80% using the nutrient solution (Pikovskaya medium, as described in Section 2.4), and the fermentation was performed at 30 °C for 96 h. After the cultivation period, the sample was homogenized in 50 mL of distilled water (shaking the suspension at 200 rpm for 60 min). The resulting material was vacuum-filtered using Whatman No. 1 filter paper and was then centrifuged for 20 min at 12000 rpm and 20 °C. Soluble P in the clear supernatant was determined by the colorimetric method described in Section 2.4. All experiments were carried out in triplicate and the data were calculated as means ± standard deviations.

2.6. Sequential solubilization

A. niger was cultivated under SmC, without the presence of IPR, for 144 h (as described in Section 2.4), followed by removal of the biomass by filtration and centrifugation. The culture medium extract obtained was used for solubilization of the IPR for a further 24 h, at 30 °C and 220 rpm, resulting in a total process time of 168 h. The medium was again filtered and centrifuged to remove the IPR particles, and the phosphorus solubilized in the liquid fraction was determined as described in Section 2.8. This strategy was evaluated using solids contents of 5, 10, and 15 g L^{-1}. All experiments were carried out in triplicate.

2.7. Simultaneous solubilization with fed-batch addition of solids

For solubilization with fed-batch addition of solids, *A. niger* was cultivated under SmC for 48 h, in the absence of IPR (as described in Section 2.4), after which the IPR was added at predetermined times (48, 72, 96, and 120 h). At each time, a solids content of 2.5 g L^{-1} was added, up to a final solids content of 10 g L^{-1}. This strategy was only performed with the solids content of 10 g L^{-1}. After 168 h, the medium was filtered and centrifuged to remove the fungal biomass and PR particles, and the phosphorus solubilized in the liquid fraction was determined as described in Section 2.8. All experiments were carried out in triplicate.

2.8. Determination of soluble phosphorus

The soluble P content was determined using a colorimetric method adapted from Murphy and Riley [27]. Briefly, a 5 mL aliquot of the clear supernatant sample was reacted with 2 mL of ascorbic acid solution (0.4 mol L^{-1}), 0.2 mL of citric acid (0.03 mol L^{-1}), and 2 mL of a reagent consisting of 25 mL of a sulfuric acid solution (4.7 mol L^{-1}), 5.5 mL of ammonium molybdate solution (0.08 mol L^{-1}), and 0.6 mL of antimony and potassium tartrate solution (0.05 mol L^{-1}). This mixture was reacted at 50 °C for 15 min, forming a phosphoantimonylmolybdenum blue complex. The concentration of the complex was determined by UV-Vis spectrometry at a wavelength of 880 nm.

2.9. Determination of soluble calcium, aluminum, and iron

The amounts of calcium (Ca), iron (Fe), and aluminum (Al) released were determined by flame atomic absorption spectroscopy (FAAS), using a Perkin Elmer PinAAcle 900T instrument operated in flame atomization mode. The analytical conditions for Ca were a wavelength of 422.67 nm, slit width of 0.7 nm, and flame mixture of synthetic air at 10 L min^{-1} and acetylene at 2.7 L min^{-1}. The conditions for Al were a wavelength of 309.27 nm, slit width of 0.7 nm, and flame mixture of nitrous oxide at 6 L min^{-1} and acetylene at 7.5 L min^{-1}. The conditions for Fe were a wavelength of 248.33 nm, slit width of 0.2 nm, and flame mixture of synthetic air at 10 L min^{-1} and acetylene at 2.5 L min^{-1}.

2.10. Determination of organic acids

The concentrations of gluconic, oxalic, and citric acids were determined using a Waters HPLC system equipped with W515 pumps, W717 injector, and W486 UV reader. An Aminex HPX-87H column (Bio-Rad) was employed, with 5 mM sulfuric acid solution as the isocratic mobile phase, at a flow rate of 0.6 mL min^{-1}. The injector and column temperatures were 4 °C and 65 °C, respectively. The organic acids were detected at 210 nm. Gluconic, oxalic, and citric acid standards were obtained from Sigma-Aldrich (organic acid kit). All the experiments were performed in triplicate and the data were calculated as means ± standard deviations.

2.11. Determination of pH, titratable acidity, and microbial dry mass

The pH of the medium was measured with a glass electrode and titratable acidity was determined by titrating a sample containing 10 mL of acid extract with 0.1 M NaOH solution, using about three drops of a solution of phenolphthalein (1 wt.%) as indicator. The microbial biomass was determined as the dry weight after drying at 70 °C for 48 h.

3. Results and discussion

3.1. Characterization of Itafós phosphate rock

A detailed characterization of the original and milled samples of IPR was carried out in order to understand the physical and chemical nature of the phosphate source used in the bioprocess. The X-ray diffractograms (Supporting Information, Section 2, Fig. S1) revealed crystalline phase constituents corresponding to alpha-quartz (SiO_2, PDF2 pattern file #01-089-8934) and apatite ($Ca_5(PO_4)_3OH$ or $Ca_5(PO_4)_3F$ or $Ca_5(PO_4)_3Cl$, PDF2 pattern file #01-086-0740). Minor phases such as kaolinite ($Al_2Si_2O_5(OH)_4$) or berlinite (aluminum phosphate, $AlPO_4$, PDF2 pattern file #01-076-0228) may also have been present, but the diffraction patterns were not conclusive. The presence of a large amount of crystalline quartz phase evidenced the igneous origin of this rock [28]. All the identified phases were consistent with the chemical analysis results shown in Table 1.

Fluoride and chloride were also detected in significant amounts (Table 1), indicating that the apatite phase was probably mostly fluorapatite and/or chlorapatite. Mineralogical analysis (Supporting Information, Section 1) suggested that the chloride may have all been in the form of KCl, while fluoride was present as fluorapatite ($Ca_5(PO_4)_3F$), considering the higher affinity of F for calcium-based phases [29, 30]. The mineralogical analyses also showed that the phosphate phase contained in this rock was about 50% (w/w).

Table 1: Chemical analysis of the Itafós phosphate rock.

Oxide species	Mass %
SiO_2	36.40
Al_2O_3	4.60
Fe_2O_3	2.03
CaO	30.40
MgO	0.52
TiO_2	0.22
P_2O_5	20.29
Na_2O	0.30
K_2O	0.88
MnO	0.10
Loss on ignition	4.33
Total	100
F*	1.87
Cl**	1.50
C***	0.96

(*) Fluoride determined by specific ion analysis. (**) Chloride determined by specific ion analysis. (***) Carbon determined by infrared spectroscopy.

Physical characterization of the IPR samples obtained using different milling times was performed by SEM. The micrographs showed that a longer milling time resulted in smaller IPR particle size (Supporting Information, Section 2, Fig. S2), while short milling times (such as 2.5 min) only resulted in de-agglomeration. An effect on particle size only occurred after 5 min of grinding, when the first submicron particles became apparent. These observations were supported by the surface area results (Table 2), which showed that the specific surface area of the sample milled for 2.5 min was approximately the same as that of the original sample. However, the specific surface area increased by about 70% for the material milled for 10 min and more than 3-fold for the material milled for 80 min.

Table 2: Specific surface area of the Itafós phosphate rock, according to milling time.

Millling Time	Surface Area ($m^2\ g_{rock}^{-1}$)
Natural	3.01
2.5 min	3.02
5 min	3.28
10 min	5.13
20 min	7.16
40 min	8.30
80 min	9.12

3.2. Effect of particle size on P solubilization

Fig. 1 shows the effect of the IPR particle size on P solubilization using *A. niger* cultivated under both SmC (Fig. 1a) and SSC (Fig. 1b) with IPR that had been milled for different periods of time (Table 2). For both cultivation methods, there were significant increases in P solubilization as the specific surface area increased, with a maximum of 70% solubilization achieved under SmC with IPR milled for 80 min. This represented an increase of 90% in P solubilization, compared to the natural IPR. Under SSC, the solubilization of P achieved using the same particle size was 61%, representing an increase of around 110%, compared to the natural IPR. In addition to the positive effect of the smaller size of the IPR, greater P solubilization could have resulted from enhanced interaction between the rock particles and the organic acids produced by *A. niger*.

These results indicated that the milling time had a greater influence in the case of igneous rocks, compared to sedimentary rocks, since in earlier work [12] we showed that this process only resulted in a limited increase in the specific surface area of Bayóvar rock (a sedimentary rock). This behavior was directly related to the rock friability, which is generally higher for igneous rocks. However, the optimum milling point had not yet been reached, with the solubilization efficiency tending to stabilize with the reduction of particle size.
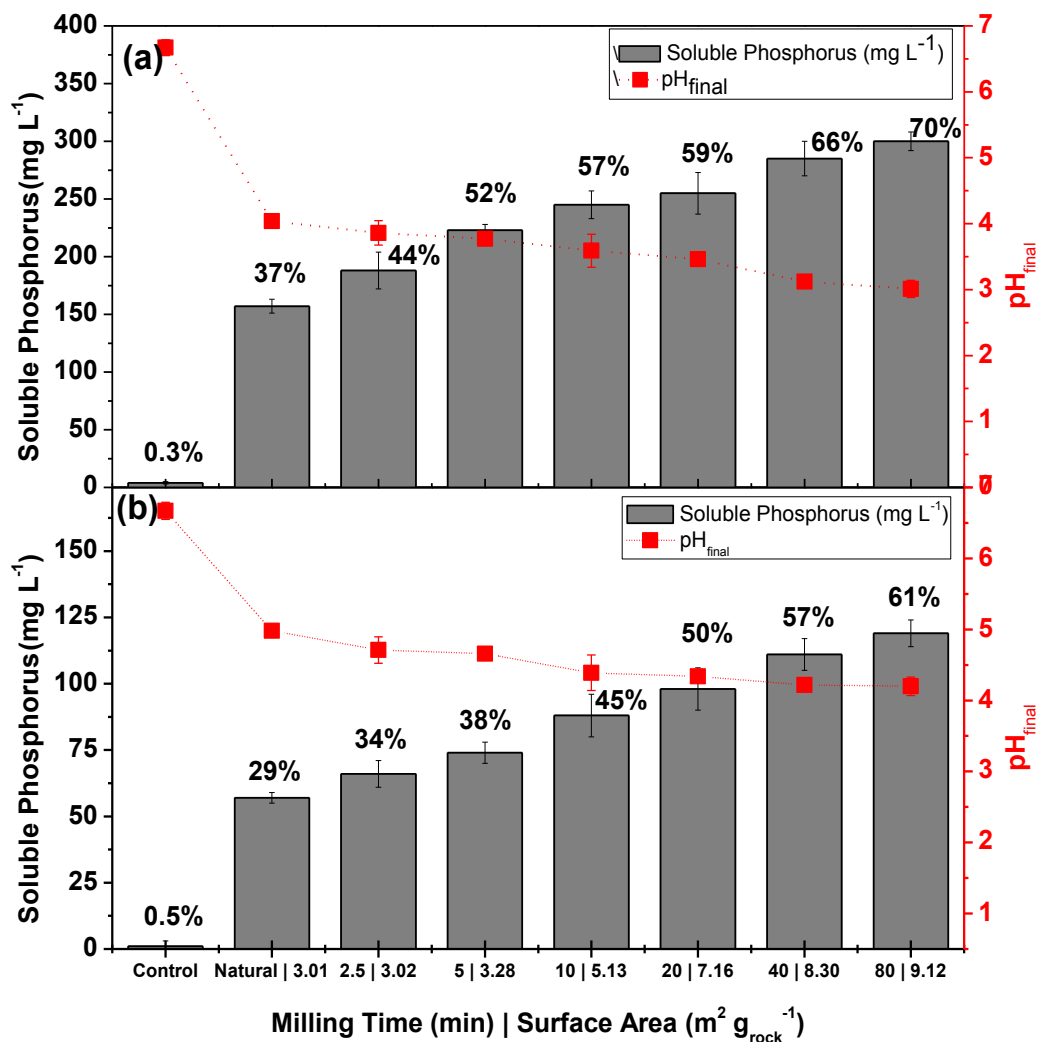
Figure 1. Phosphorus solubilization and pH$_{final}$ for *A. niger* cultivation using different particle sizes. **a)** Submerged cultivation for 96 h using Pikovskaya medium, 30 °C, 220 rpm, pH$_{initial}$ 7, and 5 g L^{-1} IPR. **b)** Solid-state cultivation for 96 h using sugarcane bagasse, 30 °C, 80% moisture, pH$_{initial}$ 7, and 5 g L^{-1} IPR.

The results showed that manipulation of the rock phosphate particle size significantly enhanced phosphorus solubilization under both SmC and SSC. However, the mechanical activation could also have affected other constituent phases of the IPR. Therefore, in order to obtain a better understanding of the effect of particle size on the solubilization of IPR, evaluation was made of solubilization of the elements Ca, Fe, and Al present in the IPR. In addition, production of the main organic acids was quantified for all the grinding times. Since SmC was more effective than SSC for phosphate solubilization, and considering that SmC

and SSC showed similar features during the solubilization processes, in the next experiments only SmC was used as a model microbial cultivation process.

3.3. Effect of particle size on Ca, Fe, and Al solubilization and organic acid production

Table 3 shows the organic acids (citric, oxalic, and gluconic) and soluble Ca, Fe, and Al produced after 96 h of SmC cultivation using the different particle sizes. Low concentrations of soluble Ca were observed in all cases, corresponding to about 1% of the total Ca in the IPR. These low values could have been due to the precipitation of calcium oxalate following reaction with oxalic acid [8, 21], which would decrease the levels of Ca and oxalic acid in the solution. This hypothesis was in agreement with the low amount of oxalic acid detected in the medium after the solubilization process. Nevertheless, the concentration of soluble Ca increased slightly with higher surface area of the IPR.

Table 3: Effect of particle size under metals solubilization and acids organic production by submerged fermentation at 30 °C, 220 rpm for 96h.

Millin/Sup. Area. (Min|m²/g)	P (%) Solubilized		Solubilized Metals (mg L^{-1})								Organic Acids (mg L^{-1})					
			P		Ca		Fe		Al		Citric		Oxalic		Gluconic	
$Natural$| 3.01	41 ± 5	a	157 ± 6	a	9.81 ± 0.52	a	0.51 ± 0.01	a	1.16 ± 0.29	a	3 ± 1	a	12 ± 1	a	151 ± 6	a
2.5	3.02	49 ± 2	b	188 ± 16	b	10.65 ± 0.38	ab	0.53 ± 0.02	a	1.78 ± 0.19	a	3 ± 1	a	14 ± 1	ab	139 ± 9	ab
5	3.28	57 ± 3	c	223 ± 5	c	11.24 ± 0.26	b	0.51 ± 0.02	a	2.87 ± 0.83	b	0		15 ± 1	bc	125 ± 7	b
10	5.13	63 ± 2	d	245 ± 12	d	11.68 ± 0.14	c	0.50 ± 0.01	a	6.54 ± 1.01	b	0		17 ± 1	cd	107 ± 2	c
20	7.16	66 ± 4	d	255 ± 18	d	11.73 ± 0.09	cd	0.52 ± 0.03	a	18.27 ± 1.10	c	2 ± 1	a	19 ± 1	de	96 ± 3	d
40	8.30	73 ± 5	de	285 ± 15	de	12.07 ± 0.27	de	0.56 ± 0.06	ab	29.66 ± 0.86	d	0		21 ± 2	ef	91 ± 2	d
80	9.14	77 ± 5	e	300 ± 8	e	12.34 ± 0.16	e	0.59 ± 0.03	b	45.03 ± 4.11	e	0		22 ± 1	f	95 ± 2	d

* Different letters mean that there is significant difference among treatments, tukey's test, 95% confidence level.

The release of Fe during the solubilization process was minimal, at around 0.5 mg L^{-1} for all IPR particle sizes, representing 0.7% of the initial amount of Fe. However, soluble Al showed a significant increase with IPR particle surface area, especially for material milled for more than 20 min. This effect was probably associated with the lower pH of the medium induced by the fungal activity. Since the Al phases are fully soluble at pH <4 (according to the Pourbaix diagram for Al [31]), local acidification leads to complete Al phase dissolution. This effect is less important for Fe solubilization, since significant solubilization is only expected at pH <2 [31].

The main mechanism of IPR solubilization was complexation involving the organic acids produced by the microorganism [8-10], which could be influenced by the particle size. The production of gluconic acid decreased with the particle surface area, probably due to an adverse effect of soluble Al [11]. Oxalic acid production was likely to have been higher than the values shown in Table 3, due to precipitation in the form of the calcium salt, as mentioned previously. Citric acid production was minimal, since the environmental conditions (C and N concentrations, pH, and dissolved oxygen) were not ideal. Furthermore, Al and Fe at low concentrations can cause substantial inhibition of citric acid production [11]. Other organic acids may also have been produced during the microbial cultivation, but were not identified.

These hypotheses were confirmed by the temporal profiles of acid production observed using the IPR sample milled for 10 min (Fig. 2). The results showed that oxalic and gluconic acids were produced in higher amounts during the initial period, followed by subsequent large decreases, while the total titratable acidity continuously increased. This strongly indicated that these acids precipitated as complexes, mainly with Ca (but possibly also with Al), with the acidity resulting from solubilization of the IPR. Citric acid production remained consistently low, as expected. These results were corroborated by the solubility of Ca in the medium, as well as by the total IPR solubilization (Figs. S3 and S4, Supporting Information). Ca showed a maximum soluble fraction after 24 h of reaction, tending to precipitate with organic acids, while IPR continued to be solubilized. On the other hand, the soluble Al and Fe fractions showed increasing trends, due to the pH reduction, despite the fact that these ions may also form complexes with organic acids [32, 33].
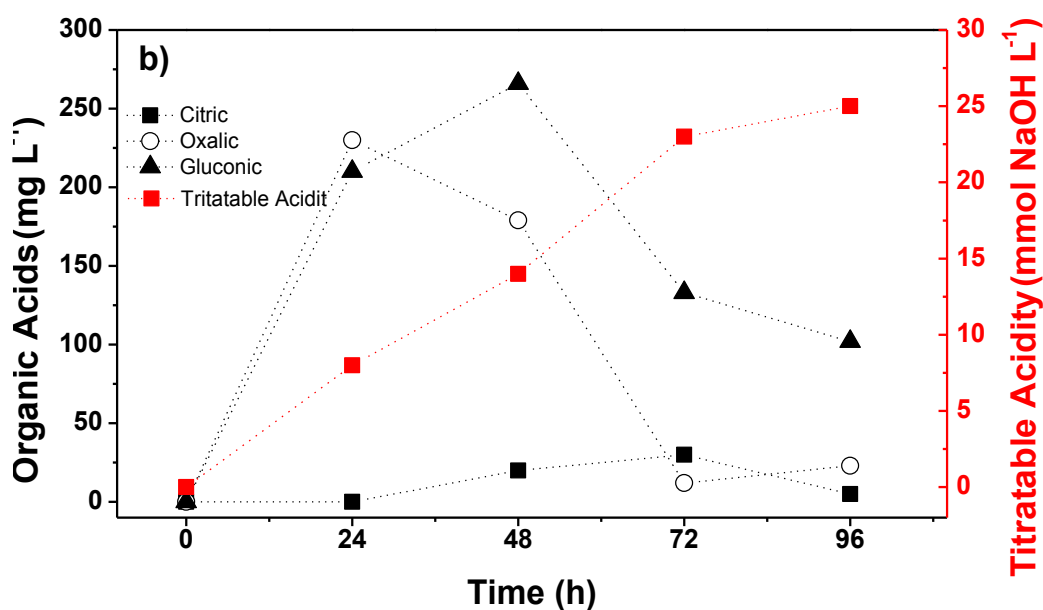
Figure 2. Temporal profiles of organic acids production during submerged cultivation for 96 h. Conditions: 30 °C, 220 rpm, $pH_{initial}$ 7, and 5 g L^{-1} IPR (5.13 m^2 g_{rock}^{-1}).

3.4. Bioprocess strategies to improve phosphate rock solubilization

The optimization of P solubilization required the selection of suitable process parameters that avoided undesirable effects of the IPR on *A. niger* growth during the reaction. In order to clearly reveal the effects of such parameters, an intermediate condition (10 min milling) was chosen. Fig. 3a shows the effect of the solids content on the production of microbial biomass. Higher solids content led to a reduction in biomass production, especially during the first 72 h, with similar trends for solids concentrations from 5 to 15 g L^{-1}. The biomass concentration at 72 h was 12.68 g L^{-1} for the cultivation without IPR, while values of 8.06 g L^{-1} (47% inhibition), 7.11 g L^{-1} (53% inhibition), and 6.20 g L^{-1} (58% inhibition) were obtained for the cultivations with solids contents of 5, 10, and 15 g L^{-1}, respectively. This could have been due to attrition and friction among the solid particles and the microorganism, which increased in line with the concentration of rock particles in the medium, hence restricting microbial growth, as observed previously by Xiao et al. [34]. Another inhibitory effect could have been associated with F^- release into the medium, as suggested by Mendes et al. [35] and Silva et al. [36], since IPR is probably a fluorapatite (Table 1).
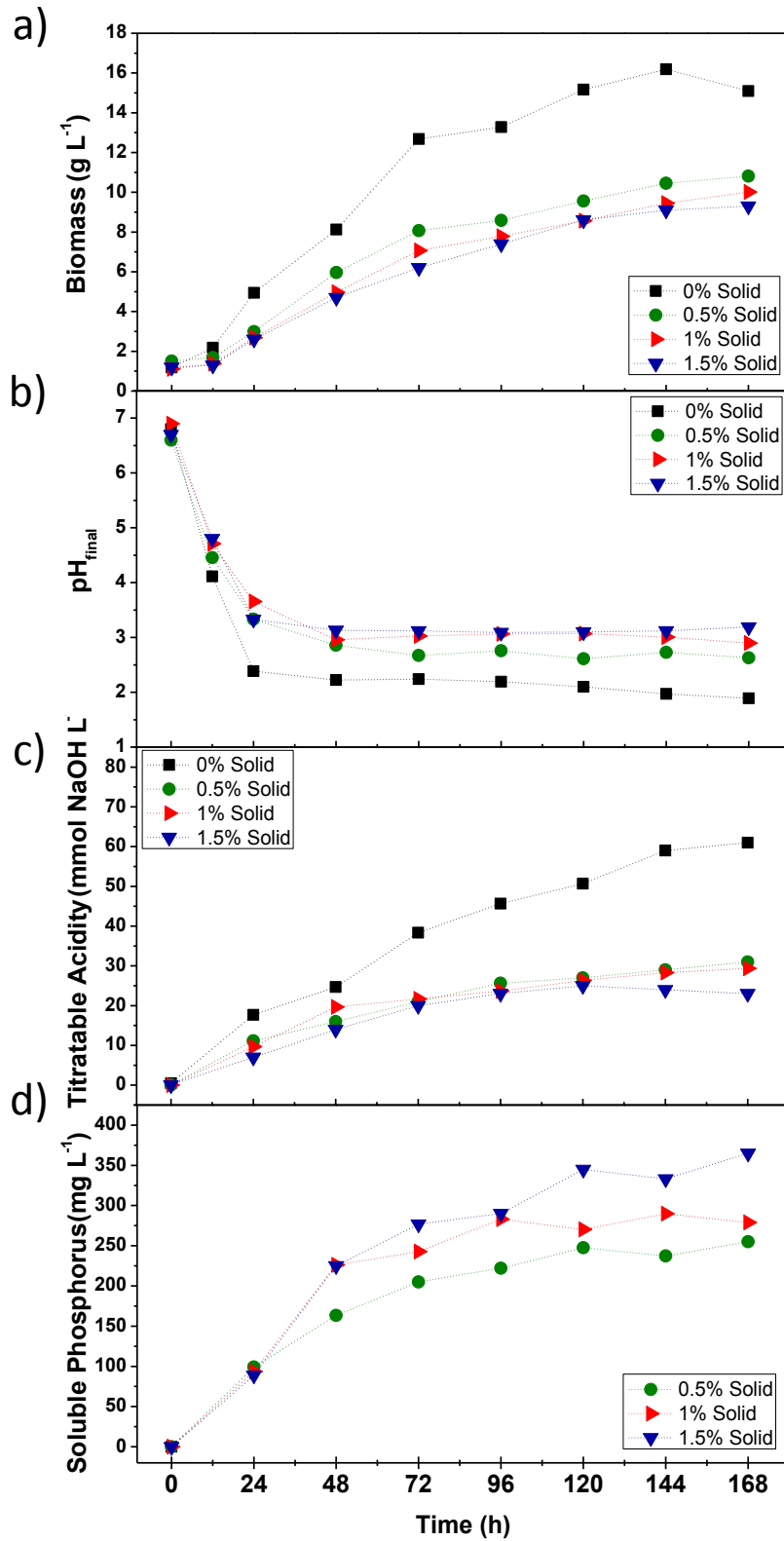
Figure 3. Temporal profiles of the effect of the solids content on **a)** biomass concentration, **b)** titratable acidity, **c)** pH$_{final}$, and **d)** phosphorus solubilization during submerged cultivation of *A. niger* at 30 °C, 220 rpm, and pH$_{initial}$ 7.

Fig. 3b shows the effect of the solids content on the pH of the cultivation medium. In the cultivation without rock, the pH showed a rapid decrease to around pH 2.3 within 48 h, followed by a decrease to pH 1.9 at 168 h. Fast decreases of pH were also observed in the cultivations with IPR, although the values were only reduced to around pH 3 within 48 h. After that, small differences were observed in the pH values, according to the solids content used in the fermentation. Therefore, addition of IPR to the medium had a negative effect on the decrease of pH, and the effect was slightly greater when higher solids contents were used. A similar trend was observed for the effect of the solids content on the titratable acidity (Fig. 3c), indicating the effect of solids content or soluble Al on the production of organic acids by *A. niger*, in agreement with Papagianni et al. [11]. Consequently, the efficiency of solubilization of PR decreased, as shown in Fig. 3d.

In order to minimize the inhibitory effects of the IPR during *A. niger* cultivation and increase the solubilization of P, two process strategies were investigated: sequential solubilization, and solubilization with fed-batch addition of solids. In the sequential solubilization strategy, the main objective was to optimize organic acid production in the first stage, by cultivation of *A. niger* without IPR, which was then followed by the solubilization of IPR in the second stage. Therefore, *A. niger* was cultivated without IPR for 144 h and the acid extract obtained was used for solubilization of the IPR during a further 24 h, totaling 168 h. Fig. 4 compares the results with those obtained for conventional solubilization with and without mechanical activation. The solubilization efficiency decreased with the solids content, despite slight increases in solubilized P, in agreement with the results shown in Fig. 3d. The use of mechanical activation resulted in a large increase in solubilized P, compared to the process without activation. However, the conventional process using mechanical activation showed no significant difference (Tukey's test, 95% confidence level) in the solubilization efficiency, compared to the sequential process with mechanical activation.
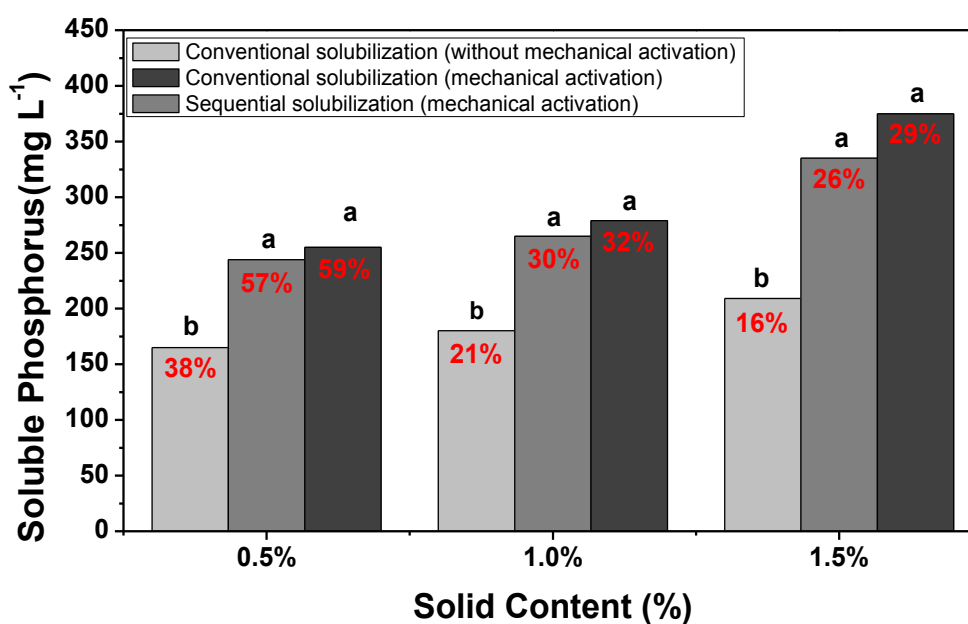
Figure 4. Phosphorus solubilized by sequential solubilization and conventional solubilization with and without mechanical activation, using three solids contents. Different letters indicate significant differences among treatments (Tukey's test, 95% confidence level).

In the fed-batch strategy, the IPR was added at predetermined times, with four additions (at 48, 72, 96, and 120 h) of 2.5 g L^{-1}, totaling 10 g L^{-1} of solids. The goal of this strategy was to optimize the organic acid production in the first 48 h, with subsequent additions of small amounts of solid throughout the cultivation, in order to reduce the inhibition effect. The temporal profiles for IPR solubilization, microbial biomass, pH, and titratable acidity using the fed-batch strategy are shown in Fig. 5.

The IPR solubilization efficiency (Fig. 5a) increased to 37% (320 mg L^{-1}) at 168 h, which was statistically superior (Tukey's test, 95% confidence level) to the efficiency achieved under sequential solubilization (30%) and conventional solubilization (32%), using the same solids content of 10 g L^{-1}. The temporal profile (Fig. 5b) for the first 48 h was similar to that for the process carried out without IPR, indicating an absence of inhibitory effects. However, after the first IPR addition, the biomass concentration in the medium decreased by 25%, the pH increased to 3, and the total acidity remained constant until the end of the cultivation.

These results showed that use of the fed-batch strategy in the IPR solubilization process led to improved solubilization efficiency, compared to the conventional simultaneous process.

The amount of P solubilized increased by 15%, relative to the conventional process (with mechanical activation), and by 21%, relative to the sequential solubilization, for a load of 10 g L^{-1} solids consisting of mechanically activated rock. Moreover, when compared with the conventional process using IPR without mechanical activation, a substantial improvement of 78% in solubilization efficiency was achieved using the integrated fed-batch process and mechanical activation.
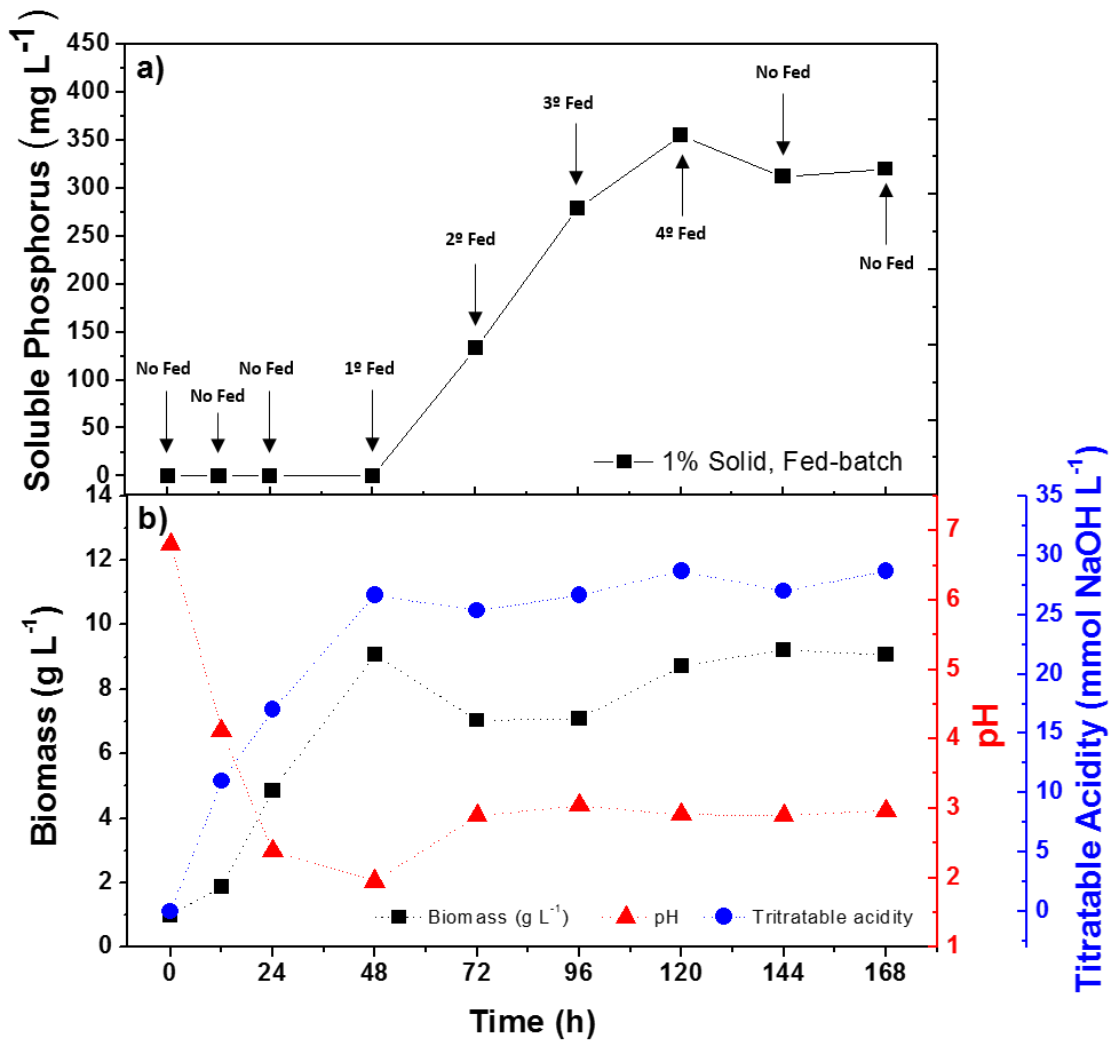
Figure 5. Effect of fed-batch addition of solids during the submerged cultivation of *A. niger* at 30 °C, 220 rpm, and pH$_{initial}$ 7. **a)** Soluble phosphorus, **b)** biomass, pH, and titratable acidity.

The solubilization achieved using the fed-batch addition of solids/mechanical activation strategy could be considered highly promising, when compared with the results reported elsewhere for conventional processes and similar PR (igneous origin). Saber et al. [17] cultivated *A. niger* under SmC using a similar igneous PR (fluorapatite rock from Giza, Egypt) and obtained 99.7 mg L^{-1} of soluble phosphorus after 216 h. Schneider et al. [21], using similar conditions, obtained 281 mg L^{-1} of soluble phosphorus after 192 h of cultivation using hydroxyapatite rock from Catalão, Brazil. Mendes et al. [24] also cultivated *A. niger* under SmC, using Araxá rock from Brazil, and obtained 74.4 mg L^{-1} of soluble phosphorus after 144 h. In this work, the maximum soluble P concentration obtained was about 350 mg L^{-1} after a process time of only 120 h. These findings showed that the fed-batch addition of solids/mechanical activation strategy was able to minimize the inhibitory effect and increase phosphate solubilization.

4. Conclusions

Bioprocess strategies were developed for improving the efficiency of solubilization of IPR. Use of a fed-batch strategy coupled with mechanical activation led to a 78% increase in solubilization, compared to a conventional process. Mechanical activation was proved to be a potential strategy for increasing the solubilization of IPR, with solubility gains of around 57% using SmC and 45% using SSC, employing IPR milled for only 10 min. Investigation of the influence of the solids content on microbial biomass, total acidity, and pH revealed negative effects on these variables, when compared to the process without phosphate rock. Such limitations were overcome by employing the fed-batch addition of solids, resulting in increased IPR solubilization. This proposed strategy could contribute to future developments aimed at implementing large-scale industrial production of environmentally sustainable phosphate fertilizers by biotechnological processes.

Supporting Information

Section 1 shows mineralogical analysis calculations. Section 2, Figure S1. X-ray diffractometry (XRD) pattern of Itafós phosphate rock; Figure S2. Field emission gun scanning electron microscopy (FEG-SEM) micrographs and specific surface area of Itafós rock phosphate subjected too different milling times; Figure S3. Temporal profiles of calcium,

aluminum and iron solubilization by submerged cultivation; Figure S4. Temporal profiles of phosphorus solubilization and pH by submerged cultivation.

References

(1)   Vassilev, N.; Vassileva, M., Biotechnological solubilization of rock phosphate on media containing agro-industrial wastes. *Applied Microbiology and Biotechnology* **2003,** *61* (5-6), 435-440.

(2)   Vassilev, N.; Vassileva, M.; Lopez, A.; Martos, V.; Reyes, A.; Maksimovic, I.; Eichler-Loebermann, B.; Malusa, E., Unexploited potential of some biotechnological techniques for biofertilizer production and formulation. *Applied Microbiology and Biotechnology* **2015,** *99* (12), 4983-4996.

(3)   Mao, X. Y.; Lu, Q.; Mo, W.; Xin, X. P.; Chen, X.; He, Z. L., Phosphorus Availability and Release Pattern from Activated Dolomite Phosphate Rock in Central Florida. *Journal of Agricultural and Food Chemistry* **2017,** *65* (23), 4589-4596.

(4)   Everaert, M.; Warrinnier, R.; Baken, S.; Gustafsson, J. P.; De Vos, D.; Smolders, E., Phosphate-Exchanged Mg-Al Layered Double Hydroxides: A New Slow Release Phosphate Fertilizer. *Acs Sustainable Chemistry & Engineering* **2016,** *4* (8), 4280-4287.

(5)   Benicio, L. P. F.; Constantino, V. R. L.; Pinto, F. G.; Vergutz, L.; Tronto, J.; da Costa, L. M., Layered Double Hydroxides: New Technology in Phosphate Fertilizers Based on Nanostructured Materials. *Acs Sustainable Chemistry & Engineering* **2017,** *5* (1), 399-409.

(6)   Vassilev, N.; Vassileva, M.; Nikolaeva, I., Simultaneous P-solubilizing and biocontrol activity of microorganisms: potentials and future trends. *Applied Microbiology and Biotechnology* **2006,** *71* (2), 137-144.

(7)   Vassileva, M.; Serrano, M.; Bravo, V.; Jurado, E.; Nikolaeva, I.; Martos, V.; Vassilev, N., Multifunctional properties of phosphate-solubilizing microorganisms grown on agro-industrial wastes in fermentation and soil conditions. *Applied Microbiology and Biotechnology* **2010,** *85* (5), 1287-1299.

(8)   Mendes, G. D.; de Freitas, A. L. M.; Pereira, O. L.; da Silva, I. R.; Vassilev, N. B.; Costa, M. D., Mechanisms of phosphate solubilization by fungal isolates when exposed to different P sources. *Annals of Microbiology* **2014,** *64* (1), 239-249.

(9)   Kpomblekoua, K.; Tabatabai, M. A., Effect of organic-acids on release of phosphorus from phosphate rocks. *Soil Science* **1994,** *158* (6), 442-453.

(10)   Illmer, P.; Schinner, F., Solubilization of inorganic calcium phosphates—Solubilization mechanisms. *Soil Biology and Biochemistry* **1995,** *27* (3), 257-263.

(11)   Papagianni, M., Advances in citric acid fermentation by Aspergillus niger: Biochemical aspects, membrane transport and modeling. *Biotechnology Advances* **2007,** *25* (3), 244-263.

(12)   Klaic, R.; Plotegher, F.; Ribeiro, C.; Zangirolami, T. C.; Farinas, C. S., A novel combined mechanical-biological approach to improve rock phosphate solubilization. *International Journal of Mineral Processing* **2017,** *161*, 50-58.

(13)   Li, Z.; Bai, T. S.; Dai, L. T.; Wang, F. W.; Tao, J. J.; Meng, S. T.; Hu, Y. X.; Wang, S. M.; Hu, S. J., A study of organic acid production in contrasts between two phosphate solubilizing fungi: *Penicillium oxalicum* and *Aspergillus niger*. *Scientific Reports* **2016,** *6*.

(14)   Hamdali, H.; Bouizgarne, B.; Hafidi, M.; Lebrihi, A.; Virolle, M. J.; Ouhdouch, Y., Screening for rock phosphate solubilizing Actinomycetes from Moroccan phosphate mines. *Applied Soil Ecology* **2008,** *38* (1), 12-19.

(15)   Morales, A.; Alvear, M.; Valenzuela, E.; Castillo, C. E.; Borie, F., Screening, evaluation and selection of phosphate-solubilising fungi as potential biofertiliser. *Journal of Soil Science and Plant Nutrition* **2011,** *11* (4), 89-103.

(16)   Nautiyal, C. S., An efficient microbiological growth medium for screening phosphate solubilizing microorganisms. *Fems Microbiology Letters* **1999,** *170* (1), 265-270.

(17)   Saber, W. I. K.; Ghanem, K. M.; El-Hersh, M. S., Rock phosphate solubilization by two isolates of *Aspergillus niger* and *Penicillium* sp. and their promotion to mung bean plants. *Research Journal of Microbiology* **2009,** *4* (7), 235-250.

(18)   Haq, I.-U.; Ali, S.; Iqbal, J., Direct production of citric acid from raw starch by Aspergillus niger. *Process Biochemistry* **2003,** *38* (6), 921-924.

(19)   Bhattacharya, S.; Das, A.; Bhardwaj, S.; Rajan, S. S., Phosphate solubilizing potential of Aspergillus niger MPF-8 isolated from Muthupettai mangrove. *Journal of Scientific & Industrial Research* **2015,** *74* (9), 499-503.

(20)   Srividya, S.; Soumya, S.; Pooja, K., Influence of environmental factors and salinity on phosphate solubilization by a newly isolated *Aspergillus niger* F7 from agricultural soil. *African Journal of Biotechnology* **2009,** *8* (9), 1864-1870.

(21)   Schneider, K. D.; van Straaten, P.; de Orduna, R. M.; Glasauer, S.; Trevors, J.; Fallow, D.; Smith, P. S., Comparing phosphorus mobilization strategies using *Aspergillus niger* for the mineral dissolution of three phosphate rocks. *Journal of Applied Microbiology* **2010,** *108* (1), 366-374.

(22)   Mendes, G. O.; Dias, C. S.; Silva, I. R.; Ribeiro, J. I.; Pereira, O. L.; Costa, M. D., Fungal rock phosphate solubilization using sugarcane bagasse. *World Journal of Microbiology & Biotechnology* **2013,** *29* (1), 43-50.

(23)   Xiao, C.-Q.; Chi, R.-A.; Huang, X.-H.; Zhang, W.-X.; Qiu, G.-Z.; Wang, D.-Z., Optimization for rock phosphate solubilization by phosphate-solubilizing fungi isolated from phosphate mines. *Ecological Engineering* **2008,** *33* (2), 187-193.

(24)   Mendes, G. D.; Galvez, A.; Vassileva, M.; Vassilev, N., Fermentation liquid containing microbially solubilized P significantly improved plant growth and P uptake in both soil and soilless experiments. *Applied Soil Ecology* **2017,** *117*, 208-211.

(25)   Plotegher, F.; Ribeiro, C., Characterization of Single Superphosphate Powders - a study of Milling Effects on Solubilization Kinetics. *Materials Research-Ibero-American Journal of Materials* **2016,** *19* (1), 98-105.

(26)   Pikvoskaya. Mobilization of phosporus in soil connection with the vital activity of some microbial species 1948, p. 362-370.

(27)   Murphy, J.; Riley, J. P., Citation-classic - a modified single solution method for the determination of phosphate in natural-waters. *Current Contents/Agriculture Biology & Environmental Sciences* **1986,** (12), 16-16.

(28)   Chien, S. H., Solubility assessment for ferlilizer containing phosphate rock. *Fertilizer Research* **1993,** *35* (1-2), 93-99.

(29)   Tribble, J. S.; Arvidson, R. S.; Lane, M.; Mackenzie, F. T., Crystal-chemistry, and thermodynamic and kinetic-properties of calcite, dolomite, apatite, and biogenic silica - applications to petrologic problems. *Sedimentary Geology* **1995,** *95* (1-2), 11-37.

(30)   Tonsuaadu, K.; Gross, K. A.; Pluduma, L.; Veiderma, M., A review on the thermal stability of calcium apatites. *Journal of Thermal Analysis and Calorimetry* **2012,** *110* (2), 647-659.

(31)   Talbot, D. E. J.; Talbot, J. D. R., *Corrosion Science and Technology*. CRC Press: 1998.

(32)   Motekaitis, R. J.; Martell, A. E., Complexes of aluminum(iii) with hydroxy carboxylic-acids. *Inorganic Chemistry* **1984,** *23* (1), 18-23.

(33)   Smith, R. M.; Martell, A. E., Critical stability-constants, enthalpies and entropies for the formation of metal-complexes of aminopolycarboxylic acids and carboxylic-acids. *Science of the Total Environment* **1987,** *64* (1-2), 125-147.

(34)   Xiao, C. Q.; Wu, X. Y.; Liu, T. T.; Xu, G.; Chi, R., Optimizations of particle size and pulp density for solubilization of rock phosphate by a microbial consortium from activated sludge. *Preparative Biochemistry & Biotechnology* **2017,** *47* (6), 562-569.

(35)   Mendes, G. d. O.; Bojkov Vassilev, N.; Araujo Bonduki, V. H.; da Silva, I. R.; Ribeiro, J. I., Jr.; Costa, M. D., Inhibition of Aspergillus niger Phosphate Solubilization by Fluoride Released from Rock Phosphate. *Applied and Environmental Microbiology* **2013,** *79* (16), 4906-4913.

(36)   Silva, U. D.; Mendes, G. D.; Silva, N.; Duarte, J. L.; Silva, I. R.; Totola, M. R.; Costa, M. D., Fluoride-Tolerant Mutants of Aspergillus niger Show Enhanced Phosphate Solubilization Capacity. *Plos One* **2014,** *9* (10), 9.

Supporting Information

Section 1

Mineralogical analysis calculations

Considering that all the fluoride determined comes only from the fluorapatite phase we can calculate the molar fractions of each element.

Chemical structure fluorapatite ($Ca_5(PO_4)_3F$)

Molar fraction of fluoride (X_F), phosphorus (X_P) and calcium (X_{Ca}):

$$X_P = \frac{MM_{Fluoride}}{MM_{Fluorapatire}} = \frac{19}{504} = 0.0377$$

$$X_P = \frac{MM_{Phosphorus}}{MM_{Fluorapatire}} = \frac{93}{504} = 0.1850$$

$$X_P = \frac{MM_{Calcium}}{MM_{Fluorapatire}} = \frac{200}{504} = 0.3970$$

Making the ratio R_{Fa} between the two molar fractions will have the molar ratio between fluoride and calcium in fluoropatite.

$$R_{FCa} = \frac{X_F}{X_{Ca}} = \frac{0.0377}{0.3970} = 0.0950$$

Having the value of the ratio and the amount of fluoride determined by the technique we can calculate the amount of calcium that makes up the fluorapatite.

$$\frac{F}{Ca} = R_{FCa} = \frac{1.87\%}{Ca} = 0.0950 \longrightarrow Ca = 19.68\%$$

Transforming this value into calcium oxide.

$$CaO_{Fa} = \frac{Ca * 56}{40} = 27.56\%$$

Subtracting the amount of calcium oxide to fluorapatite CaO$_{Fa}$ form the total value CaO$_{Total}$ determined will have the percentage of calcium oxide in other phases.

$$CaO_{Other\ phases} = CaO_{Total} - CaO_{Fa} = 30.40\% - 27.56\% = 2.84\%$$

Making the ratio of fluoride to phosphorus we can determine the amount of phosphorus that comes from this phase.

$$R_{FP} = \frac{X_F}{X_P} = \frac{0.0377}{0.1840} = 0.2050$$

Based on the fluoride content, we determine the amount of phosphorus in this phase.

$$\frac{F}{P} = R_{FP} = \frac{1.87\%}{P} = 0.205 \longrightarrow P = 9.12\%$$

Transforming this value into phosphorus peroxide.

$$P_2O_{5_{Fa}} = \frac{9.12 * 142}{62} = 20.89\%$$

Adding the percentages determined for the fluorapatite phase will have the mass quantity that it represents inside the phosphate rock.

$$\%Fa = \% F + \% CaO_{Fa} + \% P_2O_{5_{Fa}} = 1.87\% + 27.56\% + 20.89\% = 50.32\%$$

Section 2

Figures
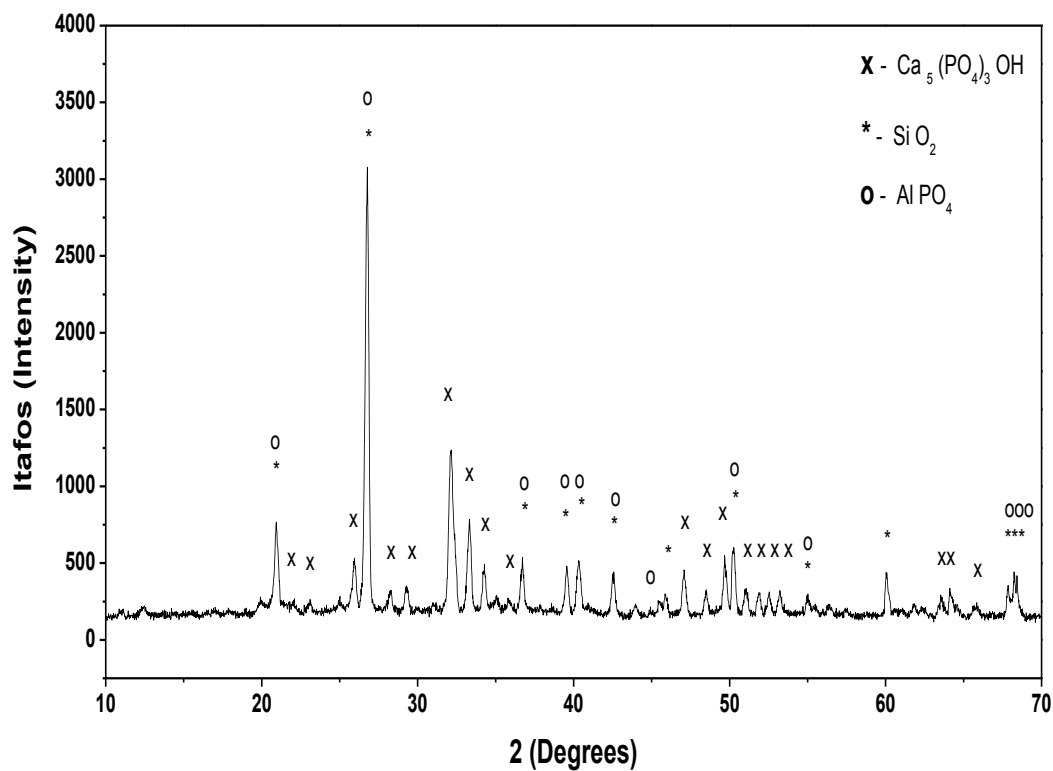
Figure S1. X-ray diffractometry (XRD) pattern of original (not milled) Itafósphosphate rock [**X** - $Ca_5(PO_4)_3(OH)$, PDF2 pattern file #01-086-0740; * - SiO_2, PDF2 pattern file #01-089-8934; ^{0} - $AlPO_4$, PDF2 pattern file #01-076-0228]
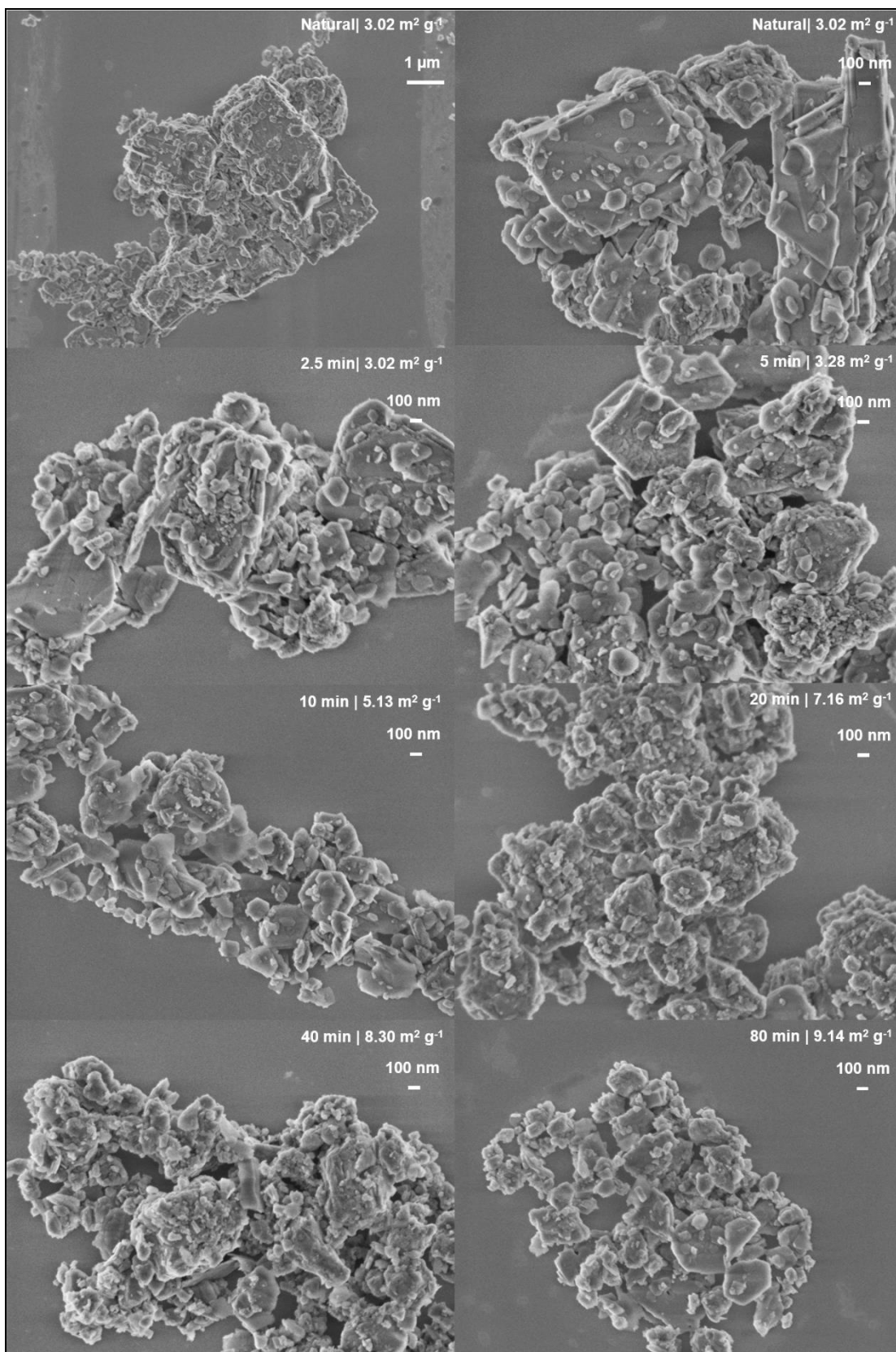
Figure S2. Field emission gun scanning electron microscopy (FEG-SEM) micrographs and specific surface area of Itafós rock phosphate subjected too different milling times.
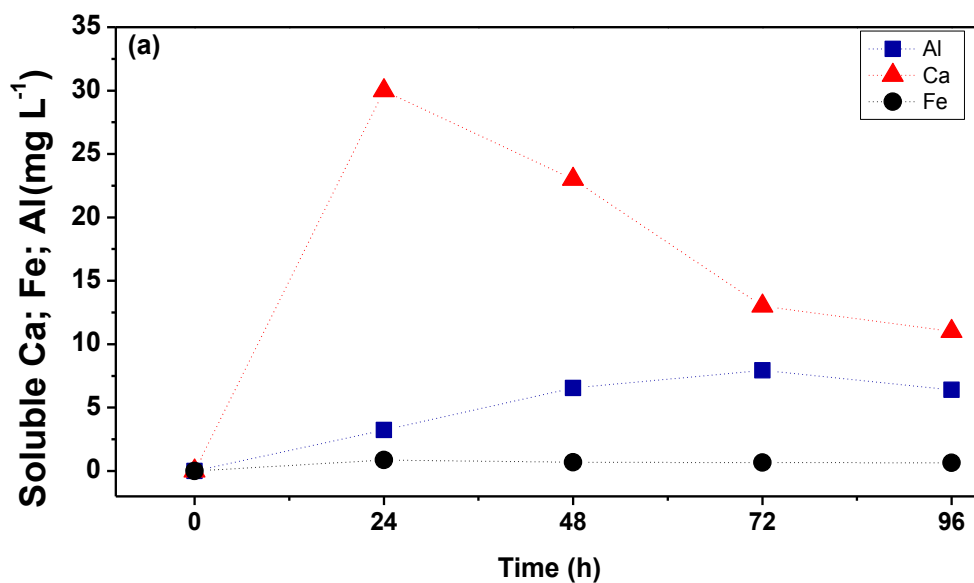
Figure S3. Temporal profiles of calcium, aluminum and iron solubilization by submerged cultivation at 96 h, 30 °C, 220 rpm, $pH_{initial}$ 7 and 5 g L^{-1} IPR (5.13 m^2 g_{rock}^{-1}).
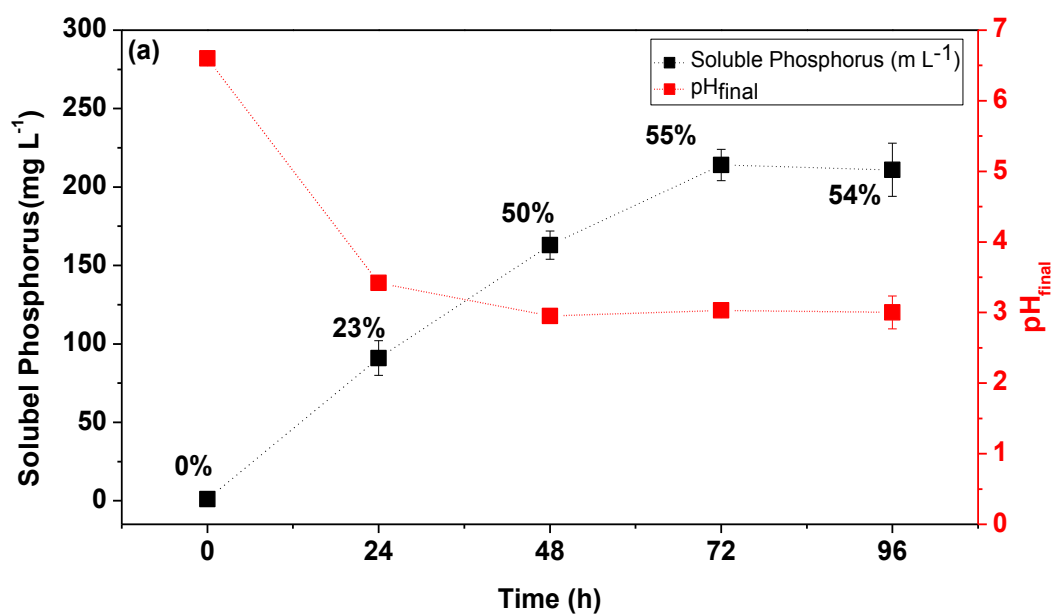
Figure S4. Temporal profiles of phosphorus solubilization and pH by submerged cultivation at 96 h, 30 °C, 220 rpm, $pH_{initial}$ 7 and 5 g L^{-1} IPR (5.13 m^2 g_{rock}^{-1}).

Capítulo 4

"Solubilization of phosphate rocks by organic acids"

Artigo em elaboração

O principal mecanismo de solubilização das rochas fosfáticas pela ação de microrganismo é a produção de ácidos orgânicos. Nesse sentido, entender o processo de solubilização de diferentes rochas fosfáticas por diferentes ácidos orgânicos é essencial para desenvolver estratégias para aumentar a eficiência de solubilização da rocha fosfática via cultivo microbiano, uma vez que o metabolismo do microrganismo pode ser manipulado para produção do ácido orgânico de interesse. Dessa forma, este estudo tem por objetivo avaliar a solubilização de três fontes de fosfatos utilizando nove ácidos orgânicos diferentes, comparando com dois ácidos inorgânicos fortes e com a solubilização em água. O fosfato de tricácio foi usado como material referência de alta solubilidade para comparação com duas rochas fosfáticas de características contrastantes, a rocha fosfática Bayóvar (origen sedimentar) e a rocha fosfática Itafós (origen ígnea), já caracterizadas e estudadas, respectivamente nos Capítulos 2 e 3. Os resultados mostraram diferentes eficiências de solubilização entre os ácidos utilizados e entre as fontes de fosfatadas. Os acidos orgânicos cítrico e principalmente o ácido oxálico foram os ácidos orgânicos mais eficientes para promover a solubilização das fontes fosfatadas. Nesse contexto, um estudo avaliando o sinergismo entre os ácidos orgânicos e a cinética de solubilização das fontes fosfatadas nos ácidos também foi realizado e observou-se uma relação de sinergismo entre ácido cítrico e oxálico (1:1) e entre ácido oxálico e gluconico (2:1) que potencializou a solubilização das rochas fosfáticas. Este estudo se refere ao objetivo específico 4: Avaliação da influência de diferentes ácidos orgânicos na solubilização de diferentes fontes de fosfato. Estes resultados fornecem um melhor entendimento dos mecanismos de ação dos ácidos orgânicos na solubilização/dissolução das rochas fosfáticas.

Abstract

The biological solubilization of phosphate rock (PR) is an attractive alternative to obtain fertilizers from biotechnological process. This method consists on the use of P-solubilizing microorganisms (PSMs), which can be cultivated by submerged cultivation or solid-state cultivation. The P-solubilizing activity of PSMs is determined by their ability to produce and release metabolites such as organic acids. However, the effectiveness of the biological solubilization of PRs depends on the type of the organic acid produced during the microbial cultivation. Therefore, a systematic study on the solubilization of PRs was carried out using nine organic acids of low molecular mass as well as two inorganic acid and water. Three phosphates sources were evaluated, including two PRs and a reference mineral. Our findings showed that the type of organic acid can significantly influence the solubilization of the PR, being that oxalic acid showed the best performance to promote the PR solubilization. In addition, a synergistic relationship between citric and oxalic acids, and between gluconic and oxalic acids was observed, which potentiated the solubilization of the PRs, compared with the same concentration of sole organic acids. The results provided a better understanding of the mechanisms of action of organic acids on the dissolution of PRs.

1. Introduction

The biological solubilization of phosphate rock (PR) is an attractive alternative to obtain fertilizers by using processes that are more environmentally sustainable. This method consists on the use of P-solubilizing microorganisms (PSMs), which can be cultivated in aerated suspensions (submerged cultivation), or using solid media (solid-state cultivation) (Mendes et al., 2015; Vassilev et al., 2017; Vassileva et al., 2010). The P-solubilizing activity of PSMs is determined by their ability to produce and release metabolites such as organic acids. However, the effectiveness of the biological solubilization of PRs depends of type of the organic acid produced (Park et al., 2017), since each organic acids have different characteristics and properties such as degree of dissociation, position and type of functional groups, and chemical affinities of chelating agents for the metals (Illmer & Schinner, 1995; Kpomblekoua & Tabatabai, 1994; Lazo et al., 2017; Mendes et al., 2014; Nahas, 1996).

In addition, the effect of organic acid on PR dissolution may change in relation to the origin of the phosphate mineral (sedimentary or igneous origin) (Lazo et al., 2017) due to the physical and chemical differences of these PR (Chien, 1993; Lim et al., 2003; McArthur, 1985; McArthur et al., 1986; Zapata, 2004). It is therefore reasonable to assume that studies on P-solubilization using distinct types of phosphate minerals are necessary to understanding the mechanisms of action of organic acids on the dissolution of the PRs. Such understanding would allow the development of strategies to improve the efficiency of biological solubilization of the PR. For instance, metabolic engineering studies could be applied to manipulate the metabolism of microorganisms in order to produce the higher levels of the organic acid specific for the solubilization of each phosphate mineral.

Here, a systematic study on the solubilization of PRs in organic acids of low molecular mass was carried out. Three different mineral phosphates were used, including two phosphate rocks (Bayóvar phosphate rock, sedimentary origin and Itafós phosphate rock, igneous origin) and a reference mineral (tricalcium phosphate). The solubilization experiments were performed using nine organic acids with different properties, and the results were compared with two strong inorganic acids and water. The kinetics of solubilization of these minerals and the synergism effects among selected organic acids were also studied by using the methodology of experimental mixture design as a statistical tool. The results provided a better understanding of the mechanisms of action of organic acids on the dissolution of PRs of different origins.

2. Materials and Methods

2.1. Organic acids

The organics acids (ascorbic, acetic, formic, gluconic, malic, succinic, oxalic, tartaric and citric acid) were supplied by Sigma-Aldrich (acids with pure phase $\geq$ 99 wt.%, except gluconic acid with a pure phase of 49-53%). The inorganic acids used were sulfuric acid (95-98% purity) and hydrochloric acid (36.5-38% purity), supplied by Synth and Dinamica, respectively.

2.2. Phosphate materials

The phosphate sources used were tricalcium phosphate (TCP) supplied by Synth with 43.46 wt.% P_2O_5, Bayóvar phosphate rock (BPR), which is a sedimentary rock originate from Sechura (Peru) with 30.72 wt.% P_2O_5 (Klaic et al., 2017) and Itafós phosphate rock (IPR), which is an igneous rock originate from Arraias (Brazil) with 20.29 wt.% P_2O_5. The two phosphate rocks were dried at 110 ºC for 48 h to reduce the humidity contents and were then ground for 10 min in an orbital mill (model CT-251, Servitec) consisting of a porcelain jar and alumina balls (Plotegher & Ribeiro, 2016). After treatment, the materials were stored in dry boxes prior to use in the solubilization experiments.

2.3. Solubilization assays

The solubilization experiments were carried out using the methodology recommended by Ministry of Agriculture and Livestock from Brazil (MAPA, 2013) to evaluate the solubility of phosphate rocks. All acid solutions were standardized relative to the citric acid solution 2 wt.% (0.104 mol L^{-1}). The total phosphorus added was also standardized to 0.886 g L^{-1} for all phosphate materials. Thus the mass added for TCP, BPR and IPR was 0.10 g, 0.33 g and 0.50 g, respectively. The experiments of solubilization were performed in 250 mL Erlenmeyer flasks, containing 50 mL of the acidic solution and the phosphate material. The solubilization was carried out for 6 h in an orbital shaker incubator (Innova 42), at 30 °C and 220 rpm. All the experiments were performed in triplicate. After the incubation period, the resulting material was vacuum filtered through Whatman No. 1 filter paper, followed by centrifugation for 15 min at 10,000 rpm and 20 °C. The clear supernatant was analyzed using the colorimetric method described in Section 2.6 to determine the amount of soluble

phosphorus released. All experiments were carried out in triplicate, and the data were calculated as means ± standard deviations.

2.4. Kinetic solubilization

The experiments to determine the temporal profile of solubilization were carried out as described in Section 2.3, but collecting samples at 6 h, 12 h and days 1, 2, 3, 4, 5, 7, 10 and 15. The phosphorus solubilized in the liquid fraction was determined as described in the Section 2.6. All experiments were carried out in triplicate, and the data were calculated as means ± standard deviations.

2.5. Experimental design

To evaluate the synergistic effect among the organic acids on the solubilization of the phosphate materials it was applied as statistical tool the methodology of experimental mixture design (EMD) set up as a *Simplex Centroid Design* of three components (Delabona et al., 2013). This methodology can evaluate the effect/synergism of three organic acids (X_1: citric acid, X_2: oxalic acid and X_3: gluconic acid). The experimental design comprised 12 experiments, including 3 center points. The randomized conditions for these experiments is presented in Table 1. The experiments were carried out as described in Section 2.3 at triplicate and phosphorus solubilized in the liquid fraction was determined as described in the Section 2.6. All the EMD and analysis was performed with Statistica® 8.0 statistical software (Statsoft Inc., Tulsa, OK, USA).

2.6. Determination of soluble phosphorus

The determination of phosphorus solubilized was based on the method reported by Murphy and Riley (1986) and modified by Drummond and Maher (1995). Briefly, a 5 mL aliquot of the clear supernatant sample was reacted with 2 mL of ascorbic acid solution (0.4 mol L^{-1}), 0.2 mL of citric acid (0.03 mol L^{-1}), and 2 mL of a reagent consisting of 25 mL of a sulfuric acid solution (4.7 mol L-1), 5.5 mL of ammonium molybdate solution (0.08 mol L^{-1}), and 0.6 mL of antimony and potassium tartrate solution (0.05 mol L^{-1}). This mixture was reacted at 50 °C for 15 min, forming a phosphoantimonylmolybdenum blue complex. The

concentration of the complex was determined by UV-Vis spectrometry at a wavelength of 880 nm.

3. Results and Discussion

3.1. Effect of the type of organic acids on phosphate solubilization

Figure 1 shows the solubility of three phosphate materials on twelve different media after 6 h of incubation at 30 °C under low agitation (40 rpm). The tricalcium phosphate was used as a reference material and the results were compared with two mineral phosphates, BPR and IPR. The media used were nine different organics acids (ascorbic, acetic, formic, gluconic, malic, succinic, oxalic, tartaric and citric acid) as well as two inorganic acids (sulfuric and hydrochloric acid). The water was used as a control owing the low solubility of these phosphate materials in this medium. The main idea of this set of solubilization experiments was to identify the organic acids with high potential for solubilization of each type of mineral phosphate.

Tricalcium phosphate TCP solubility (Figure 1a) was above 40% for all the different acids evaluated. The highest solubilization among the organic acids was observed in citric and tartaric, reaching 80% and 75%, respectively. Notably, these solubilization efficiencies are statistically the same as the ones achieved by the inorganic acids (sulfuric and hydrochloric acid). In addition, the organic acids gluconic, oxalic and succinic also showed a solubilization efficiency statistically similar to the one of sulfuric acid. Thus, the results show that there is a large amount of organic acids with potential to solubilize TCP, since they showed a solubilization comparable to strong inorganic acids.
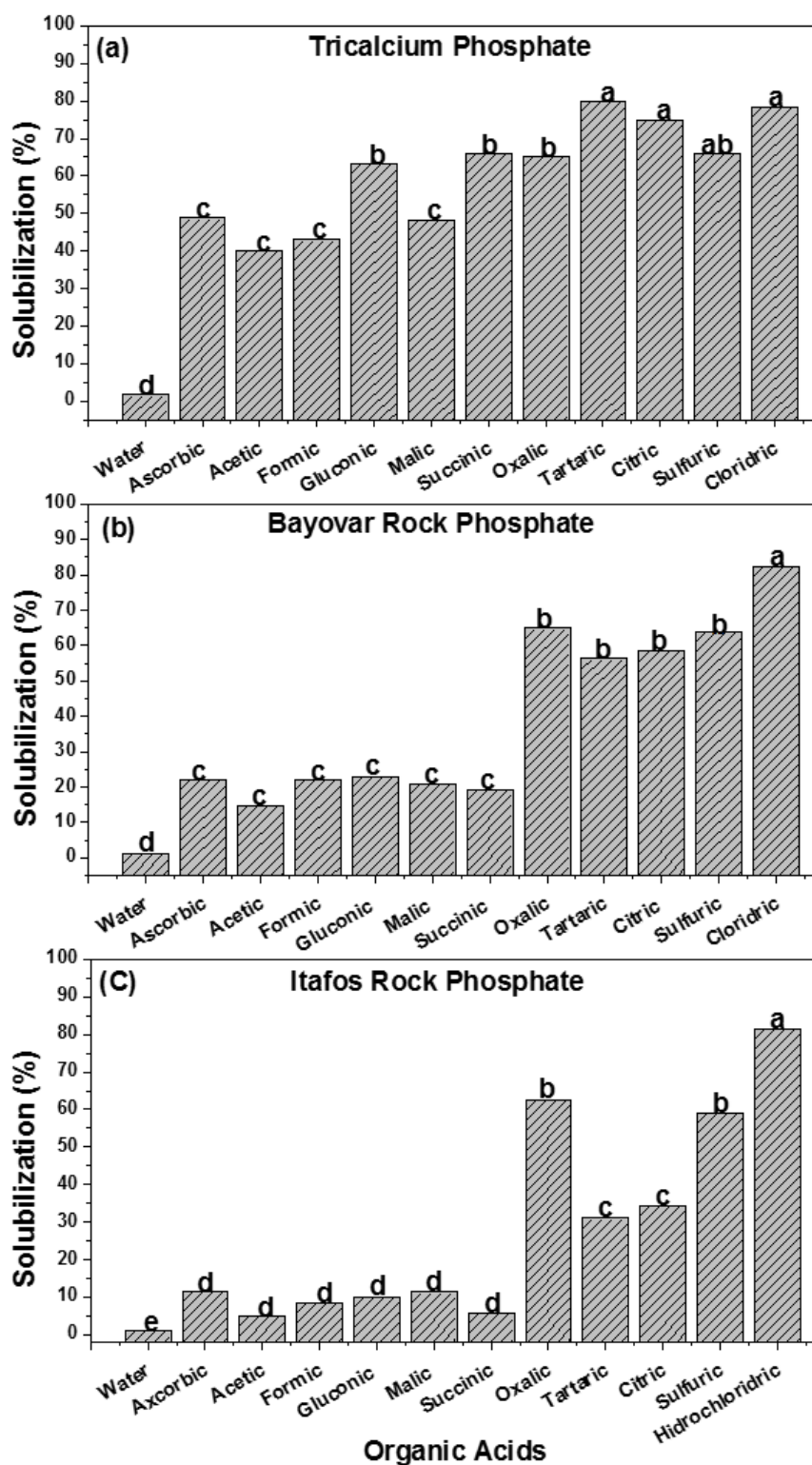
Figure 1. Efficiency solubilization of phosphate materials in organic acids at 40 rpm, 30 °C for 6 h. **a)** Tricalcium phosphate. **b)** Bayóvar rock phosphate. **c)** Itafós rock phosphate. Different letters indicate significant difference among the treatments (ANOVA with Tukey's test, 95% confidence level).

Bayóvar phosphate rock (BPR) presented an average solubilization of 60% in citric, oxalic and tartaric acids (Figure 1b), which is statistically similar to the one achieved in sulfuric acid. Maximum BPR solubilization was achieved using hydrochloric acid (82%), while in organic acids ascorbic, acetic, formic, gluconic, malic and succinic was only around 20%. For all organic acids tested, it was observed a lower solubilization efficiency for BPR when compared to TCP, except for oxalic acid. This difference in the solubility can be explained mainly by differences in chemical structure between BPR and TCP, since BPR is a natural phosphate with two crystalline phases of high chemical stability (Cao & Harris, 2008; Green & Watson, 1982) - one corresponding to alpha-quartz and another corresponding to a phosphate-rich fluorapatite phase (Klaic et al., 2017) - TCP can be easily solubilized at pH close to 4 (Bengtsson et al., 2007).

For the Itafós phosphate rock (IPR), oxalic acid was the best organic acid to promote the solubilization, reaching a solubilization of 60% which was statistically similar to the one achieved using sulfuric acid (Figure 1c). The hydrochloric acid also promoted the highest solubilization, as previously observed for BPR and TCP. In addition, the IPR solubilization in citric and tartaric acid was around 30% and in ascorbic, formic, acetic, gluconic, succinic and malic did not exceed 10%. The results show that there is a greater difficulty to promote the P solubilization from the IPR than from the BPR. This can also be explained by the difference in the chemical structure of these materials. Although both rocks have a complex composition, IPR is a mineral of igneous origin and has a higher amount of quartz and a fluoropatide phase with less isomorphic substitutions compared to the BPR (Chien, 1993; Lim et al., 2003; McArthur, 1985; McArthur et al., 1986; Zapata, 2004). This makes the IPR harder and more difficult to solubilize compared to BPR.

In overall, these results showed that the type de organic acid has a great influence in the solubilization of the different phosphate materials. A possible explanation for this influence is the number of hydroxyl and carboxylic groups as well as their position in the molecule of organic acid. Therefore, organic acids with more hydroxyl and carboxylic groups tend to be more efficient for promoting the P solubilization due to the better ability to chelate the cations (mainly calcium) bounded to phosphate, with the latter being converted into soluble form (Illmer & Schinner, 1995; Kpomblekoua & Tabatabai, 1994; Lazo et al., 2017; Mendes et al., 2014; Nahas, 1996). This effect was predominant for TCP, in which the monocarboxylic acids (acetic, formic, and gluconic) were less efficient than the dicarboxylic (malic, succinic,

tartaric) and tricarboxylic (citric acid) on phosphate solubilization. Interestingly, the oxalic acid, that is a dicarboxylic acid, was an exception to this behavior.

The differential solubilization response observed for oxalic acid on TCP was also reproduced for both PRs, which showed the highest potential to solubilize the PRs among the organic acids studied, with efficiencies comparable to the ones achieved using strong inorganic acids, sulfuric (used in the industrial fertilizer production process) and hydrochloric. A statistical analysis (Tukey's test, 95% confidence) showed that there was no significant difference in the solubilization efficiency of TCP, BPR and IPR when oxalic acid was used. This is even more interesting if we take into consideration that BPR and IPR are phosphate materials that present great complexity and their mineralogical structure makes their solubilization much more difficult when compared to TCP. Our hypothesis is that PRs that present the mineralogical constitution with phosphate phases of higher chemical stability - higher amount of quartz and apatites of low isomorphic substitution, such as observed in IPR - are more susceptible to be solubilized by organic acids with a higher degree of dissociation than tricarboxylic acids which are constantly cited as good promoters of solubilization, since that oxalic acid is a dicarboxylic acid (pKa1 = 1.27; Pka2 = 4.21) (Gelb, 1971) and citric acid is a tricarboxylic acid (pKa1 = 3.13 ; Pka2 = 4.76; pka3= 6.40) (Silva et al., 2009).

Although our results showed that the citric, tartaric and mainly the oxalic acid were the best acids to solubilize the mineral phosphates, previous literature studies have also reported the gluconic acid is a potential solubilizing agent for PRs (Taktek et al., 2017; Wagh et al., 2016; Xiao et al., 2015; Zhou et al., 2017) . Our results showed that gluconic acid seems to have more influence on calcium phosphate sources such as TCP, since the complexing constant of this acid with Ca is similar to the constants of citric and oxalic acid (Mendes et al., 2014). Based on these findings, a kinetics of solubilization was also performed using gluconic acid, oxalic acid and citric acid as well as sulfuric acid and water (control) to better understanding the mechanisms of solubilization involved in the action of these acidson TCP, BPR and IPR.

3.2. Temporal profiles of solubilization

Temporal profiles of P solubilization for TCP, BPR and IPR in the organic acids citric, oxalic, and gluconic acid as well as in sulfuric acid and water (control) are shown in Figure 2. The results confirm the low solubility of these phosphate mineral in water, since even after 15

days it was not exceed 1% of P solubilization for all phosphate sources. However, the P solubilization was very significant for all of the organic acids used, but different temporal profiles were observed. In addition, there was an oscillatory behavior in the P solubilization curves that may be due effects of precipitation and complexation of the phosphate (PO_4^{3-}) as other solubilized elements in solution (Ca^{2+}, Fe^{3+}, Al^{3+} and Mg^{2+}) (Bengtsson et al., 2007; Misra, 1999).

TCP solubilization (Figure 2a) showed a similar temporal profile of P solubilization in sulfuric, citric and oxalic acid reaching 100% in only 2 days, while the P solubilization in gluconic acid not exceed 80% even in 15 days. For the BPR (Figure 2b), there was no statistical difference in P solubilization during the first 6 h among sulfuric, oxalic and citric acid. After this period, the P solubilization was more intense in sulfuric acid reaching a solubilization close to 100% of P available in the BPR in only 3 days. In contrast, the P solubilization using gluconic acid not exceed 40% even in 15 days. It is also possible to observe that there was a higher solubilization rate using oxalic acid than in citric acid. Moreover, the temporal profile of solubilization in oxalic acid was only slightly lower than in sulfuric acid. As for the temporal profiles of solubilization for IPR (Figure 1c), acid citric and gluconic did not exceed 40% and 20%, respectively, even in 15 days. Interestingly, the temporal profile of solubilization of IPR using oxalic acid was similar to when BPR was used. Considering that IPR is a P source more complex than BPR, this indicates that oxalic acid has a better potential than citric acid to solubilize complex sources of phosphorus.

The solubilization time profile helped to confirm the positive effect of citric acid and especially of oxalic acid as phosphorus solubilizing promoting agents from complex mineral sources. Although the superior effect of oxalic acid compared to citric acid and gluconic acid is proven, these acids are produced by the same metabolic cycle (Krebs cycle) and many times when it is desired to optimize oxalic acid production during microbial cultivation there may be co-production of citric and gluconic acids (Sazanova et al., 2016; Yang et al., 2017). Therefore, due to the different characteristics and properties of these organic acids, a study was developed in the next set of experiments to evaluate the mixing effect on the solubilization of TCP, BPR and IPR.
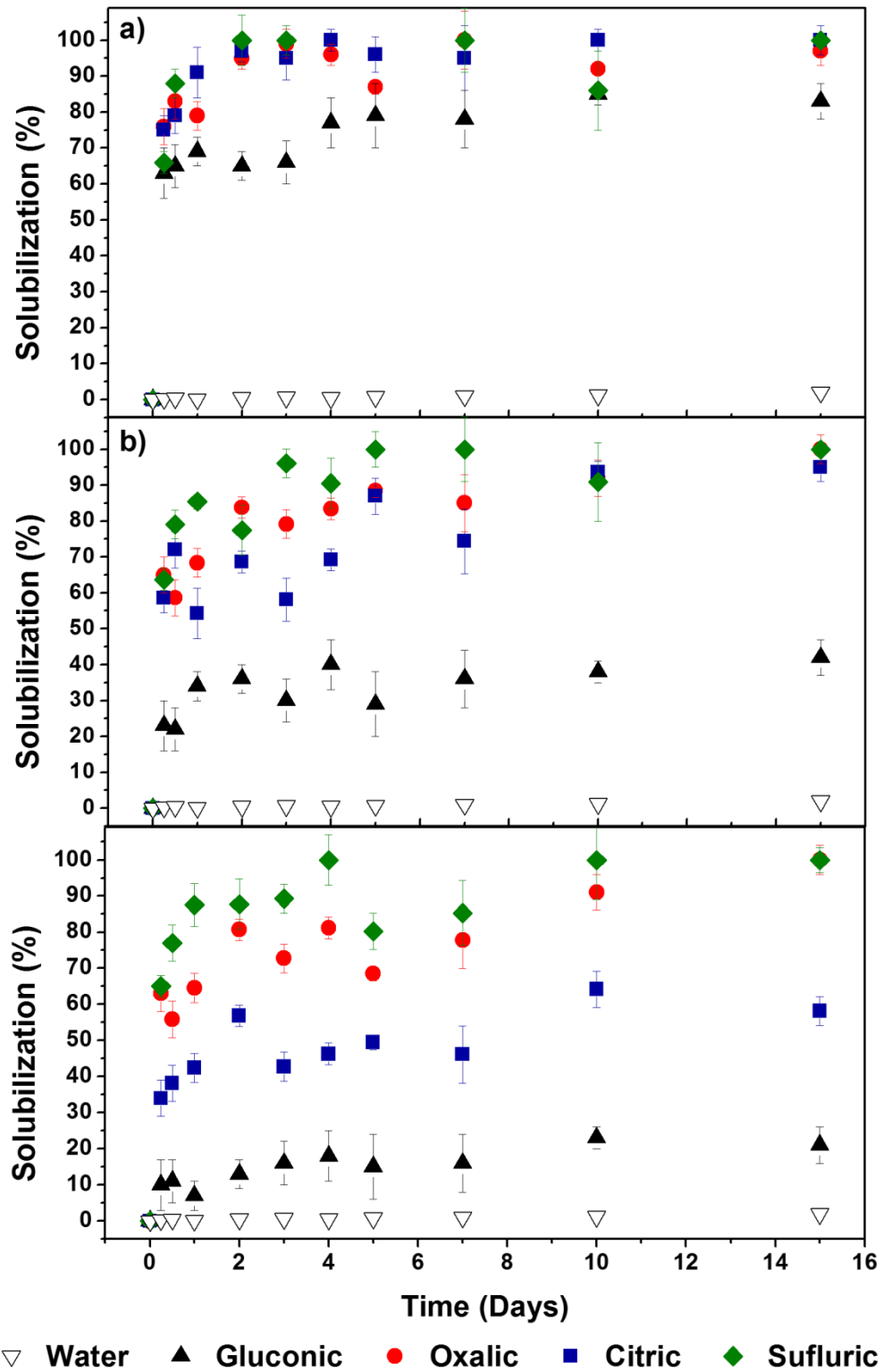
Figure 2. Temporal profiles of phosphorus solubilization in citric, oxalic, gluconic sulfuric acid and water at 30 °C and 40 rpm. **a)** Tricalcium phosphate. **b)** Bayóvar phosphate rock. **c)** Itafós phosphate rock.

3.3. Effect synergistic among organic acids

To evaluate the synergistic effect among the three organic acids: citric acid (CA), oxalic acid (OA) and gluconic acid (GA) under P solubilization from FTC, BPR and IPR, it was established a *Simplex Centroid Design* of three components. Table 1 summarizes the different combinations of citric acid, oxalic acid, and gluconic used in the experiments and the responses obtained as a percentage of P solubilized.

Table 1. Experimental matrix design, *Simplex Centroid Design* to evaluate the synergistic effect among the organic acids on the solubilization of phosphate materials.

Run	CA (mol L^{-1})	OA (mol L^{-1})	GA (mol L^{-1})	TCP (%)	BPR (%)	IPR (%)
1	0.000	0.104	0.000	67.17 ± 2.49	51.08 ± 10.96	51.85 ± 4.81
2	0.035	0.035	0.035	72.47 ± 7.30	62.48 ± 7.44	58.72 ± 8.10
3	0.520	0.520	0.000	64.83 ± 3.44	60.98 ± 2.57	72.95 ± 9.97
4	0.000	0.000	0.104	63.79 ± 5.83	28.67 ± 4.96	9.85 ± 0.29
5	0.104	0.000	0.000	69.68 ± 9.04	43.71 ± 4.57	27.16 ± 0.37
6	0.035	0.035	0.035	76.84 ± 3.45	65.68 ± 8.85	65.89 ± 2.84
7	0.017	0.017	0.070	67.27 ± 10.71	43.25 ± 0.79	38.36 ± 8.26
8	0.035	0.035	0.035	74.98 ± 4.45	55.18 ± 4.80	63.44 ± 10.65
9	0.000	0.520	0.520	72.37 ± 2.48	61.68 ± 8.87	69.12 ± 7.61
10	0.070	0.017	0.017	69.19 ± 10.30	50.79 ± 9.94	42.71 ± 10.95
11	0.520	0.000	0.520	64.81 ± 4.55	37.07 ± 4.48	22.85 ± 4.33
12	0.017	0.070	0.017	63.47 ± 5.58	46.02 ± 2.24	50.26 ± 9.18

The statistical analysis showed that for TCP solubilization all three organic acids (CA, OA and GA) presented a statistically significant positive influence on the efficiency of solubilization, since p-values were smaller than 0.05 for each of these components. Although, there were mixing points (run 2, 6 and 8) that the TCP solubility increased, interactions between the components (CA-OA, CA-GA, and OA-GA) were not significant (p-values > 0.05). Therefore, there is no synergistic effect among these organic acids in the TCP

solubilization. The statistical analysis enabled the definition of a linear model to estimate the TCP solubilization in terms of the concentrations of the components CA, OA, and GA in the solution medium, as described by Eq. (1).

$$TCP\ (\%\ solubilized) = 68.77 * [AC] + 67.71 * [OA] + 66.72 * [GA] \qquad Eq.(1)$$

In addition, these results indicated that the most significant effect on TCP solubilization was the concentration of CA, followed by the OA and GA, as revealed by Eq. (1). This result is in agreement to the efficiency observed in Figure 1a for TCP solubilization. In terms of BPR, the statistical analysis showed that all three organic acids (CA, OA and GA) are statistically significant with positive effect to promote the solubilization. Also, there were significant interactions of second-order between the components CA-OA and OA-GA which potentiate the solubilization, while the interaction between CA-GA was not significant (p-values > 0.05), as described by Eq. (2). These results agree with the results in Table 1, since that the mixing between citric acid and oxalic acid (run 3) and oxalic acid and gluconic acid (run 9) promote a better P solubilization that the pure citric, oxalic and gluconic acids (run 1, 4 and 5).

$$BPR\ (\%\ solubilized\ )$$
$$= 45.04x[CA] + 47.80x[OA] + 29.25x[GA] + 47.55[CAxOA]$$
$$+ 78.95x[OAxGA] \qquad Eq.(2)$$

In the same way, the statistical analysis showed a similar effect for IPR solubilization that resulted in a second-order relationship for the components CA-OA and OA-GA which potentiate the solubilization, however as observed for BPR, the interaction between CA-GA was not significant (p-values > 0.05), as described in Eq. (3).

$$IPR\ (\%\ solubilized)$$
$$= 26.50x[CA] + 48.02x[OA] + 14.16x[GA] + 119.24[CAxOA]$$
$$+ 129.82[OAxGA] \qquad Eq.(3)$$

It is observed that with the exception of the FTC, there were mixing effects (interactions) between citric acid and oxalic acid as well as oxalic acid and gluconic acid that potentiated the solubilization of RFs. In sequence, the models used to describe the effects on

TCP (Eq. (1)), BPR (Eq. (2)), and IPR (Eq. (3)) were used to generate the contour plots shown in Fig. 3a–c, respectively. The contour plot for BPR and IPR presented an adjust of 0.81 and 0.78, whereas the contour plot for TCP was lower than 0.1. The low adjustment for TCP is due to the low individual effect among the organic acids and due the variability of the experimental data. In addition, error of the model observed was 6.65%, 7.67% and 9.70% for TCP, BPR and IPR, respectively.

The mixture contour plot generated from models were used to delineate the optimum mixing regions that potentiated P solubilization. Although, there were no significant interaction effects for TCP, the mixture contour plot for TCP (Figure 3a) show an optimum tending to citric acid. This can be explained by the increase in the concentration of citric acid, since the solubilization effect was higher for citric acid than for oxalic and gluconic acid. In addition, the mixture contour plots for BPR and IPR (Figure 3b-c) were similar and an optimum region containing binary and ternary mixtures was found where higher solubilization efficiency was obtained when compared to the solubilization of pure acids. Therefore, by analyzing the contour plots in relation to the interaction effects, an optimal region can be observed where there is molar ratio of 1:1 between citric and oxalic acid which potentiated the solubilization, regarding to the interaction between oxalic acid and gluconic acid a molar ratio of 2:1 was observed.

The model was validated using points chosen within the regions of maximum solubilization delimited by the contour plots, as shown in Table 2. Although, the experimental results of validation differed from that obtained by the model, they are within the error predicted by the model.

Table 2. Validation of the solubilization models obtained for TCP, BPR and IPR.

Run	CA (mol L^{-1})	OA (mol L^{-1})	GA (mol L^{-1})	Experimental (Solubilized %)	Model (Solubilized %)
TCP	0.090	0.007	0.007	75.01 ± 4.59	68.53 ± 6.65
BPR	0.042	0.062	0.000	62.98 ± 6.91	58.13 ± 7.67
	0.000	0.069	0.035	60.01 ± 7.33	59.16 ± 7.67
IPR	0.042	0.062	0.000	71.88 ± 5.44	68.03 ± 9.70
	0.000	0.069	0.035	66.73 ± 7.12	65.40 ± 9.70
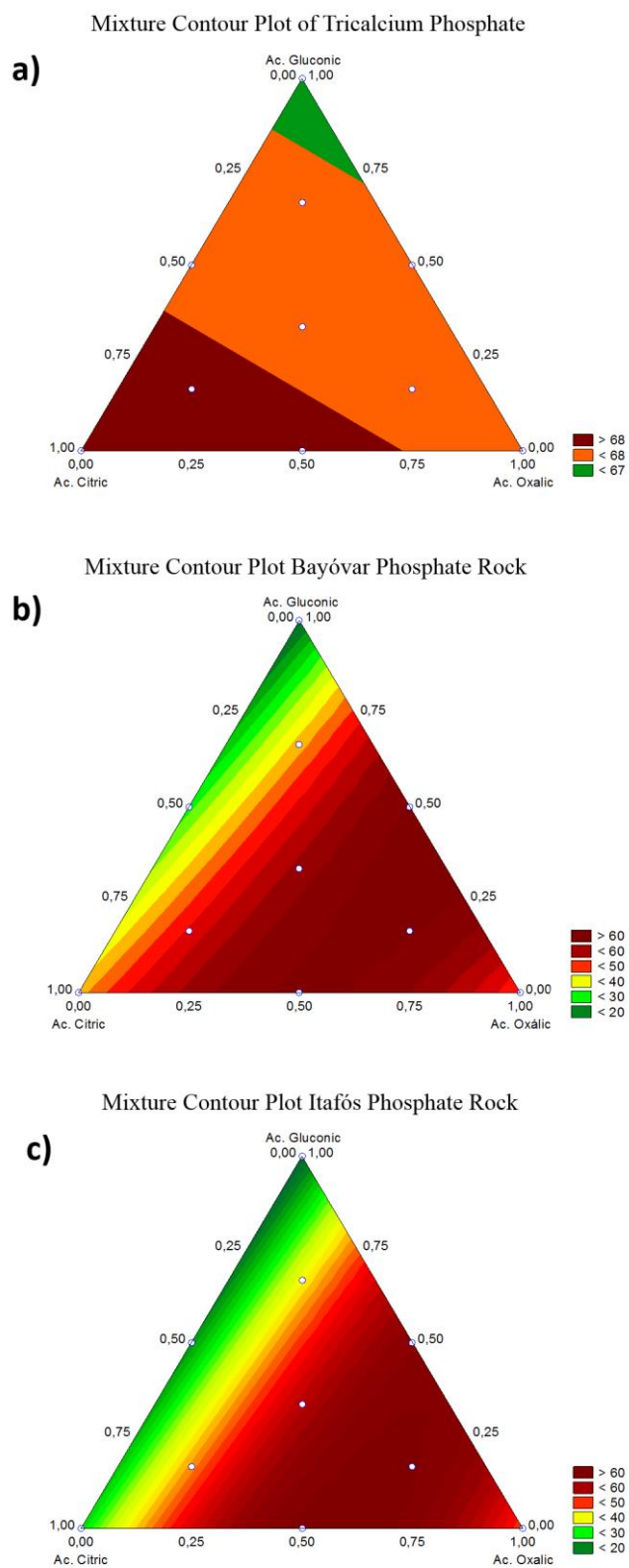
Figure 3. Contour plots showing the synergistic effect among citric, oxalic and gluconic acid on solubilization of phosphate minerals at 40 rpm, 30 °C for 6 h. **a)** Tricalcium Phosphate. **b)** Bayóvar phosphate rock. **c)** Itafós phosphate rock.

4. Conclusions

Our findings showed that the type of organic acid can significantly influence the solubilization of the phosphate rock. The oxalic acid showed a remarkable performance for the solubilization of phosphate present in complex minerals. In addition, a synergistic relationship between citric acid and oxalic acid, and between gluconic acid and oxalic acid was observed, which potentiated the solubilization of the phosphate rocks, compared with the same concentration of organic acids pure. The results support a better understanding of the mechanisms of action of organic acids on the solubilization of the PRs. These findings can contribute to the development of biotechnological routes for microbial solubilization of RP, since the cultivation conditions can be manipulated using metabolic engineering tools to favor the microbial production of organic acids with high P-solubilizing efficiency.

References

Bengtsson, A., Lindegren, M., Sjoberg, S., Persson, P. 2007. Dissolution, adsorption and phase transformation in the fluorapatite-goethite system. *Applied Geochemistry*, **22**(9), 2016-2028.

Cao, X.D., Harris, W. 2008. Carbonate and magnesium interactive effect on calcium phosphate precipitation. *Environmental Science & Technology*, **42**(2), 436-442.

Chien, S.H. 1993. Solubility assessment for ferlilizer containing phosphate rock. *Fertilizer Research*, **35**(1-2), 93-99.

Delabona, P.D., Farinas, C.S., Lima, D.J.D., Pradella, J.G.D. 2013. Experimental mixture design as a tool to enhance glycosyl hydrolases production by a new Trichoderma harzianum P49P11 strain cultivated under controlled bioreactor submerged fermentation. *Bioresource Technology*, **132**, 401-405.

Drummond, L., Maher, W. 1995. Determination of phosphorus in aqueous-solution via formation of the phosphoantimonylmolybdenum blue complex - reexamination of optimum conditions for the analysis of phosphate. *Analytica Chimica Acta*, **302**(1), 69-74.

Gelb, R.I. 1971. Conductometric determination of pka values-oxalic and squaric acids. *Analytical Chemistry*, **43**(8), 1110-&.

Green, T.H., Watson, E.B. 1982. Crystallization of apatite in natural magmas under high pressure, hydrous conditions, with particular reference to 'Orogenic' rock series. 1 ed. in: *Contributions to Mineralogy and Petrology*, pp. 1432-0967.

Illmer, P., Schinner, F. 1995. Solubilization of inorganic calcium phosphates—Solubilization mechanisms. *Soil Biology and Biochemistry*, **27**(3), 257-263.

Klaic, R., Plotegher, F., Ribeiro, C., Zangirolami, T.C., Farinas, C.S. 2017. A novel combined mechanical-biological approach to improve rock phosphate solubilization. *International Journal of Mineral Processing*, **161**, 50-58.

Kpomblekoua, K., Tabatabai, M.A. 1994. Effect of organic-acids on release of phosphorus from phosphate rocks. *Soil Science*, **158**(6), 442-453.

Lazo, D.E., Dyer, L.G., Alorro, R.D. 2017. Silicate, phosphate and carbonate mineral dissolution behaviour in the presence of organic acids: A review. *Minerals Engineering*, **100**, 115-123.

Lim, H.H., Gilkes, R.J., McCormick, P.G. 2003. Beneficiation of rock phosphate fertilisers by mechano-milling. *Nutrient Cycling in Agroecosystems*, **67**(2), 177-186.

MAPA. 2013. Manual de métodos analíticos oficiais para fertilizantes e corretivos, (Ed.) M.d.A.P.e. Abastecimento. Brazil.

McArthur, J.M. 1985. Francolite geochemistry - compositional controls during formation, diagenesis, metamorphism and weathering. *Geochimica Et Cosmochimica Acta*, **49**(1), 23-35.

McArthur, J.M., Benmore, R.A., Coleman, M.L., Soldi, C., Yeh, H.W., Obrien, G.W. 1986. Stable isotopic characterization of francolite formation. *Earth and Planetary Science Letters*, **77**(1), 20-34.

Mendes, G.D., de Freitas, A.L.M., Pereira, O.L., da Silva, I.R., Vassilev, N.B., Costa, M.D. 2014. Mechanisms of phosphate solubilization by fungal isolates when exposed to different P sources. *Annals of Microbiology*, **64**(1), 239-249.

Mendes, G.d.O., Rego Muniz da Silva, N.M., Anastacio, T.C., Bojkov Vassilev, N., Ribeiro, J.I., Jr., da Silva, I.R., Costa, M.D. 2015. Optimization of Aspergillus niger rock phosphate solubilization in solid-state fermentation and use of the resulting product as a P fertilizer. *Microbial Biotechnology*, **8**(6), 930-939.

Misra, D.N. 1999. Interaction of citric or hydrochloric acid with calcium fluorapatite: Precipitation of calcium fluoride. *Journal of Colloid and Interface Science*, **220**(2), 387-391.

Murphy, J., Riley, J.P. 1986. Citation-classic - a modified single solution method for the determination of phosphate in natural-waters. *Current Contents/Agriculture Biology & Environmental Sciences*(12), 16-16.

Nahas, E. 1996. Factors determining rock phosphate solubilization by microorganisms isolated from soil. *World Journal of Microbiology & Biotechnology*, **12**(6), 567-572.

Park, H.S., Jun, S.C., Han, K.H., Hong, S.B., Yu, J.H. 2017. Diversity, Application, and Synthetic Biology of Industrially Important Aspergillus Fungi. in: *Advances in Applied Microbiology, Vol 100*, (Eds.) S. Sariaslani, G.M. Gadd, Vol. 100, Elsevier Academic Press Inc. San Diego, pp. 161-202.

Plotegher, F., Ribeiro, C. 2016. Characterization of Single Superphosphate Powders - a study of Milling Effects on Solubilization Kinetics. *Materials Research-Ibero-American Journal of Materials*, **19**(1), 98-105.

Sazanova, K.V., Vlasov, D.Y., Osmolovskay, N.G., Schiparev, S.M., Rusakov, A.V. 2016. Significance and Regulation of Acids Production by Rock-Inhabited Fungi. *Biogenic-Abiogenic Interactions in Natural and Anthropogenic Systems*, 379-392.

Silva, A.M.N., Kong, X.L., Hider, R.C. 2009. Determination of the pKa value of the hydroxyl group in the alpha-hydroxycarboxylates citrate, malate and lactate by 13C NMR: implications for metal coordination in biological systems. *Biometals*, **22**(5), 771-778.

Taktek, S., St-Arnaud, M., Piche, Y., Fortin, J.A., Antoun, H. 2017. Igneous phosphate rock solubilization by biofilm-forming mycorrhizobacteria and hyphobacteria associated with Rhizoglomus irregulare DAOM 197198. *Mycorrhiza*, **27**(1), 13-22.

Vassilev, N., Eichler-Lobermann, B., Flor-Peregrin, E., Martos, V., Reyes, A., Vassileva, M. 2017. Production of a potential liquid plant bio-stimulant by immobilized Piriformospora indica in repeated-batch fermentation process. *Amb Express*, **7**, 7.

Vassileva, M., Serrano, M., Bravo, V., Jurado, E., Nikolaeva, I., Martos, V., Vassilev, N. 2010. Multifunctional properties of phosphate-solubilizing microorganisms grown on agro-industrial wastes in fermentation and soil conditions. *Applied Microbiology and Biotechnology*, **85**(5), 1287-1299.

Wagh, J., Chanchal, K., Sonal, S., Praveena, B., Archana, G., Kumar, G.N. 2016. Inoculation of genetically modified endophytic Herbaspirillum seropedicae Z67 endowed with gluconic and 2-ketogluconic acid secretion, confers beneficial effects on rice (Oriza sativa) plants. *Plant and Soil*, **409**(1-2), 51-64.

Xiao, C.Q., Fang, Y.J., Chi, R. 2015. Phosphate solubilization in vitro by isolated Aspergillus niger and Aspergillus carbonarius. *Research on Chemical Intermediates*, **41**(5), 2867-2878.

Yang, L., Lubeck, M., Lubeck, P.S. 2017. Aspergillus as a versatile cell factory for organic acid production. *Fungal Biology Reviews*, **31**(1), 33-49.

Zapata, F. 2004. Use of phosphate rocks for sustainable agriculture. *FAO Fertilizer and Plant Nutrition Bulletin*, 1-148.

Zhou, J.P., Wang, H.M., Cravotta, C.A., Dong, Q., Xiang, X. 2017. Dissolution of Fluorapatite by Pseudomonas fluorescens P35 Resulting in Fluorine Release. *Geomicrobiology Journal*, **34**(5), 421-433.

Capítulo 5

"Nanocomposite of starch-phosphate rock bioactivated for environmentally-friendly fertilization"

Artigo submetido na revista *Minerals Engineering*

A partir dos conhecimentos adquiridos com os estudos envolvendo a seleção do microrganismo, os ensaios de solubilidade em meio de cultura, o efeito do tamanho de partícula, assim como o efeito dos ácidos orgânicos na dissolução da rocha fosfática, foi possível propor uma estratégia para desenvolver um compósito-fertilizante granular baseado na ativação biológica. O compósito proposto é processado a partir da gelatinizarão do amido e composto por rocha fosfática mecanicamente ativada e esporos de *Aspergillus niger*. Estudos foram realizados para maximizar a carga de rocha dispersa na matriz ao mesmo tempo que uma elevada dispersão dessas partículas pude-se ser obtida. As caracterizações dos compósitos mostraram um elevado grau de dispersão das partículas de rocha fosfática na matriz de amido, além de um considerável teor de P_2O_5 entre 10-22%, comparado a fertilizantes comerciais como o superfosfato simples que apresenta um teor de P_2O_5 entre 18-22%. A solubilidade do fósforo contido no compósito foi superior a 70% em somente 96 h após realizada a bio-ativação. Estes compósitos-fertilizantes podem ser considerados um inovador conceito de um "grânulo biorreator", onde os microrganismos se desenvolvem na estrutura do grânulo, consumindo a matriz como fonte de carbono e produzindo ácidos orgânicos. Consequentemente, a acidez local aumenta promovendo a solubilização das partículas de rocha fosfática dispersas na matriz. Os resultados obtidos neste estudo suportam o desenvolvimento de uma nova classe de biofertilizantes ativados biologicamente a partir do uso de minerais fosfatados de baixa qualidade. Os resultados estão apresentados na forma de artigo e referem-se ao objetivo específico 5: (5) Desenvolvimento de novas alternativas e novos produtos-fertilizantes para aumentar a solubilidade de rochas fosfática a partir a ação de microrganismos solubilizadores.

Abstract

The use of natural phosphate rock as a source of phosphorus for plant growth is considered more environmentally friendly, compared to conventional chemical fertilizers. However, the very low solubility of the phosphate present in natural rocks limits its practical application. To overcome this limitation, a composite was developed based on the dispersion of nanoparticulate phosphate rock in a polysaccharide matrix of starch, as an integrated strategy to facilitate application and provide a supporting substrate for an acidulant microorganism, *Aspergillus niger*. The bioactivation of the nanocomposite resulted in a remarkable solubilization of up to 70% of the total available phosphate in very low solubility phosphate rocks (Bayóvar and Itafós) and 100% of the total available phosphate in a reference mineral (hydroxyapatite), in only 96 h. Such approach employing bioactivation of starch-phosphate rock nanocomposites significantly contributed to improve P-solubilization, opening new routes for the development of smart fertilizers based on polysaccharide matrix.

1. Introduction

Phosphorus (P) is an essential nutrient for plant growth, but it generally presents low availability in tropical soil due to the high reactivity of soluble forms of P with iron and aluminum, forming low solubility compounds [1, 2]. As a result, periodic phosphate fertilization is required in order to achieve high crop productivity [3]. Conventional P fertilizers are usually high solubility compounds such as mono-ammonium phosphate (MAP), but their production processes are environmentally harmful due to the chemical treatment of the phosphate rock (PR) with high concentrations of sulfuric acid and phosphoric acid [3, 4]. Furthermore, the high solubility of these fertilizers frequently leads to environmental impacts, resulting in eutrophication of water bodies in the vicinity of agricultural areas. Indirect effects include algae growth and fish mortality due to reduction of oxygen levels [5, 6]. Other studies have also reported that intensive soil fertilization with conventional P fertilizers may have an impact on the proliferation of some microorganisms present in the soil microflora [7, 8].

The direct use of ground phosphate rock (PR) is an attractive alternative for fertilization, since the absence of previous chemical treatment results in reduced environmental impacts and lower costs, with the additional advantage that the lower solubility of PR allows greater control of phosphate release [9-11]. However, the high chemical stability of phosphate rocks, due the presence of the apatite phase and apatite-related crystallization effects [12, 13], means that solubility is much lower than required in practical applications [10]. The solubility of PR is quite low even in acidic soils, limiting the direct use of PR as fertilizers, especially for short cycle crops [14-18]. Therefore, a major challenge is to identify processing strategies that allow faster solubilization of the PR, preferably from material applied in the field, accessing the entire phosphate content and ensuring that the solubilization occurs during a period of time suitable for the needs of the plants.

One way to overcome the low solubility of PR is to use P-solubilizing microorganisms (PSMs) that are able to accelerate the solubilization process [19-21]. The P-solubilizing activity of PSMs is determined by their ability to produce and release metabolites such as organic acids, which contain hydroxyl and carboxyl groups that chelate the cations (mainly calcium) bound to phosphate, with the latter being converted into soluble forms [20, 22-25]. Free and encapsulated P-solubilizing microorganisms can be applied to soil in order to increase the PR solubilization [19, 26]. The advantages of using encapsulated PSMs in soil include increased of shelf time and protection of the microorganisms from adverse environmental effects [3, 19, 26, 27].

Despite the potential advantages of using encapsulated PSMs, the traditional encapsulation techniques (such as alginate and chitosan encapsulation) do not employ the simultaneous dispersion of PR particles during the encapsulation of the microorganisms [19, 26]. Therefore, the development of a material integrating both PR particles and microorganisms could be a potential way to promote a higher interaction between the organic acids produced and the rock particles, thus maximizing the P solubilization. Gelatinized starch offers advantageous characteristics for use as a matrix for simultaneous encapsulation of PSMs and dispersion of RF particles, since is a cheap, abundant, and biodegradable natural polymer [28-30]. In addition, the polysaccharide matrix can be metabolized by PSMs (such as *Aspergillus niger*) to support growth and the production of organic acids [31, 32]. This could be considered as an innovative concept for a "bioreactor in a granule", where the microorganism development is favored by the granule structure, thus increasing the local organic acid production for efficient PR solubilization.

In this work, nanoparticulate composites were developed based on the dispersion of mineral phosphate in a polymeric gelatinized starch matrix containing spores of *Aspergillus niger*. Three different mineral phosphates were used in the experiments, including two phosphate rocks (Bayóvar and Itafós) and a reference mineral (hydroxyapatite). Detailed physical-chemical characterizations of the three materials were performed using X-ray diffraction, X-ray fluorescence, field emission scanning electron microscopy, and surface area measurements. The morphologies of the composites were investigated using X-ray tomography to observe the dispersion of the mineral particles in the starch matrix. Experiments were performed to evaluate the effect of bioactivation of the composite by *A. niger*, leading to phosphorus solubilization. The final products obtained were novel types of solid biofertilizers, suitable for application to the soil in order to supply the phosphorus requirements of plants. The results support the development of a new class of smart biofertilizer, which could open up new applications for formulations containing poorly soluble mineral phosphates.

2. Materials and Methods

2.1. Microorganisms.

The filamentous fungus *Aspergillus niger C* (BRMCTAA 82) was obtained from the Embrapa Food Technology collection (Rio de Janeiro, RJ, Brazil). This fungus was selected

from among eight filamentous fungi as the best for solubilization of phosphate rock [21] and it was used here as a model of microorganism to evaluate the biological P solubilization. Spore suspensions of the fungal strain were kept at -18 °C in a solution of water with glycerol (10 wt.%) and NaCl (0.9 wt.%). Spores were germinated at 30 °C in Petri dishes containing potato dextrose agar. After 96 h, a suspension of grown spores was harvested by adding distilled water. The spore concentration was determined using a Neubauer chamber.

2.2. Materials

Standard corn starch (St) (Amidex 3001, 30% amylose and 70% amylopectin), kindly supplied by Corn Products Brazil, and glycerol (Synth) were used to prepare the gelatinized starch matrices. The phosphate sources used were hydroxyapatite (Hap) (Sigma-Aldrich, ≥90% pure phase), Bayóvar phosphate rock (BPR), which is a sedimentary rock originating from Sechura (Peru), and Itafós phosphate rock (IPR), which is an igneous rock originating from Arraias (Brazil). The two phosphate rocks were dried at 110 °C for 48 h to reduce the humidity contents and were then ground for 10 min in an orbital mill (model CT-251, Servitec) consisting of a porcelain jar and alumina balls [9, 21]. After treatment, the materials were stored in dry boxes prior to use in preparation of the composites (Section 2.3) and for characterization (Section 2.4).

2.3. Preparation of the composites

Composites containing starch, phosphate, and spores were prepared by first gelatinizing the starch (St) by dispersion of 5 wt.% in a solution of distilled water and 1% glycerol, maintaining the mixture at about 90 °C for 30 min, under stirring, until a sticky gel was formed. The phosphate particles, at the desired sizes (mechanically activated by 10 min of grinding; Section 2.2), were then transferred to the beaker and dispersed in the starch gel by vigorous shaking for 15 min, as described by Giroto et al. [28]. After reducing the temperature to 30 °C, a suspension of *Aspergillus niger* spores (prepared as described in Section 2.1) was incorporated to a concentration of $2x10^7$ spores per g of the composite material. The mixed gel was kept at 40 °C under air circulation for at least 24 h to obtain a solid gel. The dried composite was triturated in a laboratory knife mill (model MA048, Marconi) and particles smaller than 4 mm were collected by sieving and stored in dry boxes, prior to the characterization (Section 2.4) and solubilization experiments (Section 2.5). All the composites

were prepared using the same procedure. The different proportions of the phosphates used to produce the composites are shown in Table 1, together with their nomenclatures.

Table 1. Compositions of the materials in terms of starch, phosphate source, and spores. The maximum percentage of phosphate in each material is also shown.

| Composite | Amount (g) | | | | Spores* | |
	Starch (St)	Hydroxyapatite (Hap)	Bayóvar (BPR)	Itafós (IPR)		P_2O_5 (%)
St/Hap Control	15	15	-	-	-	21.73
St/Hap 1:1	15	15	-	-	2×10^7	21.73
St/Hap 1:1.5	15	24	-	-	2×10^7	26.94
St/Hap 1:2	15	30	-	-	2×10^7	28.97
St/BPR Control	15	-	15	-	-	15.36
St/BPR 1:1	15	-	15	-	2×10^7	15.36
St/BPR 1:1.5	15	-	24	-	2×10^7	18.90
St/RPB 1:2	15	-	30	-	2×10^7	20.48
St/IPR Control	15	-	-	15	-	10.15
St/IPR 1:1	15	-	-	15	2×10^7	10.15
St/IPR 1:1.5	15	-	-	24	2×10^7	12.49
St/IPR 1:2	15	-	-	30	2×10^7	13.53

*Spores per g of total mass of composite

2.4. Characterization of the phosphate rocks and composites

All the phosphate rocks and composites were characterized by X-ray diffraction (XRD), using a LabX XDR-6000 diffractometer (Shimadzu, Japan) operated with Cu-Kα radiation (λ = 1.54056 Å), voltage of 30 kV, and current of 30 mA. XRD patterns were recorded at 2θ of 5-70°, using a continuous scanning speed of 2° min^{-1}. Chemical analyses were performed by X-ray fluorescence (XRF), using the lithium tetraborate fusion technique, with determination of the 10 commonest oxides found in ores. The morphologies of the materials were observed

by field emission gun scanning electron microscopy (FEG-SEM), using a JSM-6701F microscope (JEOL, Japan) operated at an acceleration voltage of 15 kV, with a working distance of 10 mm and a secondary electron detector. The specific surface area was determined by isothermal nitrogen adsorption, using a Micromeritics ASAP-2020 instrument, according to the 5-point B.E.T. (Brunauer–Emmett–Teller) method. The particle morphologies were analyzed using X-ray microtomography (model 1172, SkyScan), with the composite samples placed in a rotating steel support. The images were acquired using the following parameters: unaltered, spatial resolution (voxel size) of 2 mm, 0.3º step rotation, 180º rotation, and averaging of 6 frames. The images were reconstructed from the tomographic sections using NRecon software (SkyScan), using the following settings: smoothing 5, ring artifact correction 5, and beam hardening correction of 60%.

2.5. Bioactivation and solubilization of the composites

Incubation experiments were conducted to evaluate the synergy among starch matrix and the encapsulated *A. niger* for improving the solubilization of the mineral phosphorus. The incubation experiments were performed using submerged cultivation. The liquid nutrient medium used in the submerged cultivation and during P solubilization was adapted from the medium described by Pikvoskaya [33] and had the following composition (w/v): glucose, 1%; $(NH_4)_2SO_4$, 0.5%; NaCl, 0.2%; $MgSO_4.7H_2O$, 0.1%; KCl, 0.2%; $MnSO_4.H_2O$, 0.002%; $FeSO_4.7H_2O$, 0.002%; yeast extract, 0.5%. The cultivations were performed in 500 mL Erlenmeyer flasks, employing 100 mL of the nutrient medium and addition of the composites at a ratio of 2% (w/v). The incubation was carried out for 96 h in an orbital shaker incubator, at 30 °C and 220 rpm. All the experiments were performed in triplicate. After the incubation period, the resulting material was vacuum filtered through Whatman No. 1 filter paper, followed by centrifugation for 20 min at 12,000 rpm and 20 °C. The clear supernatant was analyzed using the colorimetric method described in Section 2.6 to determine the amount of soluble phosphorus released.

2.6. Determination of soluble phosphorus

The determination of phosphorus was based on the method reported by Murphy and Riley [34] and modified by Drummond and Maher [35], employing an acidified solution of ammonium molybdate (Synth, Brazil) containing ascorbic acid (Synth, Brazil) and antimony

(Synth, Brazil), which causes the formation and reduction of phosphomolybdic acid. This mixture was allowed to react at 50 ºC for 15 min, forming a phosphoantimonylmolybdenum blue complex. The concentration of this complex was determined by UV-Vis spectrometry at a wavelength of 880 nm, using a Lambda 25 spectrophotometer (Perkin Elmer).

3. Results and Discussion

3.1. Characterization of the Hydroxyapatite (Hap), Bayóvar phosphate rock (BPR), and Itafós phosphate rock (IPR)

A detailed characterization of the Hap, BPR, and IPR minerals was carried out in order to evaluate the chemical and physical natures of these sources of phosphate used to produce the composites. The XRD patterns of the minerals are shown in Figure 1. The Hap diffractogram only showed the crystalline phase corresponding to hydroxyapatite ($Ca_5(PO_4)_3OH$) (PDF2 pattern file #01-086-0740), confirming the chemical analysis by X-ray fluorescence (Table 2). No secondary phases were present.
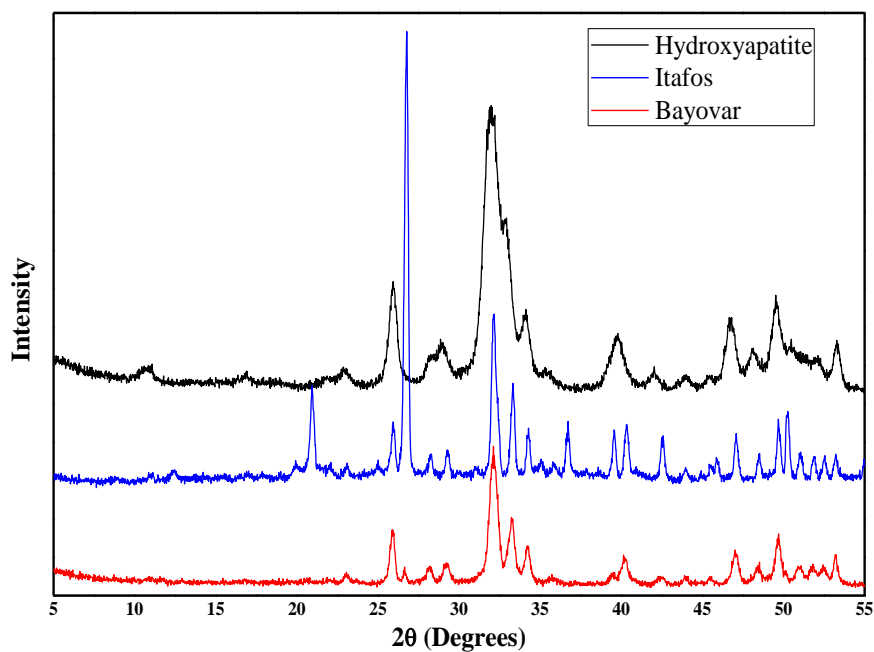
Fig. 1. XRD patterns of pure hydroxyapatite and the Itafós and Bayóvar phosphate rocks.

The XRD pattern of BPR revealed two main crystalline phases, one corresponding to alpha-quartz (SiO_2, PDF2 pattern file #01-089-8934) and another corresponding to a phosphate-rich fluorapatite phase ($Ca_5(PO_4)_3F$, PDF2 pattern file #01-087-2462). Both phases were confirmed by chemical analysis (Table 2). Previous studies have shown that the main crystalline phase in this rock is a type of modified fluorapatite [10, 36-39]. In this fluorapatite (francolite or carbonate-fluorapatite, $Ca_{10}[(PO_4)_{6-X}(CO_3, SO_4)_X]F_2$), some phosphate groups (PO_4^{3-}) in the crystalline reticulum can be substituted by carbonate (CO_3^{2-}) or sulfate (SO_4^{2-}) groups. This results in modification of physicochemical properties of the material, such as its reactivity and solubility [10, 36, 38, 40, 41]. It was not possible to identify other minor phases in the XRD pattern of BPR (Figure 1).

Table 2. Chemical analysis of the phosphate sources by X-ray fluorescence, and specific surface areas.

Oxide species	Hydroxyapatite (Hap)	Itafós (IPR)	Bayóvar (BPR)
	Mass %		
SiO_2	0.11	36.4	4.42
Al_2O_3	<0.10	4.60	0.96
Fe_2O_3	0.03	2.03	0.87
CaO	51.3	30.4	46.6
MgO	0.44	0.52	0.53
TiO_2	<0.01	0.22	0.07
P_2O_5	43.46	20.29	30.72
Na_2O	0.24	0.30	1.98
K_2O	0.02	0.88	0.30
MnO	<0.01	0.10	0.01
Loss on ignition	5.02	4.33	10.57
Total	100.74	100.07	97.03
Specific surface area ($m^2\ g^{-1}$)	59.7	5.1	22.2

The XRD pattern of IPR revealed the presence of three crystalline phase constituents. Analogously to BPR, high intensity peaks corresponded to alpha-quartz SiO_2 (PDF2 pattern file #01-089-8934). Two phosphate-rich phases were present, corresponding to an aluminum phosphate, berlinite ($Al(PO_4)_3$, PDF2 pattern file #01-076-0228), and a hydroxyapatite ($Ca_5(PO_4)_3OH$, PDF2 pattern file #01-086-0740). All the identified phases were consistent with the results obtained in the chemical analyses (Table 2).

Morphological analysis using SEM showed that Hap consisted of agglomerates of small rounded nanoparticles <100 nm in size (Figure 2a). BPR showed agglomerates around 500 nm in size (Figure 2b), while IPR showed the largest aggregates of around 1 μm (Figure 2c). These results were supported by the surface area analyses, where Hap, with the smallest particle size, had the largest surface area (59.7 m^2 g^{-1}), followed by BPR (22.2 m^2 g^{-1}) and IPR (5.1 m^2 g^{-1}). The phase identification and chemical analysis results indicated that IPR was less brittle than BPR, due to a higher concentration of alpha-quartz. When the two rocks were ground under the same conditions, lower efficiency of the grinding process was observed for IPR, resulting in a size distribution with larger particles, compared to BPR.
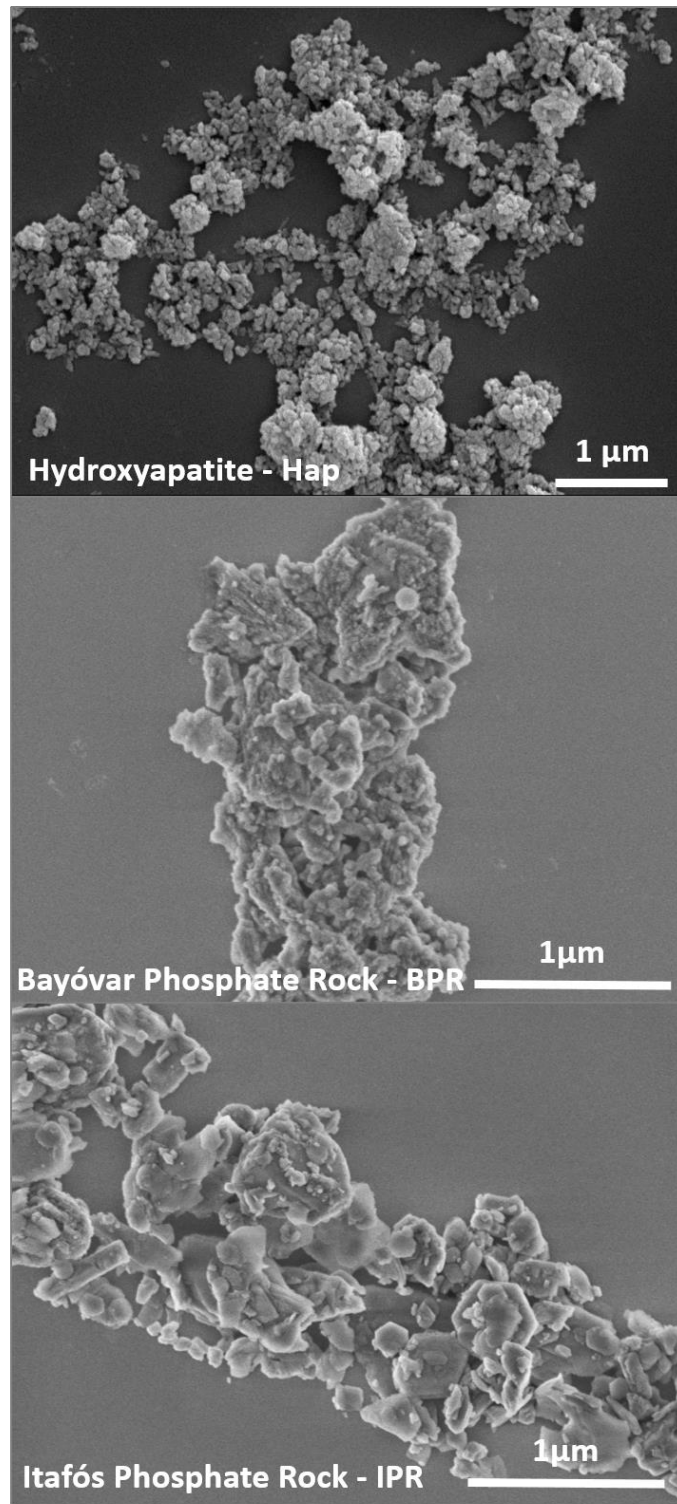
Fig. 2. X-ray tomography cross-sectional images of the composites: (a) St/Hap Control (without fungal spores), (b) St/Hap 1:1, (c) St/Hap 1:1.5, (d) St/Hap 1:2, I St/IPR Control (without fungal spores), (f) St/IPR 1:1, (g) St/IPR 1:1.5, (h) St/IPR 1:2, (i) St/BPR Control (without fungal spores), (j) St/BPR 1:1, (l) St/BPR 1:1.5, and (m) St/BPR 1:2.

Therefore, the materials presented differences in their chemical structures, with different phosphate phases as well as different morphologies. In the next step, the X-ray microtomography technique was used to characterize the dispersion of the particles in the starch matrix after formation of the composites.

3.2. Characterization of the composites

Recent studies have reported that reducing the particle size to the nanoscale can improve the solubility of PR [9, 21]. Therefore, the mechanical activation of the RF by reduction to the nanoscale before encapsulation was employed as a potential strategy to improve the interaction of the PR particle with the starch matrix and the microorganisms.

Figure 3 shows X-ray microtomography images of the composites. The bright dots in each image show the dispersion of the particles in the starch matrix. The Hap particles (Figure 3a-d) were homogeneously distributed in the matrix, due to their small size. An increase of the Hap concentration in the starch matrix did not lead to the formation of agglomerates, so it was possible to obtain composites containing higher phosphate levels (% of P_2O_5), with the same degree of particle dispersion.

The morphologies of the composites produced using IPR and BPR are shown in Figure 3e-h and Figure 3i-m, respectively, revealing a tendency for particle agglomeration. Furthermore, the larger aggregate size affected the dispersion of IPR and BPR in the matrix, resulting in composites with lower homogeneity, compared to Hap. However, the two rock-based materials showed similar dispersions, indicative of similar surface availability, despite the different particle sizes and surface areas. This suggests that considering this aspect, solubilization in these materials would be similar, so any difference could be attributed to the chemical structures. On the other hand, the presence of smaller particles in the Hap-based materials would favor greater solubilization, compared to the rock-based materials, especially considering the higher solubility of the hydroxyapatite phase, compared to fluorapatite and other phosphate phases present in the rock materials.

The XRD patterns of composites St/Hap 1:1, St/Hap 1:1.5, St/Hap 1:2, and pure Hap showed the same profiles (Figure S1, Supporting Information). It could therefore be concluded that the structure of the phosphatic material remained the same after dispersion and production of the composites. In the next step, the effect of bioactivation by *A. niger* on solubilization was evaluated for all the products (Table 1).
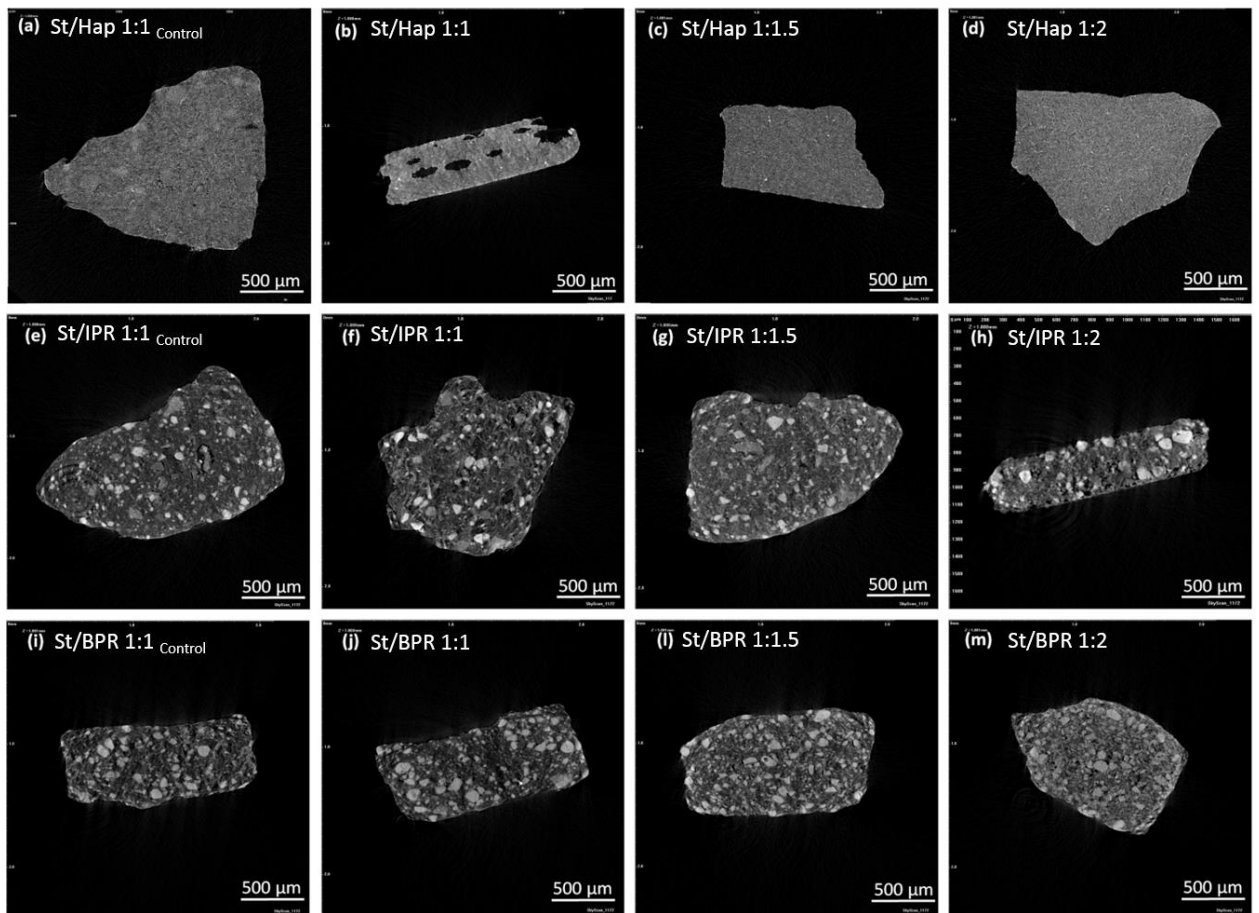
Fig. 3. FEG-SEM micrographs and specific surface areas for a) hydroxyapatite, b) Bayóvar phosphate rock, and c) Itafós phosphate rock.

3.3. Effect of bioactivation on solubilization of the composites

An initial set of experiments was carried out to evaluate the potential of the *A. niger* spores encapsulated in the starch matrix to solubilize the available phosphorus in the composites produced using the three different mineral phosphates (Hap, BRP, and IPR). In these experiments, the composites were incubated in a liquid Pikovskaya nutrient medium (described in Section 2.5) with a minimum amount of carbon (1% glucose) to provide the conditions required for spore germination and fungal growth. A visual comparison between the nanocomposite (solid granules) and the resulting structure after 96 h of bioactivation reveals that the polymeric structure is continuously replaced by the microorganism biomass (Figure S2 – Supporting Information). The microorganism biomass still keeps the

nanocomposite structure, which is supposed to be very favorable for its effects over the dispersed PR nanoparticles.

The temporal profiles of phosphorus solubilization and pH are shown in Figure 4 for the Hap, BPR, and IPR composites. As expected, when the composite was placed under favorable environmental conditions, germination occurred, with fungal growth within the composite and organic acid production. The secretion of organic acids resulted in acidification of the medium and increased phosphorus solubilization, compared to control experiments performed using composites without any fungal spores (Figure 4). In all cases, the spores in the composites remained viable after 30 days of storage at room temperature.

A)

B)

C)
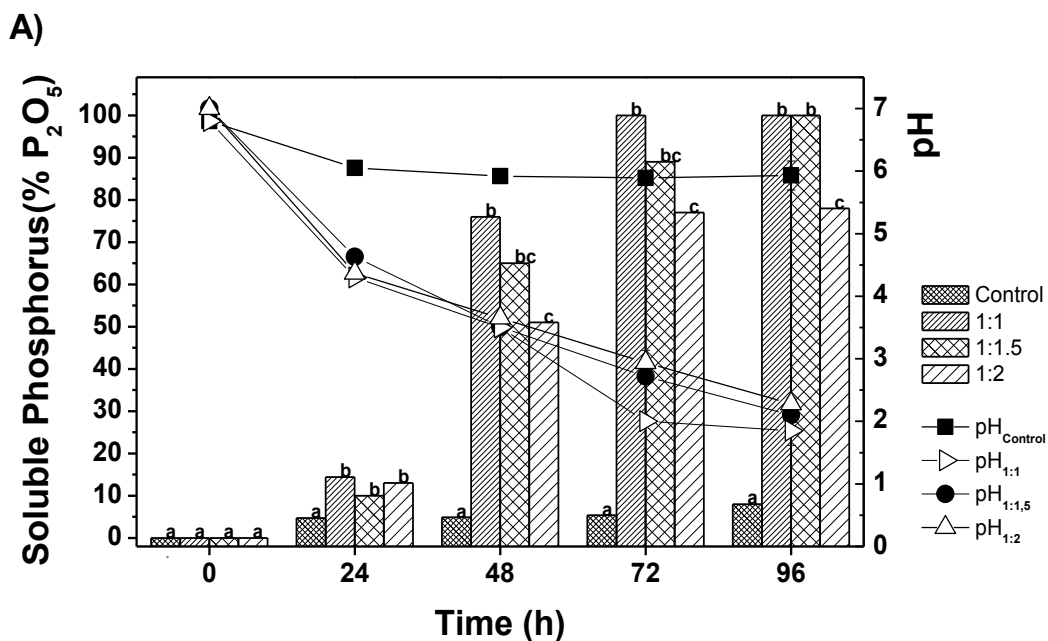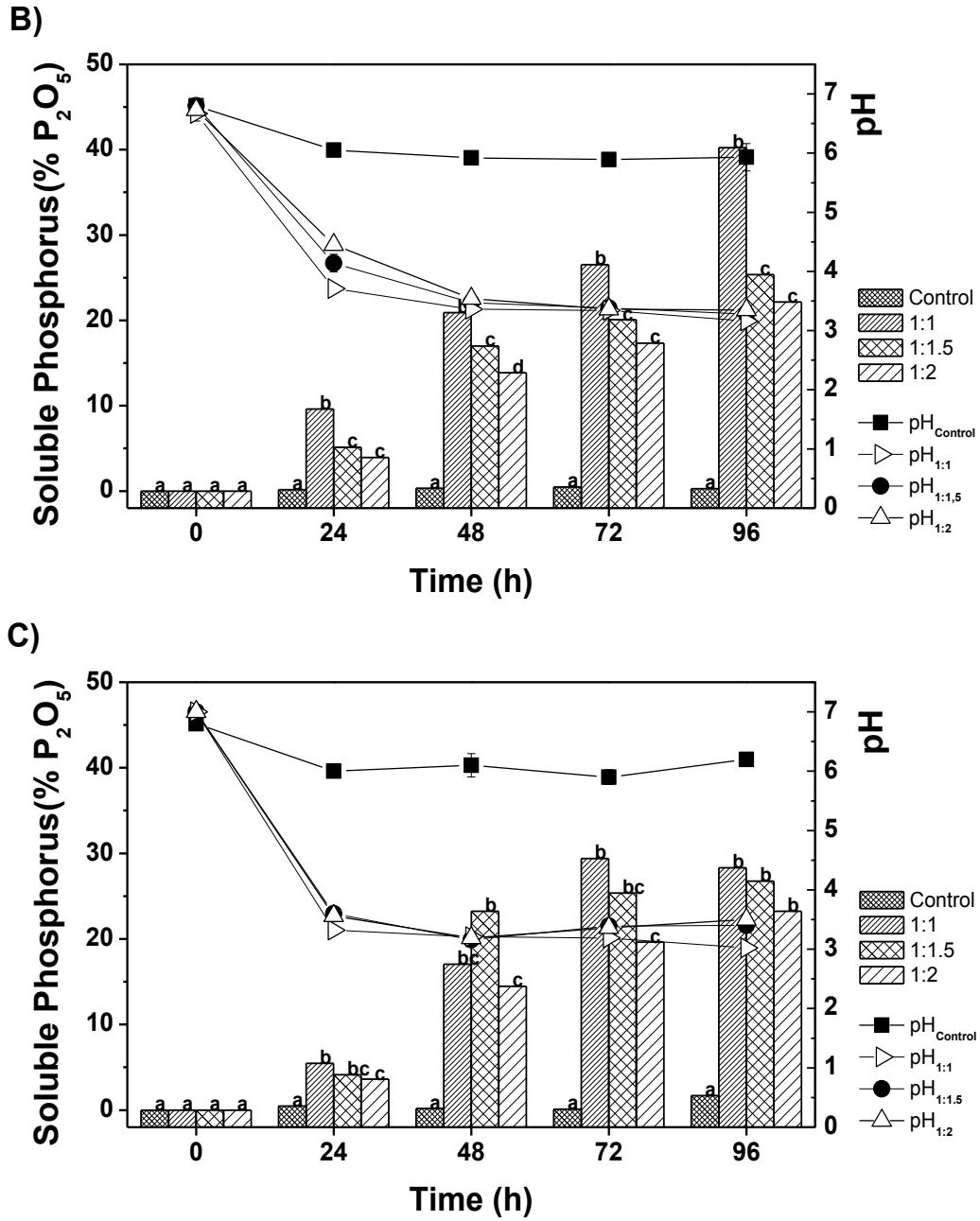
Fig. 4. Temporal profiles of phosphorus solubilization and pH for the Hap, BPR, and IPR composites. A) Composite St/Hap Control (without *A. niger* spores), St/Hap 1:1, St/Hap 1:1.5, and St/Hap 1:2. B) Composite St/BPR Control (without *A. niger* spores), St/BPR 1:1, St/BPR 1:1.5, and St/BPR 1:2. C) Composite St/IPR Control (without *A. niger* spores), St/IPR 1:1, St/IPR 1:1.5, and St/IPR 1:2. Different letters indicate significant difference among the treatments (ANOVA with Tukey's test, 95% confidence level).

Figure 4A shows the temporal profiles for the solubilization of phosphorus as P_2O_5 from the composites with three different ratios of starch to hydroxyapatite (1:1, 1:1.5, and 1:2),

117

using a fixed concentration of *A. niger* spores. The results of a control experiment (hydroxyapatite to starch ratio of 1:1), without fungal spores, are also included in Figure 4A. After 24 h of incubation, all three St/Hap composites with *A. niger* spores showed higher solubility than the control treatment. The increased P_2O_5 solubilization obtained using the inoculated composites could be attributed to the acidification of the medium by organic acid production, as shown by a decrease of the pH to around 2 after 96 h of incubation, for all three inoculated St/Hap composites.

Phosphorus solubilization increased after 48 h of incubation, with 50 to 80% of the total P_2O_5 present in the hydroxyapatite composites solubilized at pH between 3 and 4 (Figure 4A). After 72 h of incubation, with pH between 2 and 3, 100% phosphorus solubilization was observed for the St/Hap 1:1 composite, while values of 90% and 77% were obtained for St/Hap 1:1.5 and St/Hap 1:2, respectively. After 96 h of incubation, the St/Hap 1:1 composite maintained a solubilization value of 100%. However, the St/Hap 1:2 composite stabilized at 78% solubilization, despite the fact that the pH at the end of the incubation period was around 2.

In contrast, the pH of the control treatment (not inoculated) showed only a small reduction within 24 h and remained close to pH 6 until the end of the incubation period. This could be attributed the buffering capacity of the material itself, which was also observed for the control treatments of the composites obtained using BPR and IPR as phosphate sources (Figures 4B and 4C).

Behavior similar to that observed for the hydroxyapatite composite was found for phosphorus solubilization from the composites obtained with the three different ratios of BPR in starch (1:1, 1:1.5, and 1:2), using the same fixed concentration of *A. niger* spores (Figure 4B). There was intense acidification of the medium in the first 24 h, with a decrease of the pH from 6.8 to around 4, which provided a suitable acidified environment favoring phosphorus release from the St/BPR composites. However, the acidification stabilized after 48 h, with pH close to 3 reached after 96 h, indicative of lower organic acid production, compared to the medium containing St/Hap, for which the pH reached around 2 (Figure 4A). Therefore, lower P_2O_5 solubilization from the St/BPR composites could be a consequence of different effects: lower organic acid production, less particle dispersion than in the St/Hap composites, and especially differences in the chemical structures of the materials.

The St/BPR composites showed highest solubilization at a ratio of 1:1, with 40% of the available P_2O_5 solubilized after 96 h, while even lower solubilization yields were obtained for the ratios 1:1.5 and 1:2, corresponding to 25% and 22% of available P_2O_5, respectively. The St/BPR 1:1 composite showed a higher yield at all the times evaluated, with a constant increase in the release of P_2O_5 up to 96 h, while the St/BPR 1:1.5 and St/BPR 1:2 composites showed only a slight increase in the solubilization after 48 h. Hence, the St/BPR 1:1 and St/Hap 1:1 composites showed greater phosphorus solubilization efficiencies, compared to the composites containing higher amounts of phosphate, with continuous increases of phosphorus solubilization during the course of the incubation. This indicated that an optimum balance between the composite components was required in order to achieve good dispersion in the polysaccharide matrix and efficient production of organic acids.

Figure 4C shows the temporal profiles of phosphorus solubilization as P_2O_5 from the composites produced using dispersion of IPR in starch at three different ratios (1:1, 1:1.5, and 1:2), using a fixed concentration of *A. niger* spores, together with the profile for a control treatment (1:1) without fungal spores. The composites containing IPR presented P_2O_5 solubilization below 30% during the entire incubation period. Intense acidification of the culture medium was observed during the first 24 h, with the pH subsequently stabilizing at around 3. This acidic medium provided effective solubilization of P_2O_5 in all the St/IPR composites up to 72 h, but there were no further significant increases after this period.

Comparison of the composites produced using the three sources of phosphate (Figure 4) showed that St/Hap presented the highest phosphorus solubilization efficiency, followed by St/RPB and St/RPI. These differences were expected, due to the different chemical compositions and physical characteristics (surface area and structure) of these phosphate materials, as shown in the characterization analyses (Section 3.1).

The hydroxyapatite used here as a model source of phosphate had a higher surface area and smaller particle size, compared to the two PRs (Table 2), which favored the solubilization process. Hydroxyapatite is a pure source of phosphate that can be readily solubilized at pH around 4 [42]. The number of isomorphic substitutions (replacement of anionic PO_4^{3-} groups by CO_3^{2-} groups) affects the chemical structure and stability of the material, and mineral phosphate with a greater number of isomorphic replacements tends to be more soluble [10, 36-39, 41]. This could explain the higher solubility of BPR, compared to IPR, since the number of isomorphic substitutions is higher in BPR than in IPR. In addition, the heterogeneous chemical composition of PRs could reduce the solubility of these sources, compared to the

119

Hap evaluated here as model source of apatite. Elements such as Fe, Al, and Mn were present in the chemical compositions of the PRs (Table 2) and could have been simultaneously solubilized together with the phosphorus [43]. Even at low concentrations, these metals can inhibit the production of organic acids [44], hence reducing the acidification of the medium. This effect was indicated by the pH reduction profiles shown in Figure 4. For the St/Hap composites, the pH gradually decreased to pH 2 during the incubation period (evidencing a higher production of organic acids, compared to use of the PRs), while the PR-based composites showed rapid decreases of pH in the first 24 h, with stabilization at around pH 3.5 after 48 h of incubation.

The acidification of the medium and consequent lowering of pH was due to the production of organic acids such as citric, oxalic, gluconic, malic, succinic, and tartaric acids, among others, characteristic of *A. niger* metabolism [20, 45]. These acids can form complexes with calcium, iron, aluminum, and other metals present in the structure of the phosphatic material, hence releasing phosphate groups into the medium. This has been reported to be the main mechanism for solubilization of inorganic phosphate by microorganisms [20, 22-24].

In addition, the phosphorus ratios used in the composites produced with the different phosphate sources could have influenced the solubilization efficiency. Mendes et al. [46] reported a negative correlation between the amount of P_2O_5 solubilized and total P_2O_5, when the PR dose was increased. This phenomenon was also observed here, with the acidity only differing slightly among the composites produced with the same phosphate source, indicative of a limitation on the amount of PR that could be solubilized according to this mechanism. As a result, the solubilization efficiencies were lower for the composites with higher contents of P_2O_5. In order to circumvent this limitation, a second set of incubation experiments was performed with a reduction and standardization of the P_2O_5 mass added to the medium. The composites St/Hap 1:1, St/BPR 1:1, and St/IPR 1:1 were selected, due their better efficiencies shown in the bioactivation and solubilization experiments.

3.4. Effect of bioactivation on solubilization of the composites after standardization of P_2O_5 mass

This set of incubation experiments employed a standardized mass of added P_2O_5 (530 mg of P_2O_5 per kg of solution), so the amount of P added was always the same, but the total mass of the material added varied due to the different phosphorus contents of the materials.

The standardization of P_2O_5 is an established procedure for analysis of the solubilities of different phosphate sources [47]. The amount of P_2O_5 mass added was standardized according to the recommendations of Malavolta [48] and Novais [49] (around 458 mg of P_2O_5 per kg of soil). For this set of experiments, a ratio of 1 kg of liquid medium to 1 kg of soil was considered to reproduce typical conditions involving the application of phosphate fertilizers to soil.

Figure 5 shows the phosphorus solubilization and pH_{final} values for selected composites, using a fixed mass of P_2O_5 and incubation for 96 h. The St/Hap 1:1 composite showed a profile similar to that found previously (Figure 4A), with 100% solubilization of P_2O_5. However, the solubilization efficiencies obtained for the composites containing PR were significantly improved, with values of 75% for St/BPR 1:1 and 72% for St/IPR 1:1. This indicated that the organic acids produced in the first set of experiments did not provide sufficient acidity to solubilize the excess P_2O_5 content in the composite, in a finite medium, while when actual fertilization conditions were used, the quantity of organic acids produced was sufficient to provide up to 70% solubilization of the PRs, in only 96 h.
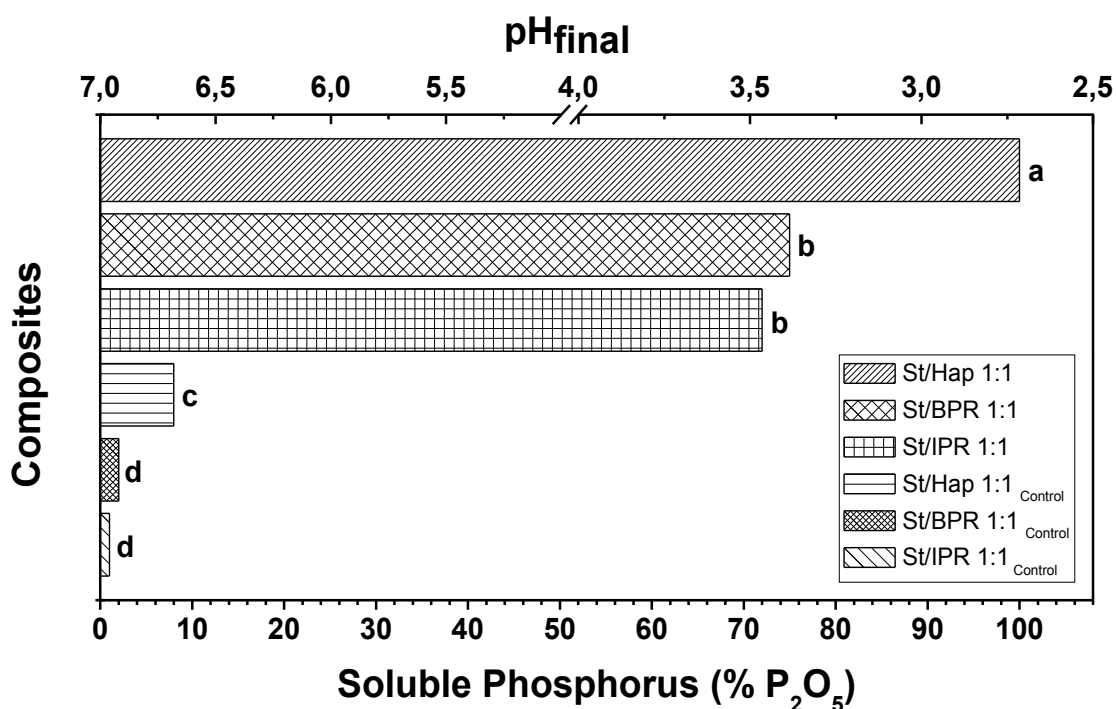

Fig. 5. Soluble phosphorus and pH_{final} for the composites St/Hap 1:1, St/BPR 1:1, St/IPR 1:1, and the control (without *A. niger* spores), with standardization of the P_2O_5 mass, after 96 h at 30 °C and 220 rpm. Different letters indicate significant difference among the treatments (ANOVA with Tukey's test, 95% confidence level).

Application of Tukey's test at the 95% confidence level (Figure 5) showed that there were no significant differences in phosphate solubilization between the St/BPR 1:1 and St/IPR 1:1 composites. This was a very promising finding, because it indicated that the composites provided the same solubilization efficiencies for sedimentary (BPR) and igneous (IPR) phosphate rocks, in only 96 h. The higher solubility of sedimentary rocks is widely reported in the literature [38, 41]. For example, Schneider et al. [50] evaluated the biosolubilization, by *A. niger*, of a sedimentary phosphate rock (from North Carolina, USA) and two igneous phosphate rocks (from Catalão, Brazil, and Kapuskasing, Canada). It was shown that the sedimentary rock (5.4% solubilization) was more soluble than the igneous rocks (4.4% and 4.0% solubilization, respectively), after 192 h. This highlights the effectiveness of the strategy applied in the present work, which provided a high solubilization efficiency, in a relatively short period of time, for phosphorus from igneous rocks with lower reactivity (such as the Itafós mineral) that are found in many countries, including Brazil [51].

The results obtained here confirmed the potential of the nanocomposites as a smart strategy for phosphate fertilization, since the granules provided adequate phosphate concentrations, as well as a source of carbon and energy for the growth of *A. niger* and production of the organic acids required for phosphate release.

4. Conclusions

Our findings showed that the gelatinized starch matrix is an ideal material for the simultaneous dispersion of rock phosphate and encapsulation of *A. niger*, thus maximizing the effect of the microbial solubilization of the P-sources. Such favored results towards P solubilization observed with the bioactivation of the starch-phosphate rock nanocomposite is likely related to the combined role of the starch as a dispersion matrix and as a carbon source for adequate microorganism development. The composites prepared with the Bayóvar (reactive) and Itafós (unreactive, low solubility) phosphate rocks demonstrated potential as biofertilizers, with phosphorus solubilization of up to 70% in 96 h from the standardized phosphorus mass employed in the medium. These nanocomposites open up new routes for the development of smart fertilizers in which microorganisms provide solubilization of inorganic phosphorus found in unreactive minerals that are abundant and inexpensive sources of phosphate.

Acknowledgments

Supporting Information Available

Contains X-ray diffraction (XRD) of the St/Hap 1:1, St/Hap 1:1.5, and St/Hap 1:2 composites and hydroxyapatite showing that the apatite phase is not altered during the processing of the composite. A visual comparison between the initial nanocomposite (solid granules) and after 96 h of bioactivation at culture medium is also include.

References

1.   de Campos, M.; Antonangelo, J. A.; Alleoni, L. R. F., Phosphorus sorption index in humid tropical soils. *Soil & Tillage Research* **2016,** *156*, 110-118.

2.   Vilar, C. C.; Costa, A. C. S. d.; Hoepers, A.; A Souza Junior, I. G. d., Capacidade máxima de adsorção de fósforo relacionada a formas de ferro e alumínio em solos subtropicais. *Revista Brasileira de Ciência do Solo* **2010,** *34*, 1059-1068.

3.   Vassilev, N.; Vassileva, M.; Lopez, A.; Martos, V.; Reyes, A.; Maksimovic, I.; Eichler-Loebermann, B.; Malusa, E., Unexploited potential of some biotechnological techniques for biofertilizer production and formulation. *Applied Microbiology and Biotechnology* **2015,** *99*, (12), 4983-4996.

4.   Vassilev, N.; Vassileva, M., Biotechnological solubilization of rock phosphate on media containing agro-industrial wastes. *Applied Microbiology and Biotechnology* **2003,** *61*, (5-6), 435-440.

5.   Conley, D. J.; Paerl, H. W.; Howarth, R. W.; Boesch, D. F.; Seitzinger, S. P.; Havens, K. E.; Lancelot, C.; Likens, G. E., Ecology Controlling Eutrophication: Nitrogen and Phosphorus. *Science* **2009,** *323*, (5917), 1014-1015.

6.   Nemery, J.; Garnier, J., Biogeochemistry The fate of phosphorus. *Nature Geoscience* **2016,** *9*, (5), 343-344.

7.   Lin, X. G.; Feng, Y. Z.; Zhang, H. Y.; Chen, R. R.; Wang, J. H.; Zhang, J. B.; Chu, H. Y., Long-Term Balanced Fertilization Decreases Arbuscular Mycorrhizal Fungal Diversity in an Arable Soil in North China Revealed by 454 Pyrosequencing. *Environmental Science & Technology* **2012,** *46*, (11), 5764-5771.

8.   Silva, U. C.; Medeiros, J. D.; Leite, L. R.; Morais, D. K.; Cuadros-Orellana, S.; Oliveira, C. A.; Lana, U. G. D.; Gomes, E. A.; Dos Santos, V. L., Long-Term Rock Phosphate Fertilization Impacts the Microbial Communities of Maize Rhizosphere. *Frontiers in Microbiology* **2017,** *8*, 11.

9.   Plotegher, F.; Ribeiro, C., Characterization of Single Superphosphate Powders - a study of Milling Effects on Solubilization Kinetics. *Materials Research-Ibero-American Journal of Materials* **2016,** *19*, (1), 98-105.

10.   Zapata, F., Use of phosphate rocks for sustainable agriculture. *FAO Fertilizer and Plant Nutrition Bulletin* **2004**, 1-148.

11.   Lessl, J. T.; Ma, L. Q., Sparingly-Soluble Phosphate Rock Induced Significant Plant Growth and Arsenic Uptake by Pteris vittata from Three Contaminated Soils. *Environmental Science & Technology* **2013,** *47*, (10), 5311-5318.

12.   Green, T. H.; Watson, E. B., Crystallization of apatite in natural magmas under high pressure, hydrous conditions, with particular reference to 'Orogenic' rock series. In *Contributions to Mineralogy and Petrology*, 1 ed.; 1982; pp 1432-0967.

13.   Cao, X. D.; Harris, W., Carbonate and magnesium interactive effect on calcium phosphate precipitation. *Environmental Science & Technology* **2008,** *42*, (2), 436-442.

14.   Fayiga, A. O.; Nwoke, O. C., Phosphate rock: origin, importance, environmental impacts, and future roles. *Environmental Reviews* **2016,** *24*, (4), 403-415.

15.   Pavinato, P. S.; Rodrigues, M.; Soltangheisi, A.; Sartor, L. R.; Withers, P. J. A., Effects of Cover Crops and Phosphorus Sources on Maize Yield, Phosphorus Uptake, and Phosphorus Use Efficiency. *Agronomy Journal* **2017,** *109*, (3), 1039-1047.

16.   de Oliveira, A.; Prochnow, L. I.; Klepker, D., Soybean yield in response to application of phosphate rock associated with triple superphosphate. *Scientia Agricola* **2011,** *68*, (3), 376-385.

17.   Vieira Fontoura, S. M.; Beber Vieira, R. C.; Bayer, C.; Ernani, P. R.; de Moraes, R. P., Agronomic performance of phosphate fertilizers in an oxisol under no-tillage. *Revista Brasileira De Ciencia Do Solo* **2010,** *34*, (6), 1907-1914.

18.   Richart, A.; Lana, M. d. C.; Schulz, L. R.; Bertoni, J. C.; Braccini, A. d. L. e., Phosphorus and sulfur availability for soybean in the presence of reactive natural phosphate, triple superphosphate and elemental sulfur. *Revista Brasileira De Ciencia Do Solo* **2006,** *30*, (4), 695-705.

19.   Jain, R.; Saxena, J.; Sharma, V., The evaluation of free and encapsulated Aspergillus awamori for phosphate solubilization in fermentation and soil–plant system. *Applied Soil Ecology* **2010,** *46*, (1), 90-94.

20.   Mendes, G. D.; de Freitas, A. L. M.; Pereira, O. L.; da Silva, I. R.; Vassilev, N. B.; Costa, M. D., Mechanisms of phosphate solubilization by fungal isolates when exposed to different P sources. *Annals of Microbiology* **2014,** *64*, (1), 239-249.

21.   Klaic, R.; Plotegher, F.; Ribeiro, C.; Zangirolami, T. C.; Farinas, C. S., A novel combined mechanical-biological approach to improve rock phosphate solubilization. *International Journal of Mineral Processing* **2017,** *161*, 50-58.

22.   Kpomblekoua, K.; Tabatabai, M. A., Effect of organic-acids on release of phosphorus from phosphate rocks. *Soil Science* **1994,** *158*, (6), 442-453.

23.   Nahas, E., Factors determining rock phosphate solubilization by microorganisms isolated from soil. *World Journal of Microbiology & Biotechnology* **1996,** *12*, (6), 567-572.

24.   Illmer, P.; Schinner, F., Solubilization of inorganic calcium phosphates—Solubilization mechanisms. *Soil Biology and Biochemistry* **1995,** *27*, (3), 257-263.

25.   Menezes-Blackburn, D.; Paredes, C.; Zhang, H.; Giles, C. D.; Darch, T.; Stutter, M.; George, T. S.; Shand, C.; Lumsdon, D.; Cooper, P.; Wendler, R.; Brown, L.; Blackwell, M.; Wearing, C.; Haygarth, P. M., Organic Acids Regulation of Chemical Microbial Phosphorus Transformations in Soils. *Environmental Science & Technology* **2016,** *50*, (21), 11521-11531.

26. Vassilev, N.; Vassileva, M.; Fenice, M.; Federici, F., Immobilized cell technology applied in solubilization of insoluble inorganic (rock) phosphates and P plant acquisition. *Bioresource Technology* **2001,** *79*, (3), 263-271.

27. Vassileva, M.; Serrano, M.; Bravo, V.; Jurado, E.; Nikolaeva, I.; Martos, V.; Vassilev, N., Multifunctional properties of phosphate-solubilizing microorganisms grown on agro-industrial wastes in fermentation and soil conditions. *Applied Microbiology and Biotechnology* **2010,** *85*, (5), 1287-1299.

28. Giroto, A. S.; de Campos, A.; Pereira, E. I.; Cruz, C. C. T.; Marconcini, J. M.; Ribeiro, C., Study of a Nanocomposite Starch-Clay for Slow-Release of Herbicides: Evidence of Synergistic Effects Between the Biodegradable Matrix and Exfoliated Clay on Herbicide Release Control. *Journal of Applied Polymer Science* **2014,** *131*, (23).

29. Giroto, A. S.; Guimaraes, G. G. F.; Foschini, M.; Ribeiro, C., Role of Slow-Release Nanocomposite Fertilizers on Nitrogen and Phosphate Availability in Soil. *Scientific Reports* **2017,** *7*, 11.

30. dos Santos, B. R.; Bacalhau, F. B.; Pereira, T. D.; Souza, C. F.; Faez, R., Chitosan-Montmorillonite microspheres: A sustainable fertilizer delivery system. *Carbohydrate Polymers* **2015,** *127*, 340-346.

31. Haq, I.-U.; Ali, S.; Iqbal, J., Direct production of citric acid from raw starch by Aspergillus niger. *Process Biochemistry* **2003,** *38*, (6), 921-924.

32. Saber, W. I. K.; Ghanem, K. M.; El-Hersh, M. S., Rock phosphate solubilization by two isolates of *Aspergillus niger* and *Penicillium* sp. and their promotion to mung bean plants. *Research Journal of Microbiology* **2009,** *4*, (7), 235-250.

33. Pikvoskaya, Mobilization of phosporus in soil connection with the vital activity of some microbial species. In Microbiology, 1948; Vol. 17, pp 362-370.

34. Murphy, J.; Riley, J. P., Citation-classic - a modified single solution method for the determination of phosphate in natural-waters. *Current Contents/Agriculture Biology & Environmental Sciences* **1986**, (12), 16-16.

35. Drummond, L.; Maher, W., Determination of phosphorus in aqueous-solution via formation of the phosphoantimonylmolybdenum blue complex - reexamination of optimum conditions for the analysis of phosphate. *Analytica Chimica Acta* **1995,** *302*, (1), 69-74.

36.   McArthur, J. M., Francolite geochemistry - compositional controls during formation, diagenesis, metamorphism and weathering. *Geochimica Et Cosmochimica Acta* **1985,** *49*, (1), 23-35.

37.   McArthur, J. M.; Benmore, R. A.; Coleman, M. L.; Soldi, C.; Yeh, H. W.; Obrien, G. W., Stable isotopic characterization of francolite formation. *Earth and Planetary Science Letters* **1986,** *77*, (1), 20-34.

38.   Chien, S. H., Solubility assessment for ferlilizer containing phosphate rock. *Fertilizer Research* **1993,** *35*, (1-2), 93-99.

39.   Lim, H. H.; Gilkes, R. J.; McCormick, P. G., Beneficiation of rock phosphate fertilisers by mechano-milling. *Nutrient Cycling in Agroecosystems* **2003,** *67*, (2), 177-186.

40.   Schuffert, J. D.; Kastner, M.; Emanuele, G.; Jahnke, R. A., Carbonate-ion substitution in francolite - a new equation. *Geochimica Et Cosmochimica Acta* **1990,** *54*, (8), 2323-2328.

41.   Loureiro, F. E. L.; Monte, M. B. d. M.; Nascimento, M., *Agrominerais - Fosfato*. 2ª ed.; CETEM-MCT: Rio de Janeiro, 2008; p 141-180.

42.   Bengtsson, A.; Lindegren, M.; Sjoberg, S.; Persson, P., Dissolution, adsorption and phase transformation in the fluorapatite-goethite system. *Applied Geochemistry* **2007,** *22*, (9), 2016-2028.

43.   Mendes, G. d. O.; Bojkov Vassilev, N.; Araujo Bonduki, V. H.; da Silva, I. R.; Ribeiro, J. I., Jr.; Costa, M. D., Inhibition of Aspergillus niger Phosphate Solubilization by Fluoride Released from Rock Phosphate. *Applied and Environmental Microbiology* **2013,** *79*, (16), 4906-4913.

44.   Papagianni, M., Advances in citric acid fermentation by Aspergillus niger: Biochemical aspects, membrane transport and modeling. *Biotechnology Advances* **2007,** *25*, (3), 244-263.

45.   Li, Z.; Bai, T. S.; Dai, L. T.; Wang, F. W.; Tao, J. J.; Meng, S. T.; Hu, Y. X.; Wang, S. M.; Hu, S. J., A study of organic acid production in contrasts between two phosphate solubilizing fungi: Penicillium oxalicum and Aspergillus niger. *Scientific Reports* **2016,** *6*.

46.   Mendes, G. O.; Dias, C. S.; Silva, I. R.; Ribeiro, J. I.; Pereira, O. L.; Costa, M. D., Fungal rock phosphate solubilization using sugarcane bagasse. *World Journal of Microbiology & Biotechnology* **2013,** *29*, (1), 43-50.

47. MAPA, Manual de métodos analíticos oficiais para fertilizantes e corretivos. In Abastecimento, M. d. A. P. e., Ed. Brazil, 2013.

48. Malavolta, E., *Elementos de nutrição mineral de plantas*. 1980; p 251.

49. NOVAIS, R. F.; NEVES, J. C. L.; BARROS, N. F., Ensaio em ambiente controlado. In ***Métodos de pesquisa em fertilidade do solo***, 1 ed.; OLIVEIRA, A. J.; GARRIDO, W. E.; ARAÚJO, J. D.; LOURENÇO, S., Eds. Brasil: Brasília: Embrapa-SEA, 1991; Vol. 3, pp 189-253.

50. Schneider, K. D.; van Straaten, P.; de Orduna, R. M.; Glasauer, S.; Trevors, J.; Fallow, D.; Smith, P. S., Comparing phosphorus mobilization strategies using Aspergillus niger for the mineral dissolution of three phosphate rocks. *Journal of Applied Microbiology* **2010,** *108*, (1), 366-374.

51. Atencio, D., The discovery of new mineral species and type minerals from Brazil. *Brazilian Journal of Geology* **2015,** *45*, (1), 143-158.
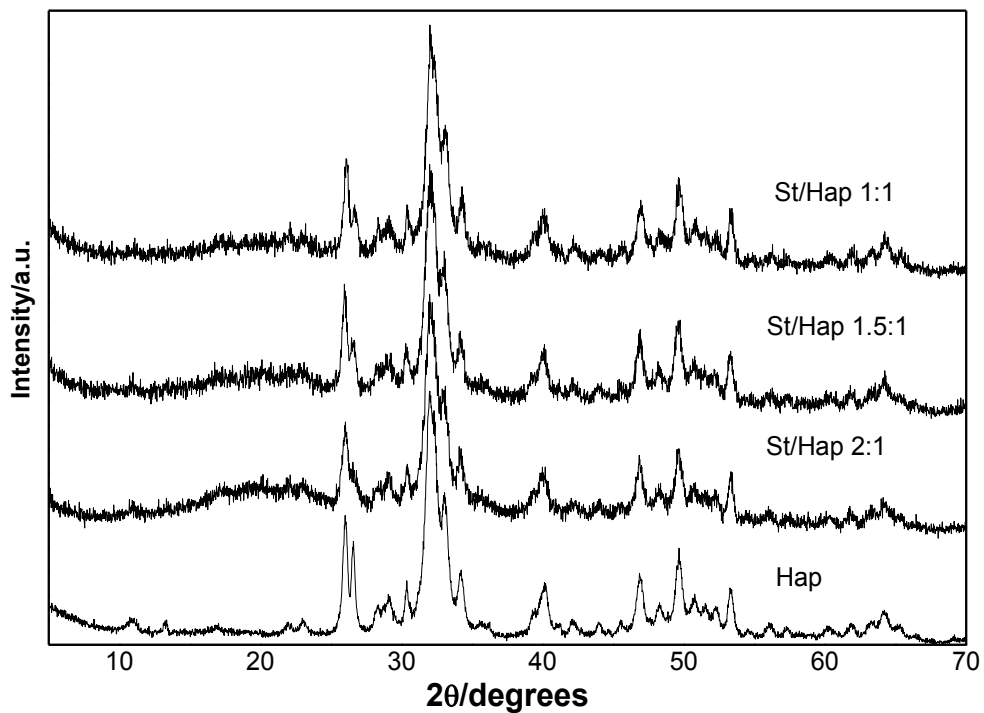
Fig. S1. XRD patterns of the St/Hap 1:1, St/Hap 1:1.5, and St/Hap 1:2 composites and hydroxyapatite.
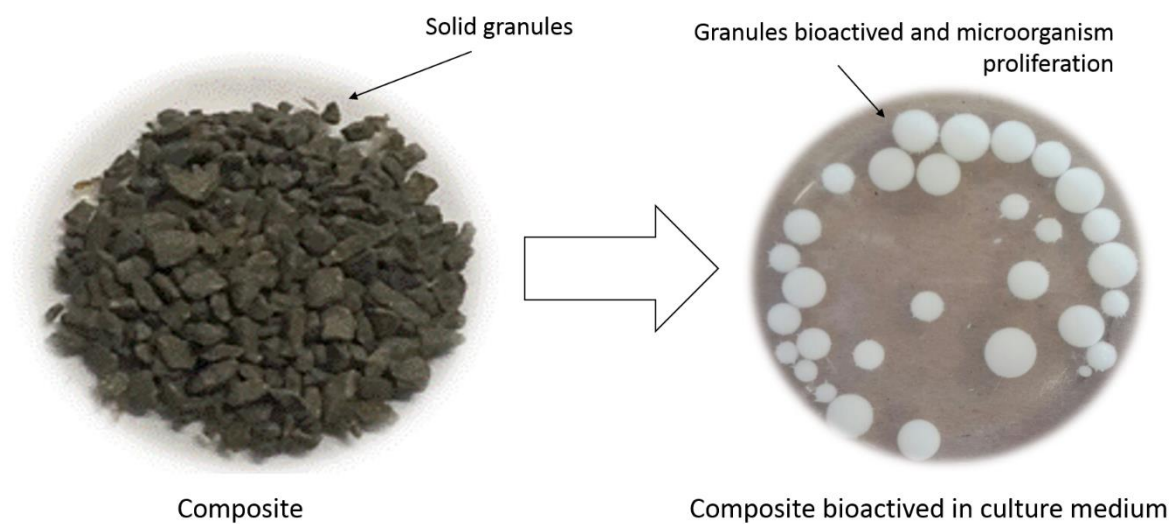
Fig. S2. Visual comparison between the initial nanocomposite (solid granules) and after 96 h of bioactivation at culture medium.

Capítulo 6

"Nanocomposites fertilizers biologically activated for an efficient supply of sulfur and micronutrients to plants"

Artigo em elaboração

São crescentes as pesquisas relacionadas à tecnologia de fertilizantes e um tema em evidência é o desenvolvimento de estratégias para aumentar a solubilidade de fontes de nutrientes de baixa reatividade, de forma a fornecê-los adequadamente às plantas. Nesse contexto, destaca-se o potencial dos compósitos-fertilizantes apresentados no Capítulo 5, que se mostraram eficientes para aumentar a solubilidade de fontes fosfatadas de baixa solubilidade. Entretanto, a tecnologia desenvolvida também pode ser aplicada a outras fontes de nutrientes de baixa solubilidade como minerais ricos em macro e micronutriente, entre outras fontes pouco reativas, mas com interesse para o setor de fertilizantes. Assim, nesta etapa do trabalho foi avaliado o potencial dessa estratégia para promover o aumento de solubilidade de óxidos minerais (fonte de micronutriente) e para a oxidação do enxofre elementar (fonte de macronutriente) pela ação de um microrganismo usando o conceito de "granulo biorreator" desenvolvido no Capítulo 5. Os resultados deste estudo mostraram que a tecnologia dos compósitos-fertilizantes também foi eficiente para comportar uma alta carga de óxidos e enxofre elementar, além do encapsulamento de *A. niger*, garantido proteção ao microrganismo e tempo de prateleira ao produto. O produto final obtido foi um grânulo multi-nutriente, fonte de Zn, Mn, Cu e S para as plantas. Experimentos realizados em casa de vegetação no sistema solo-planta comprovaram o potencial destes compósitos fertilizantes, com resultados similares aos obtidos com fertilizantes comerciais. Os resultados estão apresentados na forma de artigo e referem-se aos objetivos específicos 5 e 6: (5) desenvolvimento de novas alternativas de produtos para aumentar a solubilidade de rochas fosfática e outras fontes de nutrientes de baixa solubilidade a partir a ação de microrganismos solubilizadores, (6) Avaliação da eficácia dos biofertilizantes propostos no sistema solo-planta em casa de vegetação.

Abstract

Many commercial fertilizers are based on the application of elemental sulfur (S°) and oxides to supply sulfate and micronutrients to plants. However, the soil ability to solubilize oxides and promote the S° oxidation is low, since it is dependent of the presence of microorganisms capable of carrying out such biological reactions. To overcome this limitation, different strategies have been explored to increase the availability of sources of nutrients of low solubility, such as oxides and S°. Herein, we proposed to develop a composite based in the gelatinization of starch with dispersion of oxides and S°, and addition of *Aspergillus niger* spores, which act towards increasing the availability of these sources of micronutrients. All the different composites produced (St/Zn, St/Mn, St/Cu, St/Mix and St/Mix+S) increased solubility of the dispersed material. Nevertheless, the St/Mix+S presented the best results of solubilization for oxides, besides being a source of multi-nutrient (S, Zn, Mn and Cu). The St/Mix+S also showed considerable shelf time and when evaluated under greenhouse conditions, it showed an efficiency comparable to the experiment carried out with soluble commercial fertilizer for the cultivation of Italian ryegrass (*Lolium multiflorum* Lam.). This strategy opens a new route for development of smart fertilizer capable of making feasible the use of source of micronutrients of low solubility for plant nutrition.

Keywords: Oxides solubilization, Elemental sulfur oxidation, Starch gelatinization, *Aspergillus niger*.

1. Introduction

Although micronutrients are required in small amounts, they are indispensable for the plant to close its vegetative cycle and increase productivity (Liu & Lal, 2015; Malavolta, 1980; Martinez-Ballesta et al., 2010). Until sometime ago, there was almost no concern about the monitoring of micronutrients in the soil, but with the constant use of the land, lack of crop rotation as well as erosion and leaching there was a reduction of these elements to critical levels, mainly in soils poor in organic matter (Malavolta, 1980). Currently, monitoring of micronutrients in soil has become more common, with the micronutrients such as boron (B), copper (Cu), manganese (Mn), zinc (Zn), molybdenum (Mo), among others being added to the soil in the form of fertilizer of high solubility such as salts, sulfates, nitrates and phosphates (Malavolta, 1980; Martinez-Ballesta et al., 2010). However, these types of fertilizers besides high cost, are produced from the chemical processing of their respective oxides with inorganic acids, which can cause several environmental impacts.

The direct use of oxides is an attractive alternative for fertilization, since the absence of previous chemical treatment results in reduced environmental impacts and lower costs, with the additional advantage of presenting a higher content of the element than the salts. Although many commercial fertilizers are based on the use of oxides, the high chemical stability of the oxides limits the solubility of these materials to a level much lower than the required in practical applications (Heinonen et al., 2017). Therefore, there is a need to identify alternatives that allow improving the solubilization of the oxides, preferably of the material which will be applied in the field, thus accessing the entire micronutrient available and ensuring that the solubilization occurs during a period of time suitable for the needs of the plants.

An interesting alternative is the application of microorganisms to promote the solubilization of the oxides in the field. The filamentous fungi *Aspergillus niger* has been applied to promote the phosphorus solubilization from phosphate minerals (Klaic et al., 2017; Mendes et al., 2015) as well as bioremediation and bioleaching of metals from mining ores (Bhalerao, 2012; Bhalerao & Puranik, 2007; Ong et al., 2017; Sutjaritvorakul et al., 2017; Tejomyee, 2013). Besides, previous studies also revealed that *A. niger* can promote the biological oxidation of elemental sulfur that presents similar limitation towards solubilization as the oxides (Grayston et al., 1986). However, the application of microorganisms to improve the solubilization of oxides is still little explored as well as the development of efficient ways of promoting the interaction of the oxide with the microorganism when applied to the field.

Thus, the major challenge is to develop a material that would favor the integration of both oxides particles and microorganisms in a single granule to promote oxide solubilzation that could be processed and stored, thus when applied in the field the granule would be activated to allow microorganism growth to solubilize the oxide.

The purpose of this work was to evaluate whether *A. niger* is able to solubilize metals from oxides and understand the mechanisms of solubilization. An innovative method to produce a composite was proposed based on the dispersion of nanoparticles of oxides in a polysaccharide matrix (polymeric gelatinized starch) and simultaneous encapsulation of *A. niger* spores. Three oxides model (ZnO, MnO and CuO) besides elemental sulfur (S°) were used to produce different configurations of composites. The oxides were physical-chemical characterized as well as the composites produced. Experiments were performed to evaluate the effect of bio-activation of the composite by *A. niger* and consequent oxides solubilization. The shelf time of the composites was also evaluated. The final products obtained were novel types of composite-fertilizer bio-activated with *A. niger* to promote the solubilization of source of nutrients of low solubility to plants. This study provides a basis for the development of a new class of smart biofertilizer, which could open up new applications for formulations containing poorly soluble mineral oxides.

2. Materials and Methods

2.1. Microorganism

The filamentous fungi *Aspergillus niger C* (BRMCTAA 82) was obtained from the Embrapa Food Technology collection (Rio de Janeiro, RJ, Brazil) and selected among 8 filamentous fungi as the best to solubilize phosphate rock by Klaic et al. (2017). Spores suspensions of the fungi strain were kept at -18 °C in a solution of water with glycerol (10% wt.) and NaCl (0.9% wt.). Spores were germinated on Petri dishes containing potato dextrose agar at 30 °C. After 96 h, a suspension of grown spores was harvested by adding distilled water. The spore concentration was determined using a Neubauer chamber.

2.2. Materials

Standard corn starch (St) (Amidex 3001, 30% amylose and 70% amylopectin) was kindly supplied by Corn Products Brazil and urea was from Synth, SP, Brazil. Elemental

Sulfur (86 wt.%) was from Sigma-Aldrich, St. Louis, MO. Zinc oxide (ZnO), manganese oxide (MnO) and copper oxide (CuO) were supplied by Heringer Fertilizers Brazil. All the materials were used as received. Detailed characterizations of the three oxides were carried out in order to evaluate the chemical and physical natures of these sources (described in Section 2.5).

2.3. Preparation of the composites

The nanocomposites were prepared first by starch (St) gelatinization, through dispersion of starch 8 wt.% and urea 1 wt.% in distilled water (250 ml). The gelatinization process was carried out by keeping the dispersed starch at about 90 ºC for 30 min under stirring until a sticky starch paste gel was formed, following the protocol proposed by Giroto et al. (2014). Then the oxides particles were transferred to the medium and their dispersion in the starch gel was accomplished by vigorous agitation for 15 min. The oxides were added to the starch paste gel in a proportion of 1:2 among starch (33.6 wt.%) and oxide/mix of oxides (66.4 wt.%). For the composites with elemental sulfur, the oxides were mixed with the elemental sulfur using a beaker and spatula for further dispersion in the starch gel. The different proportion of the starch, oxides and elemental sulfur used to produce the nanocomposites are shown in Table 1 as well as their nomenclatures. After the oxides dispersion, the temperature was reduced to 30 ºC, and *Aspergillus niger* spores were incorporated (spore suspension were prepared as described in Section 2.1) to achieve a concentration of 1×10^8 spores per gram of the material. The mixed gel was kept at 30 ºC with air circulation for at least 12 h to obtain a solid gel. The dried composite was ground in a laboratory knife mill (Marconi, model MA048) and the particles between 1-4 mm were collected with a sieve and stored in dry boxes prior to characterization (described in Section 2.4) and for experiments of bio-activation (described in Section 2.6). All composites were prepared using the same procedure.

Table 1: Composition of composites produced in terms of starch, metallic oxides and elemental sulfur. The final available percentage of Zn, Mn and Cu in each material is also included.

Composite	% in Mass								
	% of the material added in the formulation					% of element in final product			
	Starch	Zinc Oxide	Manganese Oxide	Copper Oxide	Elemental Sulfur	Zinc	Manganese	Copper	Sulfur
	(St)	(ZnO)	(MnO)	(CuO)	(S°)	(Zn)	(Mn)	(Cu)	(S)
St/ZnO	33.44	66.66	-	-	-	39.48	-	-	-
St/MnO	33.44	-	66.66	-	-	-	33.31	-	-
St/CuO	33.44	-	-	66.66	-	-	-	14.70	-
St/Mix	33.44	13.70	16.23	36.73	-	8.11	8.11	8.11	-
St/Mix+S	33.44	6.40	7.58	17.17	35.52	3.79	3.79	3.79	30.55

2.4. Characterization of oxides and composites

The specific surface area of the three oxides were determined by isothermal nitrogen adsorption using a Micromeritics ASAP-2020 instrument, according to the 5-point B.E.T. (Brunauer–Emmett–Teller) method.

The particle size for the three oxides was also determined. For that, aliquots (2 mg) were transferred to a 25 ml glass bottle, which contained 10 ml of distilled water and sonicated using Ultrasonic Homogenizer Sonicate for 5 min and 30% of intensity, posteriorly the particle size distribution was measured using a Particle Zetasizer analyzer (Malvern Instruments).

X-ray fluorescence (XRF) for the three oxides were performed to identify the most common chemical components present in oxide structure using the lithium tetraborate fusion technique.

The morphologies of the three oxides and of the nanocomposites produced were observed by field emission gun scanning electron microscopy (FEG-SEM), using a JSM-6701F microscope (JEOL, Japan) operated at an acceleration voltage of 15 kV, with a working distance of 10 mm and a secondary electron detector. Then, the disc was coated with carbon in a Leica EMSCD050 chamber and imaged using the secondary electron mode. Semi-

quantitative atomic compositions were evaluated by energy-dispersive X-ray (EDX) spectroscopy using an EDX Link Analytical device (Isis System Series 200) coupled with a LEO 440 scanning electron microscope.

In addition, the nanocomposites were also analyzed using X-ray microtomography (MicroCt) (model 1172 SkyScan) to observe the particle morphologies and degree of particle dispersion of oxides in the starch matrix. The composite samples were placed in a rotating steel support and the images were acquired using the following parameters: unaltered, spatial resolution (voxel size) of 2 mm, 0.3º step rotation, 180º rotation, and averaging of 6 frames. The images were reconstructed from the tomographic sections using NRecon software (SkyScan), applying the following settings: smoothing 5, ring artifact correction 5, and beam hardening correction of 60%.

2.5. Submerged cultivation

Experiments were carried out to evaluate the potential of *A. niger* to solubilize metallic oxides under submerged culture. First, the pre-culture was initiated in 250 mL Erlenmeyer flasks using 50 ml of nutrient medium by adding a volume of spore suspension calculated to give a concentration of $1.2x10^7$ spores per mL of the nutrient medium. Czaped Dox nutrient medium was used as described by Grayston et al. (1986) contained (w/v): sucrose, 3%; $NaNO_3$, 0.3%; NaCl, 0.2%; $MgCl_2.7H_2O$, 0.05%; KCl, 0.05%; KH_2PO_4, 0.1%. The incubation for the pre-culture step was carried out for 48 h in an orbital shaker incubator, at 30 °C and 220 rpm. Solubilization of oxides was initiated by transferring a volume of pre-culture suspension corresponding to 10% (v/v) to 50 mL of culture medium with the same composition. In this cultivation step, oxides were added and the suspension consisting of cells and oxides were kept for 96 h in an orbital shaker incubator at 30 °C and 220 rpm. The mass of oxides added was standardized at 2.5 mg in relation to the element for 50 ml of volume. Thus, the masses of ZnO, MnO and CuO added were 4.22 mg, 5.00 mg and 11.34 mg, respectively. After the bio-activation period, the resulting suspension was vacuum-filtered using Whatman No. 1 filter paper, followed by centrifugation for 20 min at 12000 rpm and 20 °C. The clear supernatant was analyzed for the determination of Zn, Mn and Cu solubilized using Inductively Coupled Plasma (ICP). All experiments were carried out in triplicate and the data were calculated as means ± standard deviations.

2.6. Bio-activation of the composites

Incubation of the nanocomposites in a liquid medium was conducted to evaluate the potential of *A. niger* encapsulated in matrix germinate and solubilize the metallic oxides as fungi grew. The nutrient medium used was Czapek Dox as described in Section 2.5. Cultivations were performed in 250 mL Erlenmeyer flasks by adding a volume of 50 mL of the nutrient medium. The incubation was carried out in an orbital shaker incubator, at 30 °C and 220 rpm. The mass of element added was standardized to obtain the same concentration in solution (50 mg L^{-1}). Thus, the masses of composites St/Zn, St/Mn, St/CuO, St/Mix and St/Mix+S added were 6.33, 7.50, 17.00, 30.8 and 65.96 mg, respectively. All experiments were carried out at triplicates. After this period, the resulting material was vacuum filtered using Whatman No. 1 filter paper and then centrifuged for 15 min at 11000 rpm and 20 °C. The clear supernatant was analyzed to determination of Zn, Mn and Cu solubilized using Inductively Coupled Plasma (ICP).

2.7. Determination of sulfur-oxidation in liquid medium

The sulfate (SO_4^{2-}) from the oxidation of S° were analyzed for turbidmetric as proposed by Camargo et al. (2009). The method is based on the $BaSO_4$ precipitation after addition of $BaCl_2$ into the solution and the SO_4^{2-} concentration was estimated by the solution turbidity. Then concentration of SO_4^{2-} were determined by UV-Vis spectrometry at a wavelength of 420 nm in a Lambda 25 UV-Vis Spectrophotometer (Perkin Elmer).

2.8. Soil-plant experiments

The efficiency of St/Mix+S composites as fertilizer sources of Zn, Mn, Cu and S to plants was evaluated in a greenhouse experiment conducted at Embrapa Pecuaria Sudeste, in São Carlos, São Paulo State, Brazil. The composites were applied in two Oxisols, a sandy loam and a clay soils, which are low in organic matter and poor in Zn, Mn, Cu and S content. The both soils were collected from a pasture site at a depth of 0-20 cm. Before use, the soil was air-dried, crushed to pass through a 2 mm screen for obtaining a homogeneous soil granulometry, and chemically and physically characterized (van Raij et al., 2001; Vanraij et al., 1986). The chemical and physical properties of both soil is shown in Table S1 at Supplementary Material.

Following a randomized complete block design with three treatments and four replications, and four additional pots to serve as unlabeled controls (without fertilization of S, Cu, Zn, Mn), thus, the 6 pots were each filled with 3 kg of soil. At the start of the experiment, the base saturation "V" of the soils were increase to 60% by applying liming, according by Cantarella and Furlani (1997). The soil samples were homogenized and incubated for 30 days with the moisture content of the soil maintained close to 70% of its water retention capacity.

About 20-30 Italian ryegrass (*Lolium multiflorum* Lam.) seeds were sown at 1 cm depth in soil surface. The initial fertilization with macro and micronutrients (except Zn, Mn, Cu and S) was performed immediately after the sowing of Italian ryegrass, with applied 82 mg kg^{-1} of P and 70 mg kg^{-1} of N as diammonium phosphate (DAP) in soil surface. Also, was applied into each pot a solution containing: 130 mg kg^{-1} of N (as urea); 118 mg kg^{-1} of P and 150 mg kg^{-1} of K (as KH_2PO_5); 0.8 mg kg^{-1} of B (as H_3BO_3); and 0.15 mg kg^{-1} (as $(NH_4)_6Mo_7O_{24}$), which was prepared according to Novais et al. (1991). The St/Mix+S composites fertilizer was transferred to the surface of the soil, at a rate to supply 100 mg kg^{-1} of S and 12 mg kg^{-1} of Cu, Zn and Mn, respectively. The S and micronutrients also were supplied in the same ratio as (mixture of oxides + elemental Sulphur) or as (soluble sources of micronutrients "$CuCl_2$; $ZnCl_2$ and $MnCl_2$" + source commercial S° "Sulphurgan®"). The fertilizers applied in each treatment were implemented to the surface of the soil. After fertilization and sowing of Italian ryegrass, soil moisture was adjusted by irrigation whenever necessary (visual determination) by gently applying water. After emergence of Italian ryegrass, thinning was carried to obtain a final stand of five plants per pot.

The dry matter production by Italian ryegrass was evaluated in 5 consecutive cuts, made to a height of 5 cm for subsequent regrowth at 40, 55, 70, 90, and 130-days days after fertilization. Plant material collected in each cut was dried in a forced-air oven at 70°C for 72 h, and the material was then weighed and ground to < 1 mm with a Wiley mill.

3. Results and Discussion

3.1. Zinc oxide, manganese oxide, copper oxide, and composites characterizations

A detailed characterization of the ZnO, MnO, and CuO was carried out in order to evaluate the chemical and physical nature of these commercial materials for subsequent production of the composites. Table 2 shows the chemical composition of these materials, their particle size and superficial area. The ZnO and MnO showed relatively high purity, but

the purity of the CuO was only 28% having also significant concentrations of Al_2O_3 (11%), SiO_2 (19%), SO_3 (8%), CaO (11%) and Fe_2O_3 (15%). We emphasize that Ca and S are also important macronutrients for the development of plants and are generally in low availability in soils, being present in the composition of commercial fertilizer such as single superphosphate (Martinez-Ballesta et al., 2010).

Table 2. Chemical analysis by X-ray fluorescence for zinc, manganese and copper oxide, their superficial area and particle size.

Composition	Oxides (% in Mass)		
	ZnO	MnO	CuO
ZnO	**73.726**	0.105	2.462
MnO	0.069	**64.572**	0.724
CuO	0.060	0.028	**27.618**
Na_2O	22.967	0.07	0.786
MgO	0.330	0.038	0.799
Al_2O_3	0.766	4.271	10.749
SiO_2	0.557	6.185	18.923
P_2O_5	0.004	0.258	0.690
SO_3	0.873	0.079	8.365
K_2O	0.044	1.264	0.827
CaO	0.209	0.504	11.125
TiO_2	Nd*	1.619	0.503
Fe_2O_3	0.285	17,705	14.71
NiO	0.038	0.054	0.093
SnO_2	Nd*	0.016	0.454
BaO	0.005	3.224	0.965
PbO	0.067	0.009	0.207
Total	**100**	**100**	**100**
Specific surface area ($m^2\ g^{-1}$)	**1.0627**	**9.2588**	**5.3589**
Particle Size (nm)	**446±46**	**325±56**	**302±51**

*Nd: Not detected

Regarding the physical properties of the materials, ZnO presented a larger particle size (around 446 nm) and a lower surface area (1 $m^2\ g^{-1}$) when compared to other two materials, probably due to the more crystalline morphology of this material, as can be observed in micrographs shown in Figure 1 A. On the other hand, a rough morphology was observed for

MnO and CuO, as shown in Figure 1B and 1C, respectively. In addition, it was possible to observe from the morphological analyzes a tendency of formation of agglomerates for the three oxides (Figure 1 A-C).

The dispersion of the particles of oxides in the starch matrix forming the composites was analyzed using X-ray microtomography, as shown in Figure 1 (D-H) for composites St/Zn, St/Mn, St/Cu, St/Mix and St/Mix+S, respectively. The bright dots in each image show the dispersion of the particles in the starch matrix. This analysis revealed that ZnO particles were homogeneously distributed in the starch matrix. In addition, for the composites St/Mn and St/Cu as well as St/Mix it was observed a higher tendency for particle agglomeration, resulting in composites with lower homogeneity when compared to St/Zn. The composite St/Mix+ S was also very homogeneous, but some small agglomerate smaller than 100 µm were observed. This shows that the elemental sulfur (S°) added in this composite had a good interaction with the matrix of starch, thus increasing dispersion of the oxides, despite their smaller quantity. The elemental distribution in the composite St/Mix+S was also analyzed by Energy-Dispersive X-ray (EDX) spectroscopy (Figure 1 I), corroborating the results and showing that S, Zn, Mn and Cu are homogeneously distributed in the matrix.
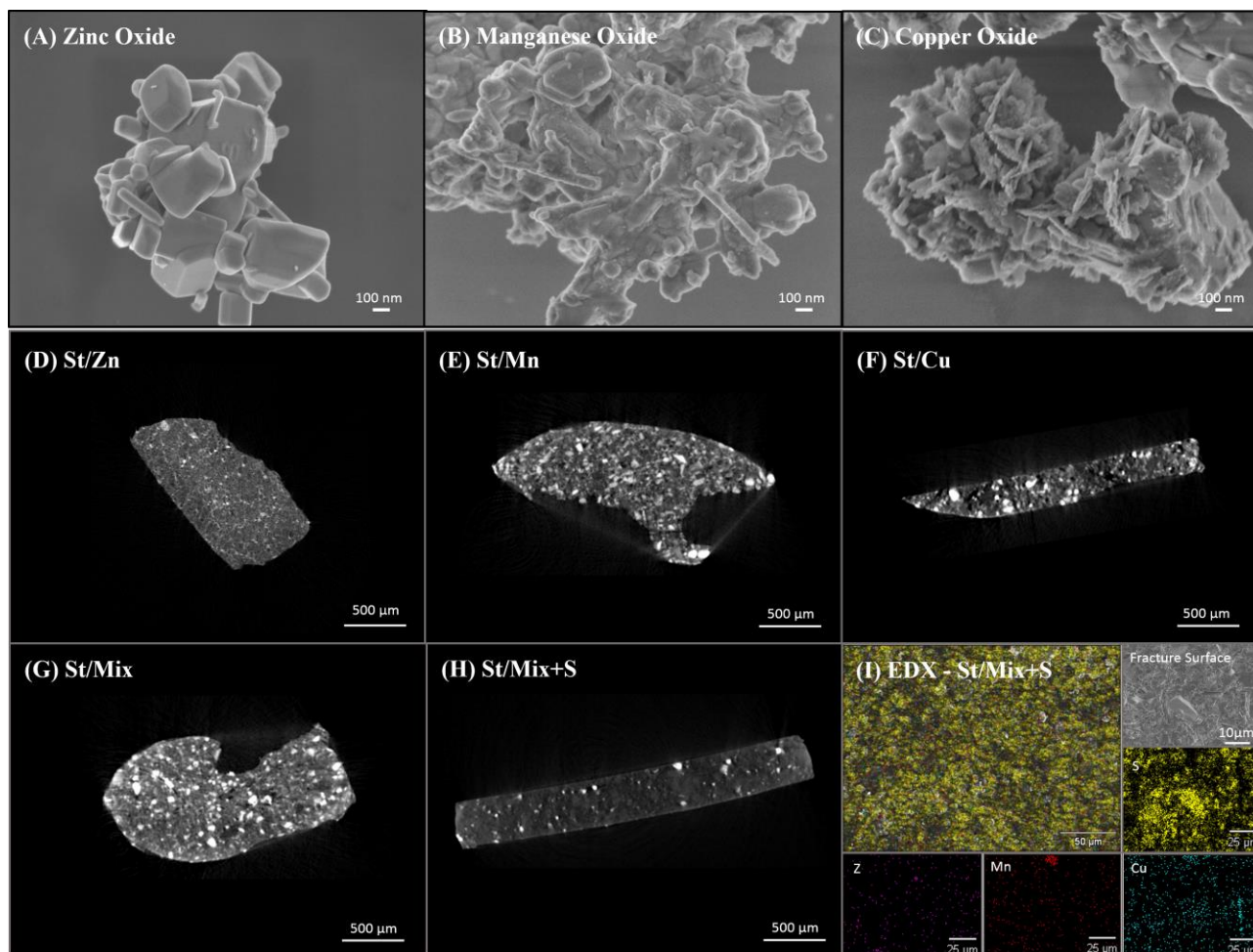
Figure 1. FEG-SEM micrographs for **A)** ZnO, **B)** MnO and **C)** CuO. The X-ray tomography cross-sectional images of the composites are also included in **D)** St/Zn, **E)** St/Mn, **F)** St/Cu, **G)** St/Mis and **H)** St/Mix+S. **I)** Scanning electron micrographs of distribution of the elements (S, Zn, Mn and Cu) in the composite St/Mix+S by EDX analysis

3.2. Biosolubilization of the oxides under submerged cultivation

This set of experiments was carried out to evaluate the potential of *A. niger* in solubilizing the oxides under submerged cultivation and to understand the mechanisms of solubilization involved. Figure 2 A shows the temporal profiles of solubilization for ZnO, MnO and CuO during submerged cultivation of *A. niger* (free-cells) as well as the control experiments (without *A. niger* inoculation). In the first 24 h of *A. niger* cultivation, all three oxides showed a remarkable higher solubility than the control treatment. The increased in the solubilization could be attributed to the acidification of the medium owing the organic acid production by *A. niger*, since the solubilization increase with the reduction of the pH (Figure

2B). The solubility of ZnO and MnO was around of 41% and 50% after only 24 h of cultivation, respectively. Nevertheless, the solubilization for the three oxides increased gradually to 80% for ZnO, 74% for MnO and 45% for CuO at 96 h. The temporal profiles of solubilization for the ZnO and MnO were similar, while the temporal profile for the CuO was less intense, probably due to some antimicrobial effect that this type of oxide can present when in high concentrations (Araujo et al., 2018; Mayorga et al., 2018). A similar study evaluating the potential of microbial solubilization of oxides (MnO_2, Fe_2O_3,CuO and granular metallic zinc) had been previously performed using the filamentous fungi *Trichoderma harzianum* (Altamore et al. 1999). However, the results found in this study in terms of efficiency of solubilization of oxides by *A. niger* were much superior.

These results indicate that the mechanisms for oxides solubilization are similar to the mechanisms reported for bioleaching wherein the solubilization of the oxides is a consequence of acidification of medium by the production of organic acids such as citric acid, oxalic acid, gluconic acid among others (Bahaloo-Horeh & Mousavi, 2017; Chaerun et al., 2017; Rasoulnia & Mousavi, 2016). The effect these three organic acids as promoter agents of oxide solubilization was demonstrated by carrying out solubilization experiments using water as a control (Figure S1, Supplementary Material). For the three oxides analyzed, the solubility in water was less than 0.1%, while the solubility of the three oxides was highly significant for most of the organic acids, except for zinc oxide and manganese oxide in oxalic acid.

Other possible mechanisms involved in the oxides solubilization could be related to the presence of some compounds with at least two hydrophilic reactive groups (e.g., phenol derivatives) which can also be excreted into the culture medium during the cultivation process. Such compounds also dissolve heavy metals by direct displacement of metal ions from the ore matrix by hydrogen ions and by the formation of soluble metal complexes and chelates (Bosecker, 1997). In the case of manganese, metal solubilization may also be due to enzymatic reduction of highly oxidized metal compounds (Bosecker, 1997; Mohanty et al., 2017).

In overall, these results demonstrate the potential of *A. niger* to improve the solubilization of metallic oxides and open up new routes for the development of smart fertilizers in which microorganisms promote the solubilization of oxides to supply micronutrients for plants. Given such positive results, in the next step of the study we proposed to design a composite based in the dispersion of oxides nanoparticles with simultaneous encapsulation of *A. niger* with the objective of obtaining a composite-fertilizer

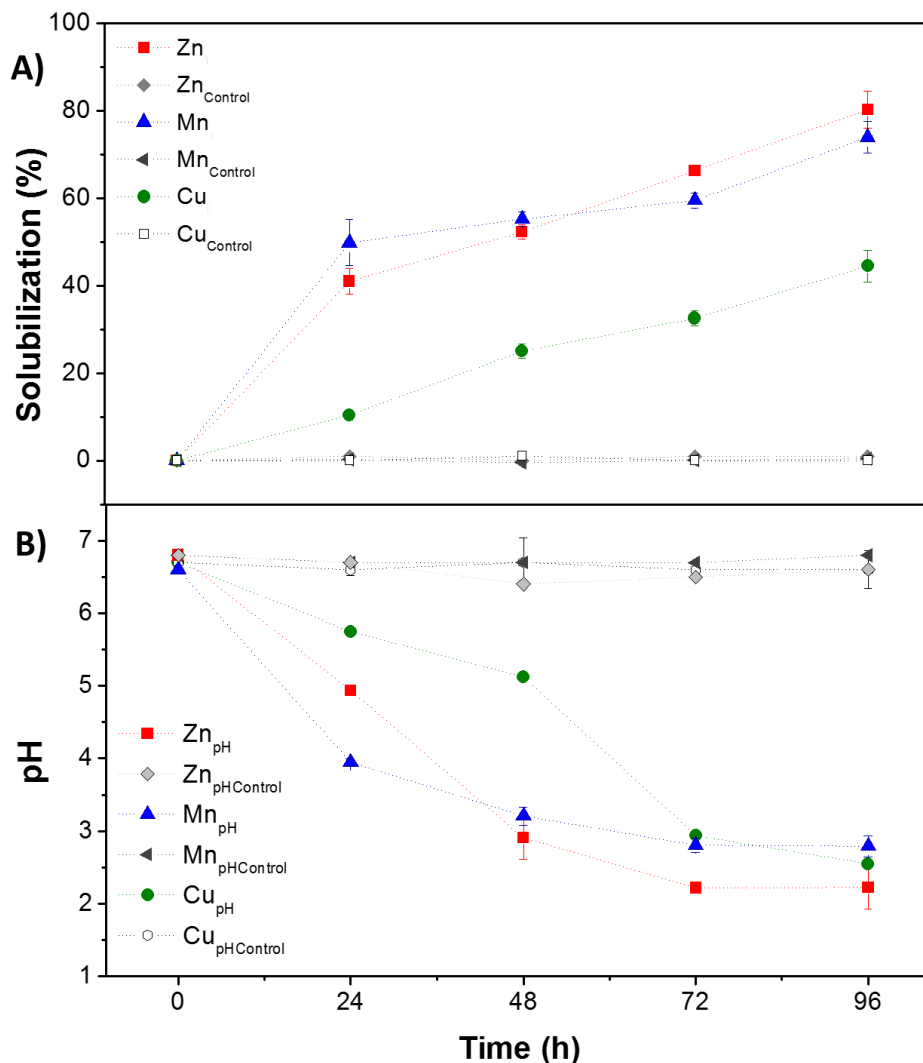granular product that could be easily applied in the field.

Figure 2. Temporal profiles of solubilization (A) and pH values (B) for ZnO, MnO and CuO and controls (without *A. niger*) during submerged cultivation of *A. niger* using Czapek Dox medium, 30 °C, 220 rpm, pH$_{initial}$ 7.

3.3. Bio-activation of composites prepared using individual oxide dispersion

Three composites were initially designed (St/Zn, St/Mn and St/Cu, described in Section 2.3) and an initial set of experiments was carried out to evaluate the possible synergy among starch matrix, oxide particles and encapsulated *A. niger* to promote the solubilization of the oxides present in the materials. In these experiments, the composites were incubated in a

liquid nutrient medium (described in Section 2.6) to provide the minimum conditions required for spore germination and fungal growth.

The Figure 3 shows the results in terms of solubilization achieved by the bio-activation of the composites St/Zn, St/Mn and St/Cu and their respective controls (without *A. niger* spores). The temporal profiles of solubilization (Figure 3A) show that the composites were bio-activated at different times. The St/Zn and St/Mn were rapidly bio-activated by *A. niger* spore germination and proliferation of fungal biomass in the granule structure, resulting in the reduction of pH and increase of the solubilization of the respective oxides. However, St/Cu was only bio-activated after 48 h of incubation, as evidenced by the starting of pH reduction and oxides solubilization. These delay in *A. niger* spores activation can be due to the protection (physical barrier) conferred by encapsulation with starch that may impair the water diffusion for spore germination. The longer delay observed for St/Cu can also be attributed to fungicidal effect of CuO, as observed in previous studies (Araujo et al., 2018; Mayorga et al., 2018).

Despite the delay observed in the bio-activation of the composites, the starch matrix was efficient to maintain the *A. niger* spores viable after the processing step, as bio-activation was very efficient to promote the solubilization. For instance, the composite of St/Mn showed an intense positive temporal profile of solubilization during the first 96 h reaching a solubilization of around 80%. After that, the solubilization increased at smaller rate, reaching close to 100% in 288 h. As for the composites of St/Zn and St/Cu, the temporal profile of solubilization were less intense during the first 96 h, but reached final values of solubilization around 90% and 70% in 288 h, respectively. In general, St/Mn and St/Cu composites promoted similar solubilization efficiencies to the experiments using only oxide under submerged culture during 96 h, but solubilization using St/Zn was slightly lower. Although there was no increase in the solubilization of these materials the strategy of processing of these composite as a granule allow the application of these materials in the field.
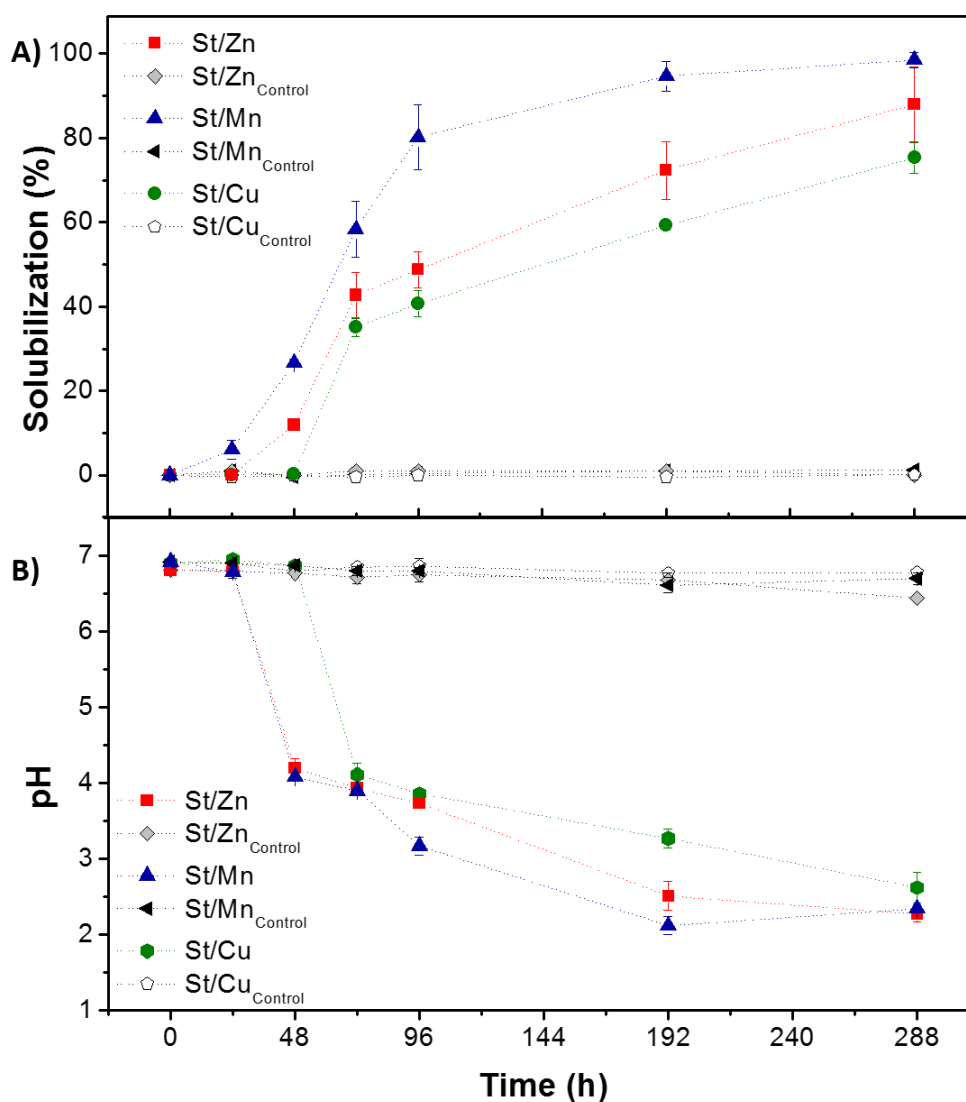
Figure 3. Bio-activation of St/Zn, St/Mn, St/Cu composites and controls (without *A. niger* spores) using Czapek Dox medium, 30 °C, 220 rpm, $pH_{initial}$ 7. **A)** Temporal profile of solubilization. **B)** Temporal profile of pH values in the medium.

3.4. Bio-activation of composites using a mix composition

The effect of dispersion of three oxides in the same matrix was also evaluated as a proposal for a composite multi nutrient with ability to solubilize simultaneously the micronutrients Zn, Mn and Cu. This designed composite was named as St/Mix. Figure 4 shows the temporal profile of solubilization for micronutrients from the bio-activation St/Mix besides of temporal profile of pH during the incubation period in submerged culture. The micronutrients solubilization intensified from 48 h due to the increase of the acidity of the culture medium. The oxides mixture in the bio-fertilizer did not affect the activation of the *A. niger* spore which occurred at the same time observed for the St/Zn, St/Mn and St/Cu

145

composites (Fig. 3). The Zn and Mn solubilization from St/Mix composite remained high, with values above 90% after 288 hours of incubation. However, the Cu solubilization shown a small decrease compared to the St/Cu composite, reducing its solubilization from 75 to 65%. As expected, oxides solubilization from without *A. niger* spores were less than 1% up to 288 h, due to their small pH change during the incubation period. On the other hand, the culture medium acidification provided by organic acids production was the main key factor nanocomposite St/Mix solubilization.

Therefore, the biocomposite St/Mix was effective to solubilizing simultaneously three oxides besides enabling the simultaneous application of micronutrients in the soil through a single bioactive granule for plant nutrition. However, to optimize the effect this innovative concept of granule composite multi nutrient, we studied the integration of the elemental sulfur in matrix, since the oxidation of elemental sulfur promotes acidity generation that can potentiate the solubilization of the oxides present in the matrix. In addition, the elemental sulfur is a macronutrient important to plant.
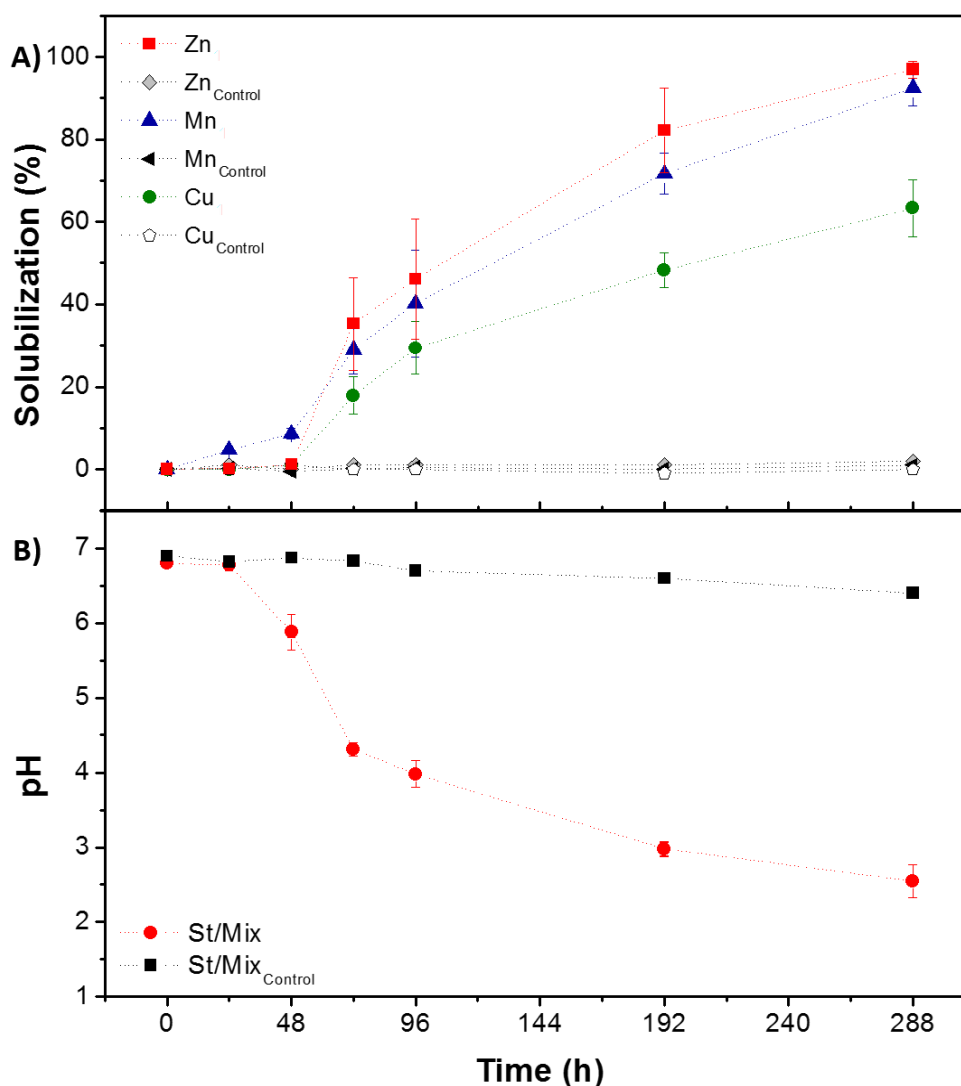
Figure 4. Bioactivation of St/Mix composite and control (without *A. niger* spores) using Czapek Dox medium, 30 °C, 220 rpm, pH$_{initial}$ 7. **A)** Temporal profile of solubilization. **B)** Temporal profile of pH values in the medium.

3.5. Bio-activation of composites using a mix composition with sulfur

Sulfur is currently a bottleneck for agronomical productivity, and the vast majority of available commercial fertilizer products does not provide adequate conditions for SO_4^{2-} production in soil, which is the actual form that this nutrient is absorbed by plants (Scherer, 2001, Evans et al., 2006; Stanisławska-Glubiak et al., 2014). Many commercial products are based on the application of elemental sulfur (S°), which is cheap and widely available, but the soil ability to oxidize them is heterogeneous and dependent of the presence of oxidizing microorganisms (Horowitz & Meurer 2007). In this context, *A. niger* fungus has also the

ability to oxidize sulfur (Grayston et al, 1986; Li et al, 2010). The oxidation reaction of S°
also produces acidity in the medium, so this acidity can also contribute to the solubilization of
the oxides (Calle-Castaneda et al., 2018; Grayston et al., 1986; Mattiello et al., 2017). Given
these characteristics, this element is ideal to be used in the matrix, since it is an important
macronutrient for the plants and when oxidized generates acidity in medium which potentiates
the solubilization of the oxides. Therefore, composites using S° were also produced (Table 1)
and incubation experiments to evaluate the bio-activation, oxides solubilization and S°
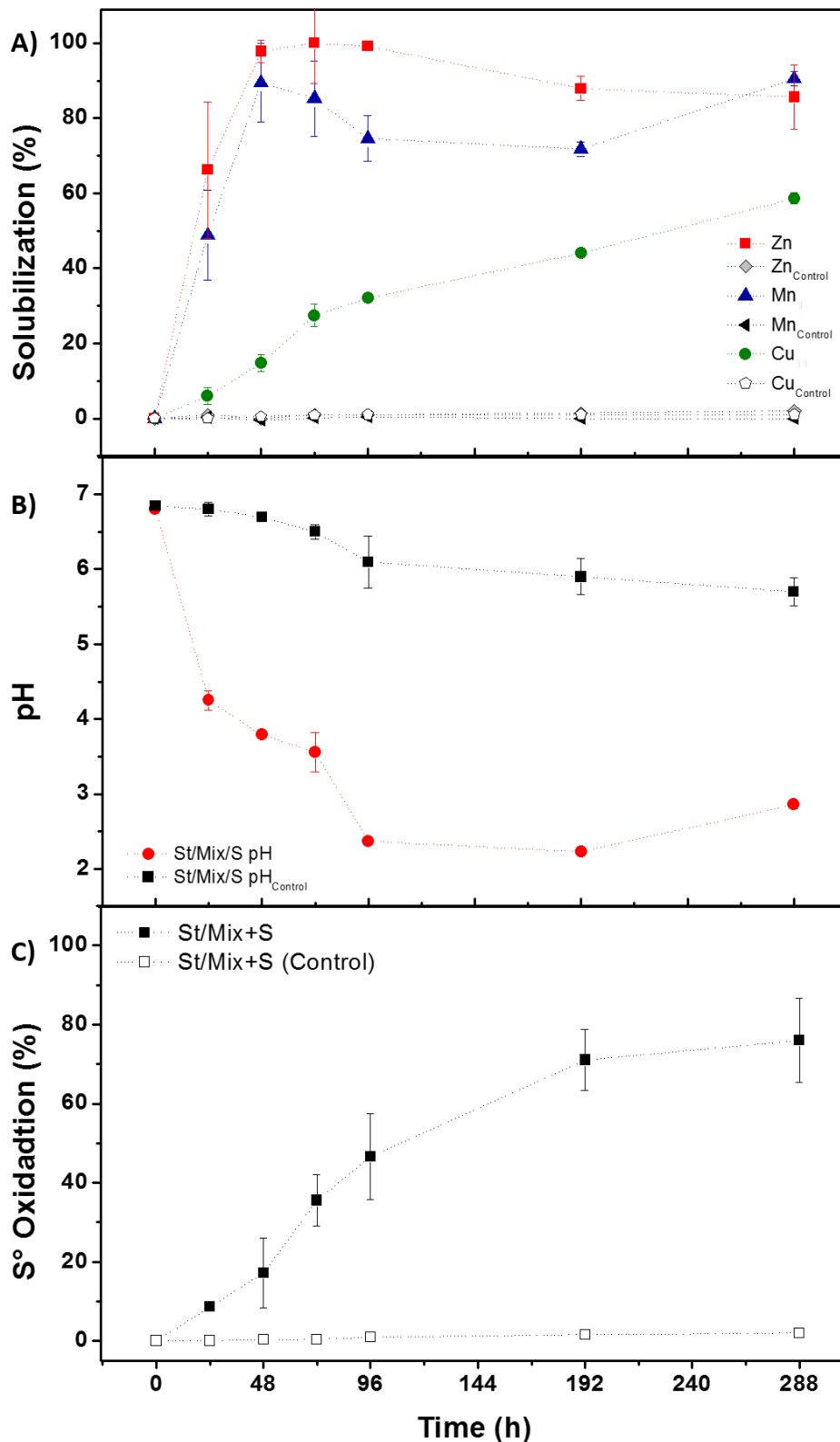oxidation were carried out.

Figure 5. Bioactivation of St/Mix+S composite and control (without *A. niger* spores) using Czapek Dox medium, 30 °C, 220 rpm, pH$_{initial}$ 7. **A)** Temporal profile of solubilization. **B)** Temporal profile of pH values in the medium. **C)** Temporal profile of sulfur-oxidation.

Figure 5 shows the bio-activation of St/Mix+S and temporal profiles of solubilization for Zn, Mn and Cu, as well as the temporal profiles of pH and sulfur oxidation. The St/Mix+S composite presented a faster bio-activation when compared to the composites analyzed previously (St/Mix, St/Zn, St/Mn and St/Cu). This could be possible due to the lower amount of oxides present in the matrix, specially CuO. In the first 24 h of incubation, there was an intense acidification of medium with a pH reduction to around 4.5. In contrast, the pH of the St/Mix and other composites showed no acidification in this same period. The acidification of the medium continued to increase, as evidenced by a pH reduction to around 4 at 48 h. This acidification was efficient to promote a large increase in the solubility of ZnO and MnO, close to 100% in only 48 h of the total of Zn and Mn available in St/Mix+S. Nevertheless, the temporal profile of solubilization CuO from St/Mix+S was similar to the composite St/Mix and St/Cu, not exceeding 60% even after 288 h. It was also observed that after the solubility of ZnO and MnO reached 100%, there was a small reduction in the amount of Zn and Mn in solution, which could be related to the complexation and precipitation effects (Lau & Hsu-Kim, 2008; Michael et al., 2014; Nie et al., 2014).

The S° oxidation was also evaluated, showing that approximately 50% of the S° available in composite was oxidized in only 96 h (Figure 5 C). This could have contributed to an increase in the acidity of the medium, which may have potentiated the solubilization of the oxides, mainly for ZnO and MnO. After 96 h of incubation, *A. niger* continued to promote S° oxidation but with a lower intensity, and the oxidation did not exceed 80% even in 288 h (12 days). These results demonstrate the potential of this composite as a fertilizer granule source of multi nutrient (S, Zn, Mn and Cu) to plant nutrition. Despite these very promising results, it is important that the composite maintain efficiency over time, so experiments evaluating the shelf time of St/Mix+S were performed, since that is an important property for the development of commercial products based on microorganisms.
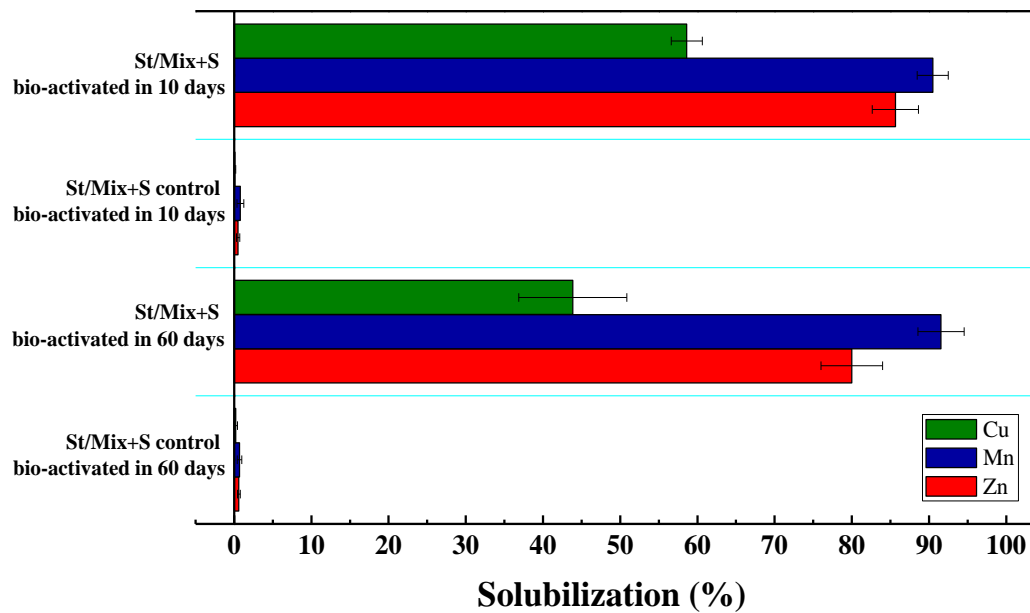
Figure 6. Effect of the shelf time on bio-activation of St/Mix+S and control (without *A. niger* spores) using Czapek Dox medium, 30 °C, 220 rpm, $pH_{initial}$ 7 after 288 h of incubation.

Figure 6 shows the effect of the shelf time on the bio-activation of the *A. niger* spores encapsulated in the starch matrix of St/Mix+S after 10 and 60 days of storage in plastic bags at room temperature. The results show that the composite was bio-activated and fungal growth promoted a similar solubilization after being stored for 10 and 60 days. This result demonstrates that the composite St/Mix+S has a high potential to be used as commercial product. Therefore, in the next step of the study, the effect of St/Mix+S composite was evaluated in a soil-plant system and its performance was compared to the ones achieved using commercial fertilizer and controls treatments.

3.6. Soil-plant experiments

This set of experiments was carried out to evaluate the bio-activation of the efficacy of the composite St/Mix+S in a soil-plant system in comparison to commercial fertilizers. Figure 7 summarizes the results for the dry matter production from Italian ryegrass during 130 days of growing on two types soils of distinct characteristics, namely a clay soil and a sandy loam soil. As expected, the two selected soils responded differently to fertilization, as can be visualized in the images of the ryegrass in the fifth cut and after 130 days of planting (Figure 7A-B).

After 130 days, the average of dry matter production among all treatments in the clay

soil (24 g pot^{-1}) (Figure 7 A) was higher than sandy loam soil (20 g pot^{-1}) (Figure 7 B). However, the actual increase due to fertilization was higher in the sandy loam soil with an increase of up to 16 g pot^{-1} provided by fertilization with the St/Mix+S composites, compared to control treatment. This result can be attributed to the lower S concentration of the sandy loam soil (Table S1, Supplementary Material) that limited the ryegrass growth from the 3rd cut (70 days after planting/fertilization) as shown in Figure 7 F.

The total dry matter produced of ryegrass cultivated in clay soil after 130 days (Figure 7 C) when fertilized with St/Mix+S was around 30 g pot^{-1}, which is similar to the values achieved using commercial sources of high solubility (CuCl$_2$; ZnCl$_2$; MnCl$_2$ + Sulphurgan$^{®}$) and statistically (Tukey's test at the 95% confidence level) higher than the treatment with the insoluble sources (Oxides + Elemental Sulfur) and the control as well. For the ryegrass cultivated in sandy loam soil (Figure 7 D), the dry matter after 130 for all the treatments with fertilizer application were higher than the control, but they did not show any statistically difference (Tukey's test at the 95% confidence level). Nevertheless, the treatment with St/Mix+S composite showed the highest average dry matter produced (25 g pot^{-1}). Such positive results achieved using the composite St/Mix+S are also evidenced in the data of the dry mass over time, for both type of soils (Figure 7 E-F).

Therefore, the results demonstrate the remarkable potential of the St/Mix+S composite to increase the solubility of these materials mainly in the soil, showing similar results to sources used commercially. However, it is also necessary to quantify the S, Cu, Zn and Mn content in the plants, as well as the recovery efficiency from each fertilizer to fully evaluate the efficacy of the proposed St/Mix+S composite, since the higher nutrient content in the dry matter reflects in a better nutritional quality of the forage. Therefore, chemical analyzes for nutrients quantification in the dry matter is being carried out and the results will be included to this work/section.
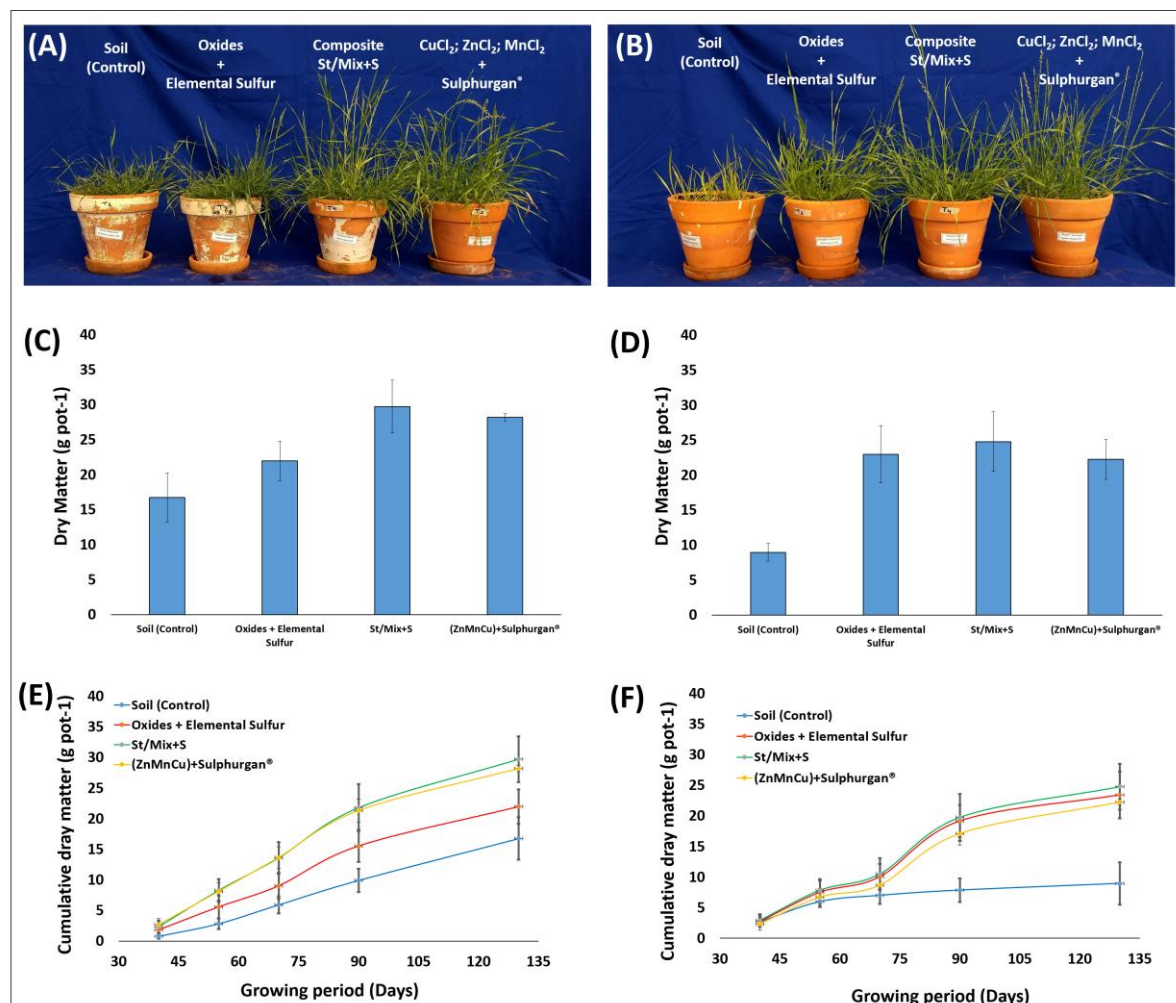
Figure 7. Soil-plant experiments. Effect of accumulated dry matter of Italian ryegrass (*Lolium multiflorum* Lam.) using four treatments of fertilizers "soil (Control)", "Oxides + Elemental Sulfur", "St/Mix+S composite" and sources "CuCl$_2$; ZnCl$_2$; MnCl$_2$ + Sulphurgan®". **A)** Picture, Italian ryegrass cultivated in clay soil after 130 days. **B)** Picture, Italian ryegrass cultivated in sandy loam soil after 130 days. **C)** Dry matter of Italian ryegrass cultivated in clay soil after 130 days. **D)** Dry matter of Italian ryegrass cultivated in sandy loam soil after 130 days. **E)** Dry matter accumulation of Italian ryegrass cultivated in clay soil. **F)** Dry matter accumulation of Italian ryegrass cultivated in sandy loam soil.

4. Conclusion

Our findings show that the proposed composite based on the dispersion of nanoparticles of oxides and sulfur in a polysaccharide matrix with *A. niger* spores is a promising source of multi-nutrient for plant development. We demonstrated that the *A. niger* is a potential fungus to promote the biological solubilization of oxides as well as the bio-oxidation of S°. All the composites produced (St/Zn, St/Mn, St/Cu, St/Mix and St/Mix+S) increased solubility of the

dispersed material in the matrix, with the St/Mix+S composite presenting the best results of solubilization of the oxides, besides being a source of multi-nutrient. A good interaction of the S° with the starch matrix was observed which increased the dispersion of the oxides and potentiated the solubilization due to the higher medium acidity. A high oxidation of S° was also observed, showing that *A. niger* was efficient to promote both reactions during the bio-activation of the composite. The St/Mix+S composite was also evaluated after two months of storage and the efficiency remained similar to the initial one. Greenhouse experiments in a soil-plant system showed a similar efficiency to the ones achieved using commercial fertilizer in terms of plant biomass. These findings demonstrate the application of the St/Mix+S composite as a fertilizer granule which is a source of multi-nutrients (S, Zn, Mn and Cu) and open new routes for development of smart fertilizer capable of making feasible the use of low solubility source of nutrients required for efficient plant development.

References

Altomare, C., Norvell, W.A., Bjorkman, T., Harman, G.E. 1999. Solubilization of phosphates and micronutrients by the plant-growth-promoting and biocontrol fungus Trichoderma harzianum Rifai 1295-22. *Applied and Environmental Microbiology*, **65**(7), 2926-2933.

Araujo, I.M.S., Silva, R.R., Pacheco, G., Lustri, W.R., Tercjak, A., Gutierrez, J., Junior, J.R.S., Azevedo, F.H.C., Figueredo, G.S., Vega, M.L., Ribeiro, S.J.L., Barud, H.S. 2018. Hydrothermal synthesis of bacterial cellulose-copper oxide nanocomposites and evaluation of their antimicrobial activity. *Carbohydrate Polymers*, **179**, 341-349.

Bhalerao, T.S. 2012. Bioremediation of endosulfan-contaminated soil by using bioaugmentation treatment of fungal inoculant Aspergillus niger. *Turkish Journal of Biology*, **36**(5), 561-567.

Bhalerao, T.S., Puranik, P.R. 2007. Biodegradation of organochlorine pesticide, endosulfan, by a fungal soil isolate, Aspergillus niger. *International Biodeterioration & Biodegradation*, **59**(4), 315-321.

Bahaloo-Horeh, N., Mousavi, S.M. 2017. Enhanced recovery of valuable metals from spent lithium-ion batteries through optimization of organic acids produced by Aspergillus niger. *Waste Management*, **60**, 666-679.

Bosecker, K. 1997. Bioleaching: Metal solubilization by microorganisms. *Fems Microbiology Reviews*, **20**(3-4), 591-604.

Calle-Castaneda, S.M., Marquez-Godoy, M.A., Hernandez-Ortiz, J.P. 2018. Phosphorus recovery from high concentrations of low-grade phosphate rocks using the biogenic acid produced by the acidophilic bacteria Acidithiobacillus thiooxidans. *Minerals Engineering*, **115**, 97-105.

Camargo, O.A., Moniz, A.C., Jorge, J.A., Valadares, J.M.A.S. 2009. *Métodosde Análise Química, Mineralógica e Física de Solos do Instituto Agronômico deCampinas*, Instituto Agronômico, Campinas, SP, Brazil.

Cantarella, H., Furlani, P.R. 1997. *Arroz de sequeiro*, Instituto Agronômico, Campinas, SP, Brazil.

Chaerun, S.K., Sulistyo, R.S., Minwal, W.P., Mubarok, M.Z. 2017. Indirect bioleaching of low-grade nickel limonite and saprolite ores using fungal metabolic organic acids generated by Aspergillus niger. *Hydrometallurgy*, **174**, 29-37.

Giroto, A.S., de Campos, A., Pereira, E.I., Cruz, C.C.T., Marconcini, J.M., Ribeiro, C. 2014. Study of a Nanocomposite Starch-Clay for Slow-Release of Herbicides: Evidence of Synergistic Effects Between the Biodegradable Matrix and Exfoliated Clay on Herbicide Release Control. *Journal of Applied Polymer Science*, **131**(23).

Grayston, S.J., Nevell, W., Wainwright, M. 1986. Sulphur oxidation by fungi. *Transactions of the British Mycological Society*, **87**(2), 193-198.

Heinonen, S., Nikkanen, J.P., Huttunen-Saarivirta, E., Levanen, E. 2017. Investigation of long-term chemical stability of structured ZnO films in aqueous solutions of varying conditions. *Thin Solid Films*, **638**, 410-419.

Klaic, R., Plotegher, F., Ribeiro, C., Zangirolami, T.C., Farinas, C.S. 2017. A novel combined mechanical-biological approach to improve rock phosphate solubilization. *International Journal of Mineral Processing*, **161**, 50-58.

Lau, B.L.T., Hsu-Kim, H. 2008. Precipitation and growth of zinc sulfide nanoparticles in the presence of thiol-containing natural organic ligands. *Environmental Science & Technology*, **42**(19), 7236-7241.

Liu, R.Q., Lal, R. 2015. Potentials of engineered nanoparticles as fertilizers for increasing agronomic productions. *Science of the Total Environment*, **514**, 131-139.

Malavolta, E. 1980. *Elementos de nutrição mineral de plantas*.

Martinez-Ballesta, M.C., Dominguez-Perles, R., Moreno, D.A., Muries, B., Alcaraz-Lopez, C., Bastias, E., Garcia-Viguera, C., Carvajal, M. 2010. Minerals in plant food: effect of agricultural practices and role in human health. A review. *Agronomy for Sustainable Development*, **30**(2), 295-309.

Mattiello, E.M., da Silva, R.C., Degryse, F., Baird, R., Gupta, V., McLaughlin, M.J. 2017. Sulfur and Zinc Availability from Co-granulated Zn-Enriched Elemental Sulfur Fertilizers. *Journal of Agricultural and Food Chemistry*, **65**(6), 1108-1115.

Mayorga, J.L.C., Rovira, M.J.F., Mas, L.C., Moragas, G.S., Cabello, J.M.L. 2018. Antimicrobial nanocomposites and electrospun coatings based on poly(3-hydroxybutyrate-co-3-hydroxyvalerate) and copper oxide nanoparticles for active packaging and coating applications. *Journal of Applied Polymer Science*, **135**(2), 11.

Mendes, G.d.O., Rego Muniz da Silva, N.M., Anastacio, T.C., Bojkov Vassilev, N., Ribeiro, J.I., Jr., da Silva, I.R., Costa, M.D. 2015. Optimization of Aspergillus niger rock phosphate solubilization in solid-state fermentation and use of the resulting product as a P fertilizer. *Microbial Biotechnology*, **8**(6), 930-939.

Michael, G., Bahri-Esfahani, J., Li, Q.W., Rhee, Y.J., Wei, Z., Fomina, M., Liang, X.J. 2014. Oxalate production by fungi: significance in geomycology, biodeterioration and bioremediation. *Fungal Biology Reviews*, **28**(2-3), 36-55.

Mohanty, S., Ghosh, S., Nayak, S., Das, A.P. 2017. Bioleaching of manganese by Aspergillus sp isolated from mining deposits. *Chemosphere*, **172**, 302-309.

Nie, Z.R., Ma, L.W., Xi, X.L. 2014. "Complexation-precipitation" metal separation method system and its application in secondary resources. *Rare Metals*, **33**(4), 369-378.

Novais, R.F., Neves, J.C.L., Barros, N.F. 1991. Ensaio em ambiente controlado. 1 ed. in: *Métodos de pesquisa em fertilidade do solo*, (Eds.) A.J. Oliveira, W.E. Garrido, J.D. Araújo, S. Lourenço, Vol. 3, Brasil. Brasília: Embrapa-SEA, pp. 189-253.

Ong, G.H., Ho, X.H., Shamkeeva, S., Fernando, A., Wong, L.S. 2017. Biosorption study of potential fungi for copper remediation from Peninsular Malaysia. *Remediation-the Journal of Environmental Cleanup Costs Technologies & Techniques*, **27**(4), 59-63.

Rasoulnia, P., Mousavi, S.M. 2016. Maximization of organic acids production by Aspergillus niger in a bubble column bioreactor for V and Ni recovery enhancement from power plant residual ash in spent-medium bioleaching experiments. *Bioresource Technology*, **216**, 729-736.

Sutjaritvorakul, T., Chutipaijit, S., Sihanonth, P. 2017. Solubilization and bioprecipitation of zinc oxide nanoparticles by fungi isolated from zinc sulfide mineral ores. *Materials Today-Proceedings*, **4**(5), 6562-6566.

Tejomyee, S.B. 2013. Biominerlization and Possible Endosulfan Degradation Pathway Adapted by Aspergillus niger. *Journal of Microbiology and Biotechnology*, **23**(11), 1610-1616.

van Raij, B., Andrade, J.C., Cantarella, H., Quaggio, J.A. 2001. *Chemical Analysis to Assess the Fertility of Tropical Soils*, Instituto Agronômico, Campinas, SP, Brazil

Vanraij, B., Quaggio, J.A., Dasilva, N.M. 1986. Extraction of phosphorus, potassium, calcium, and magnesium from soils by an ion-exchange resin procedure. *Communications in Soil Science and Plant Analysis*, **17**(5), 547-566.
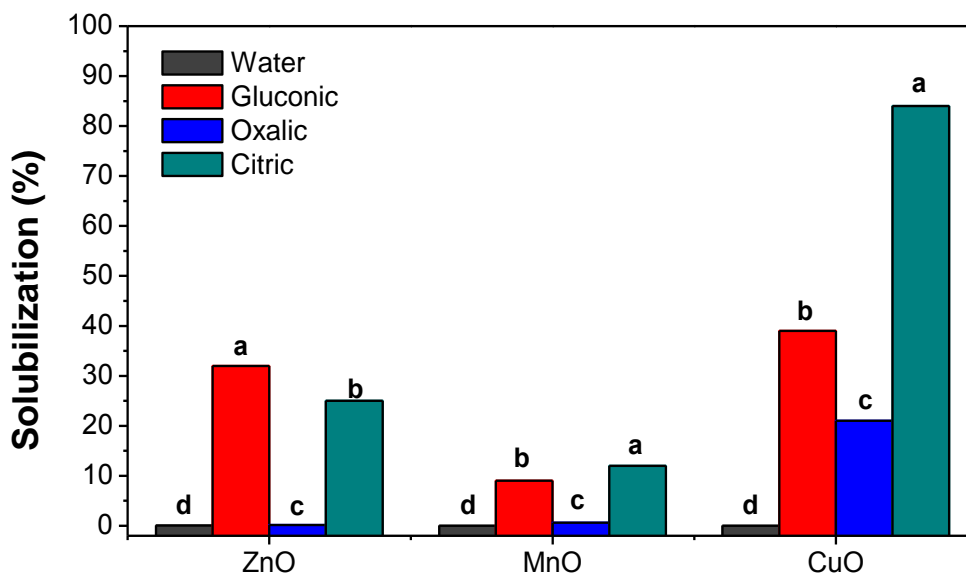
FS 1. Solubility of oxides in a solution of organic acids 2 wt.%.

Prepare 100 ml of an organic acid solution (2 wt%) in a 250 ml beaker. Heat until slightly boiled and add 1 g of the sample (oxide). Cover the beaker with watch glass and keep in slight boiling for 10 min. Then, turn off and allow to cool to room temperature, transfer to a 200 ml volumetric flask and complete the volume with distilled water and homogenise. Keep at rest for 10 min and filter using filter paper (medium to fine porosity). From the filtrate obtained the concentration of the micronutrient was determined by ICP.

Ministério da Agricultura, Pecuária e Abastecimento (MAPA). 2013. Manual de métodos analíticos oficiais para fertilizantes e corretivos. Brazil.

.

Table S1: Chemical and physical properties of soil studied

Soil	pH[1]	K	Ca	Mg	H+Al	CTC[2]	V[3]	P	S	Zn	Cu	Fe	Mn	OC[4]	Sand	Silt	Clay
		.... $mmol_c\ kg^{-1}$					%	.... $mg\ kg^{-1}$							.... $g\ kg^{-1}$		
Sandy loam	5.1	1.3	9.0	2	35	47	26	4	5	0.6	0.9	14	2	8	663	34	303
Clay	5.8	0.7	19	9	25	54	53	4	15	0.3	9.6	21	2.5	13	319	218	463

[1]pH = determined in H_2O

[2]CEC = cation-exchange capacity.

[3]V = percentage of soil base saturation.

[4]OC = total organic C.

Capítulo 7

Conclusões

A produção de fertilizantes a partir da solubilização biológica de minerais de baixa reatividade é uma tecnologia em desenvolvimento e encontra-se diante de desafios para aumentar a competitividade frente aos produtos já disponíveis no mercado. Desenvolver novas estratégias de processo para aumentar a eficiência de solubilização via cultivo microbiano, desenvolver novas alternativas de produtos fertilizantes e identificar microrganismos com potencial para solubilização são algumas das contribuições que deste estudo. Pelos resultados apresentados neste trabalho e considerando os objetivos estabelecidos inicialmente, podemos concluir:

➢ O fungo *Aspergillus niger* tem potencial para promover a solubilização de diferentes fontes de fosfatos minerais, entre rochas fosfáticas de origem sedimentar e ígnea. O fungo *A. niger* também foi eficiente para solubilizar óxido de zinco, óxido de magnésio e óxido de cobre, além de promover a oxidação do enxofre elementar.

➢ A ativação mecânica da rocha fosfática promove a redução do tamanho de partícula aumentando a interação deste material com os ácidos orgânicos produzidos durante o cultivo microbiano e consequentemente a solubilização. Os resultados mostram que a estratégia de associar a ativação mecânica ao processo de solubilização foi determinante para aumentar a eficiência de solubilização da rocha fosfática via cultivo submerso e cultivo estado sólido. Embora, devido as diferentes propriedades físico-químicas das rochas a ativação mecânica resulta em diferentes eficiências de solubilização. Observou-se que a rocha Bayóvar (sedimentar) foi menos suscetível moagem tendendo a formar aglomerados que limitaram a solubilização durante o cultivo, já para rocha Itafós (ígnea) houve aumento de solubilidade para todos os tempos de moagem estudados.

➢ Os sólidos presentes no meio de cultivo exercem efeito negativo sob a biomassa microbiana, diminuindo a acidez do meio e prejudicando a solubilização da rocha fosfática. A estratégia de batelada alimentada de sólidos foi eficiente para diminuir os efeitos de inibição, aumentado a acidez e promovendo aumento da solubilidade da rocha fosfática. A estratégia integrada utilizando ativação mecânica da rocha

fosfática, seguida de um processo de cultivo submerso utilizando batelada alimentada de sólidos promoveu um aumento de solubilidade de 77%, quando comparada com o material natural sem ativação mecânica utilizando processo convencional de solubilização.

➢ Os estudos de solubilidade das rochas fosfáticas em ácidos orgânicos mostraram diferentes eficiências de solubilização entre os ácidos utilizados, sendo que entre os ácidos orgânicos a solubilidade das fontes fosfatadas testadas (fosfato de tricálcio, rocha fosfática Bayóvar e rocha fosfática Itafós) foi maior em ácidos cítrico e oxálico. Observou-se uma relação de sinergismo entre ácido cítrico e oxálico (1:1) e entre ácido oxálico e gluconico (2:1) que potencializou a solubilização das rochas fosfáticas.

➢ Os compósitos-fertilizantes constituem uma tecnologia com elevado potencial para promover o aumento de solubilidade da rocha fosfáticas e de fontes de nutrientes de baixa solubilidade como óxidos e enxofre elementar que podem ser utilizadas para nutrição vegetal. A matriz polimérica produzida a partir da gelatinizarão do amido tem papel chave na produção destes compósito-fertilizantes, pois proporciona uma elevada dispersão de partículas com simultâneo encapsulamento de esporos do microrganismo. Essas condições promovem sinergia entre microrganismo e partículas que maximiza a solubilização devido ao elevado grau de dispersão obtido durante o processamento do compósito. O encapsulamento promoveu uma proteção aos esporos que aumenta o tempo de prateleira do produto, logo abre condições para ser comercializado.

Sugestões para trabalhos futuros

Para trabalhos futuros, sugere-se:

➢ Avaliar o efeito do co-cultivo de *Aspergillus niger* com outros microrganismos por cultivo submerso e estado sólido a fim de tentar maximizar a solubilização de rochas fosfáticas e outras fontes de baixa solubilidade.

➢ Desenvolver estudos avaliando a co-inoculação nos compósitos. O fungo *Trichoderma harzianum* pode ser uma boa opção, pois é amplamente utilizado como agente de biocontrole. Logo, pode-se agregar valor ao compósito, fornecendo um compósito-fertilizante ativado biologicamente por *Aspergillus niger* junto a um microrganismo promotor de biocontrole. Alguns fungos do gênero *Trichoderma* também podem produzir bioestimulantes que potencializam o crescimento das plantas.

➢ Avaliar o encapsulamento bactérias do gênero *Thiobacillus* principalmente nos compósitos-fertilizantes a base de enxofre e óxidos, uma vez que, essas bactérias são eficientes para promover a oxidação do enxofre elementar, logo podem ser mais hábeis que os fungos para esta função.

➢ Pesquisar por novas alternativas de polímeros de baixo custo que podem ser utilizados para desenvolver compósitos-fertilizantes e aumentar o tempo de prateleira dos microrganismos encapsulados.

➢ Avaliar o efeito da adição de microrganismos solubilizados em fertilizantes agro-minerais a fim de potencializar a solubilização dos minerais presentes nestes fertilizantes.

Referências

Avdalovic, J., Beskoski, V., Gojgic-Cvijovic, G., Mattinen, M.L., Stojanovic, M., Zildzovic, S., Vrvic, M.M. 2015. Microbial solubilization of phosphorus from phosphate rock by iron-oxidizing Acidithiobacillus sp B2. *Minerals Engineering*, **72**, 17-22.

Ahuja, A., and S. F. D'Souza, 2009, Bioprocess for Solubilization of Rock Phosphate on Starch Based Medium by Paecilomyces marquandii Immobilized on Polyurethane Foam: Applied Biochemistry and Biotechnology, v. 152, p. 1-5.

Barroso, C. B., G. T. Pereira, and E. Nahas, 2006, Solubilization of CAHPO(4) and ALPO(4) by Aspergillus niger in culture media with different carbon and nitrogen sources: Brazilian Journal of Microbiology, v. 37, p. 434-438.

Bhattacharya, S., A. Das, S. Bhardwaj, and S. S. Rajan, 2015, Phosphate solubilizing potential of Aspergillus niger MPF-8 isolated from Muthupettai mangrove: Journal of Scientific & Industrial Research, v. 74, p. 499-503.

Calle-Castaneda, S.M., Marquez-Godoy, M.A., Hernandez-Ortiz, J.P. 2018. Phosphorus recovery from high concentrations of low-grade phosphate rocks using the biogenic acid produced by the acidophilic bacteria Acidithiobacillus thiooxidans. *Minerals Engineering*, **115**, 97-105

Canovas, C.R., Macias, F., Perez-Lopez, R., Basallote, M.D., Millan-Becerro, R. 2018. Valorization of wastes from the fertilizer industry: Current status and future trends. *Journal of Cleaner Production*, **174**, 678-690

Chien, S. H., 1993, Solubility assessment for ferlilizer containing phosphate rock: Fertilizer Research, v. 35, p. 93-99.

CONAMA, 2011, Limites de emissão de poluentes atmosféricos gerados na produção de fertilizantes, ácido sulfúrico, ácido nítrico e ácido fosfórico, *in* C. N. d. M. A.-. CONAMA, ed., Brazil, p. 33.

Conley, D.J., Paerl, H.W., Howarth, R.W., Boesch, D.F., Seitzinger, S.P., Havens, K.E., Lancelot, C., Likens, G.E. 2009. ECOLOGY Controlling Eutrophication: Nitrogen and Phosphorus. *Science*, **323**(5917), 1014-1015.

de Oliveira, S. C., G. D. Mendes, U. C. da Silva, I. R. da Silva, J. I. Ribeiro, and M. D. Costa, 2015, Decreased mineral availability enhances rock phosphate solubilization efficiency in Aspergillus niger: Annals of Microbiology, v. 65, p. 745-751.

Farinas, C. S., 2015, Developments in solid-state fermentation for the production of biomass-degrading enzymes for the bioenergy sector: Renewable and Sustainable Energy Reviews, v. 52, p. 179-188.

Fazenda, M. L., R. Seviour, B. McNeil, and L. M. Harvey, 2008, Submerged Culture Fermentation of "Higher Fungi": The Macrofungi, Advances in Applied Microbiology, v. Volume 63, Academic Press, p. 33-103.

Fontes, M. P. F., and S. B. Weed, 1996, Phosphate adsorption by clays from Brazilian Oxisols, relationships with specific surface area and mineralogy: Geoderma, v. 72, p. 37-51.

Giroto, A.S., de Campos, A., Pereira, E.I., Cruz, C.C.T., Marconcini, J.M., Ribeiro, C. 2014. Study of a Nanocomposite Starch-Clay for Slow-Release of Herbicides: Evidence of Synergistic Effects Between the Biodegradable Matrix and Exfoliated Clay on Herbicide Release Control. *Journal of Applied Polymer Science*, **131**(23).

Giroto, A.S., Guimaraes, G.G.F., Foschini, M., Ribeiro, C. 2017. Role of Slow-Release Nanocomposite Fertilizers on Nitrogen and Phosphate Availability in Soil. *Scientific Reports*, **7**, 11.

Goldstein, A. H., R. D. Rogers, and G. Mead, 1993, Mining by Microbe: Nat Biotech, v. 11, p. 1250-1254.

Hamdali, H., B. Bouizgarne, M. Hafidi, A. Lebrihi, M. J. Virolle, and Y. Ouhdouch, 2008, Screening for rock phosphate solubilizing Actinomycetes from Moroccan phosphate mines: Applied Soil Ecology, v. 38, p. 12-19.

Heffer, P., Prud'home M., 2017, Short-term fertilizer Outlook 2017-2018, *in* IFA Strategic Forum, Zurich (Switzerland).

Illmer, P., and F. Schinner, 1995, Solubilization of inorganic calcium phosphates—Solubilization mechanisms: Soil Biology and Biochemistry, v. 27, p. 257-263.

Jain, R., J. Saxena, and V. Sharma, 2010, The evaluation of free and encapsulated Aspergillus awamori for phosphate solubilization in fermentation and soil–plant system: Applied Soil Ecology, v. 46, p. 90-94.

Kontic, B., and D. Kontic, 2012, A viewpoint on the approval context of strategic environmental assessments: Environmental Impact Assessment Review, v. 32, p. 151-155.

Kpomblekoua, K., and M. A. Tabatabai, 1994, EFFECT OF ORGANIC-ACIDS ON RELEASE OF PHOSPHORUS FROM PHOSPHATE ROCKS: Soil Science, v. 158, p. 442-453.

Krishnaraj, P. U., and S. Dahale, 2014, Mineral Phosphate Solubilization: Concepts and Prospects in Sustainable Agriculture: Proceedings of the Indian National Science Academy, v. 80, p. 389-405.

Lim, H. H., R. J. Gilkes, and P. G. McCormick, 2003, Beneficiation of rock phosphate fertilisers by mechano-milling: Nutrient Cycling in Agroecosystems, v. 67, p. 177-186.

Loureiro, F.E.L., Monte, M.B.d.M., Nascimento, M. 2008. *Agrominerais - Fosfato. 2ª ed.* CETEM-MCT, Rio de Janeiro.

Malavolta, E., 1980. Elementos de nutrição de Plantas.

Mattiello, E.M., da Silva, R.C., Degryse, F., Baird, R., Gupta, V., McLaughlin, M.J. 2017. Sulfur and Zinc Availability from Co-granulated Zn-Enriched Elemental Sulfur Fertilizers. *Journal of Agricultural and Food Chemistry*, **65**(6), 1108-1115.

Mendes, G. D., A. L. M. de Freitas, O. L. Pereira, I. R. da Silva, N. B. Vassilev, and M. D. Costa, 2014a, Mechanisms of phosphate solubilization by fungal isolates when exposed to different P sources: Annals of Microbiology, v. 64, p. 239-249.

Mendes, G. D., D. L. Zafra, N. B. Vassilev, I. R. Silva, J. I. Ribeiro, and M. D. Costa, 2014b, Biochar Enhances Aspergillus niger Rock Phosphate Solubilization by Increasing Organic Acid Production and Alleviating Fluoride Toxicity: Applied and Environmental Microbiology, v. 80, p. 3081-3085.

Mendes, G. d. O., N. Bojkov Vassilev, V. H. Araujo Bonduki, I. R. da Silva, J. I. Ribeiro, Jr., and M. D. Costa, 2013, Inhibition of Aspergillus niger Phosphate Solubilization by Fluoride Released from Rock Phosphate: Applied and Environmental Microbiology, v. 79, p. 4906-4913.

Mendes, G. d. O., N. M. Rego Muniz da Silva, T. C. Anastacio, N. Bojkov Vassilev, J. I. Ribeiro, Jr., I. R. da Silva, and M. D. Costa, 2015, Optimization of Aspergillus niger

rock phosphate solubilization in solid-state fermentation and use of the resulting product as a P fertilizer: Microbial Biotechnology, v. 8, p. 930-939.

Mendes, G.D., Galvez, A., Vassileva, M., Vassilev, N. 2017. Fermentation liquid containing microbially solubilized P significantly improved plant growth and P uptake in both soil and soilless experiments. *Applied Soil Ecology*, **117**, 208-211

Mullins, G., 2009, Phosphorus, Agriculture & the Environment, Virginia Polytechnic Institute and State University, Virginia State University, and the U.S. Department of Agriculture cooperating.

Nahas, E., 1996, Factors determining rock phosphate solubilization by microorganisms isolated from soil: World Journal of Microbiology & Biotechnology, v. 12, p. 567-572.

Nautiyal, C. S., 1999, An efficient microbiological growth medium for screening phosphate solubilizing microorganisms: Fems Microbiology Letters, v. 170, p. 265-270.

Nemery, J., Garnier, J. 2016. BIOGEOCHEMISTRY The fate of phosphorus. *Nature Geoscience*, **9**(5), 343-344

Novais, R.F., Neves, J.C.L., Barros, N.F., 1991. Ensaio em ambiente controlado. 1 ed. in: Métodos de pesquisa em fertilidade do solo, (Eds.) A.J. Oliveira, W.E. Garrido, J.D. Araújo, S. Lourenço, Vol. 3, Brasil. Brasília: Embrapa-SEA, pp. 189-253

Papagianni, M., 2007, Advances in citric acid fermentation by Aspergillus niger: Biochemical aspects, membrane transport and modeling: Biotechnology Advances, v. 25, p. 244-263.

Schoebitz, M., Ceballos, C., Ciampi, L. 2013. Effect of immobilized phosphate solubilizing bacteria on wheat growth and phosphate uptake. *Journal of Soil Science and Plant Nutrition*, **13**(1), 1-10.

Silva, U. D., G. D. Mendes, N. Silva, J. L. Duarte, I. R. Silva, M. R. Totola, and M. D. Costa, 2014, Fluoride-Tolerant Mutants of Aspergillus niger Show Enhanced Phosphate Solubilization Capacity: Plos One, v. 9, p. 9.

Souza, A. E., and D. S. Fonseca, 2010, Fosfato, *in* D. N. P. Minérios, ed., Brasil, p. 22.

Srividya, S., S. Soumya, and K. Pooja, 2009, Influence of environmental factors and salinity on phosphate solubilization by a newly isolated Aspergillus niger F7 from agricultural soil: African Journal of Biotechnology, v. 8, p. 1864-1870.

Stanton, R., 2002, Solid State Fermentation in Biotechnology: Fundamentals and Applications, Ashok Pandey, Carlos R. Soccol, Jose A. Rodriguez-Leon, Poonam Nigon; Asiatech Publishers, Inc., New Delhi, 2001, hardback, 221 pages, $45, ISBN 81-87680-06-7: Bioresource Technology, v. 82, p. 305.

Tayibi, H., Choura, M., Lopez, F.A., Alguacil, F.J., Lopez-Delgado, A. 2009. Environmental impact and management of phosphogypsum. *Journal of Environmental Management*, **90**(8), 2377-2386.

Toledo, M. C. M., 2001, A variabilidade da composição da apatita associada a carbonatos: Revista do Instituto Geológico, v. 22, p. 37.

Vassilev, N., M. T. Baca, M. Vassileva, L. Franco, and R. Azcon, 1995, Rock phosphate solubilization by Aspergillus niger grown on sugar-beet waste medium: Applied Microbiology and Biotechnology, v. 44, p. 546-549.

Vassilev, N., M. Fenice, F. Federici, and R. Azcon, 1997, Olive mill waste water treatment by immobilized cells of Aspergillus niger and its enrichment with soluble phosphate: Process Biochemistry, v. 32, p. 617-620.

Vassilev, N., A. Medina, R. Azcon, and M. Vassileva, 2006, Microbial solubilization of rock phosphate on media containing agro-industrial wastes and effect of the resulting products on plant growth and P uptake: Plant and Soil, v. 287, p. 77-84.

Vassilev, N., and M. Vassileva, 1992, Production of organic acids by immobilized filamentous fungi: Mycological Research, v. 96, p. 563-570.

Vassilev, N., and M. Vassileva, 2003, Biotechnological solubilization of rock phosphate on media containing agro-industrial wastes: Applied Microbiology and Biotechnology, v. 61, p. 435-440.

Vassilev, N., M. Vassileva, V. Bravo, M. Fernández-Serrano, and I. Nikolaeva, 2007, Simultaneous phytase production and rock phosphate solubilization by Aspergillus niger grown on dry olive wastes: Industrial Crops and Products, v. 26, p. 332-336.

Vassilev, N., M. Vassileva, M. Fenice, and F. Federici, 2001, Immobilized cell technology applied in solubilization of insoluble inorganic (rock) phosphates and P plant acquisition: Bioresource Technology, v. 79, p. 263-271.

Vassilev, N., M. Vassileva, A. Lopez, V. Martos, A. Reyes, I. Maksimovic, B. Eichler-Loebermann, and E. Malusa, 2015, Unexploited potential of some biotechnological techniques for biofertilizer production and formulation: Applied Microbiology and Biotechnology, v. 99, p. 4983-4996.

Vassileva, M., R. Azcon, J. M. Barea, and N. Vassilev, 1998, Application of an encapsulated filamentous fungus in solubilization of inorganic phosphate: Journal of Biotechnology, v. 63, p. 67-72.

Vassileva, M., M. Serrano, V. Bravo, E. Jurado, I. Nikolaeva, V. Martos, and N. Vassilev, 2010, Multifunctional properties of phosphate-solubilizing microorganisms grown on agro-industrial wastes in fermentation and soil conditions: Applied Microbiology and Biotechnology, v. 85, p. 1287-1299.

Vassilev, N., Eichler-Lobermann, B., Flor-Peregrin, E., Martos, V., Reyes, A., Vassileva, M. 2017. Production of a potential liquid plant bio-stimulant by immobilized Piriformospora indica in repeated-batch fermentation process. *Amb Express*, **7**, 7.

Zapata, F., 2004, Use of phosphate rocks for sustainable agriculture: FAO Fertilizer and Plant Nutrition Bulletin, p. 1-148.